MORPHOLOGICAL STUDIES AND FT-IR ANALYSIS OF SKIN AND ITS APPENDAGES OF WILD ANIMALS

G. N. NAGARAJU

DEPARTMENT OF VETERINARY ANATOMY AND HISTOLOGY

VETERINARY COLLEGE, HEBBAL, BANGALORE

KARNATAKA VETERINARY, ANIMAL & FISHERIES SCIENCES UNIVERSITY, BIDAR

MAY, 2012

MORPHOLOGICAL STUDIES AND FT-IR ANALYSIS OF SKIN AND ITS APPENDAGES OF WILD ANIMALS

Thesis submitted to the

Karnataka Veterinary, Animal & Fisheries Sciences University, Bidar

In partial fulfillment of the requirements

For the award of the degree of

DOCTOR OF PHILOSOPHY

In

VETERINARY ANATOMY AND HISTOLOGY

By

G. N. NAGARAJU

DEPARTMENT OF VETERINARY ANATOMY AND HISTOLOGY

VETERINARY COLLEGE, HEBBAL, BANGALORE

KARNATAKA VETERINARY, ANIMAL & FISHERIES SCIENCES UNIVERSITY, BIDAR

MAY, 2012

KARNATAKA VETERINARY, ANIMAL & FISHERIES SCIENCES UNIVERSITY, BIDAR
DEPARTMENT OF VETERINARY ANATOMY AND HISTOLOGY
VETERINARY COLLEGE, BANGALORE

CERTIFICATE

This is to certify that the thesis entitled ***"MORPHOLOGICAL STUDIES AND FT-IR ANALYSIS OF SKIN AND ITS APPENDAGES OF WILD ANIMALS"*** submitted by **Mr. G.N. NAGARAJU, ID No. DVHK 901,** for the award of degree of **DOCTOR OF PHILOSOPHY in VETERINARY ANATOMY** is a record of research work carried out by him during the period of his study in this University, under my guidance and supervision, and the thesis has not previously formed the basis of the award of any degree, diploma, associateship, fellowship or other similar titles.

Bangalore
May, 2012

Dr. R.V. PRASAD
Professor and Head

APPROVED BY:

Chairperson : _____
(R. V. PRASAD)

Nominated External Examiner : _____

Members : 1. _____
(K. V. JAMUNA)

2. _____
(M.L. SATHYANARAYANA)

3. _____
(K. JAYAKUMAR)

Affectionately Dedicated to

my Teachers,

my wife R. Rathnamma

and

my daughters

G.N. Sandhya and G.N. Ashwini

ACKNOWLEDGEMENTS

I am extremely grateful to ***Dr. R.V. PRASAD,*** *Professor and Head of the Department of Veterinary Anatomy, Veterinary College, Bangalore for his valuable guidance and critical suggestions as chairman of my advisory committee constant encouragement and affectionate dealing throughout the period of research and during the preparation of this thesis.*

I wish to express my sincere gratitude ***Dr. K.V. JAMUNA,*** *Professor, Department of Anatomy and Histology, and member of my advisory committee for her guidance and constructive criticisms offered during this study.*

I wish to express my deep sense of gratitude and heart felt thanks to ***Dr. V. Ramkrishna,*** *Rtd. Professor Department of Anatomy and Histology, for his selfless guidance and suggestions throughout the period of study without which this work would have been simply impossible. I admire his simplicity, approachability and encyclopedic knowledge of the subject.*

I consider myself fortunate to have advice, constructive suggestions and friendly support from ***Dr. M.L. Sathyanarayana,*** *Professor and Head, Department of Veterinary Pathology and member of my advisory committee.*

I sincerely express my gratitude to ***Dr. K. Jayakumar,*** *Professor and Head Department of Pharmacology and Toxicology, Veterinary College, Bangalore for his valuable suggestions, whole hearted support and guidelines throughout my course of study.*

I express my heartfelt thanks to ***Mr. Narayana Gowda****, lab technician, Department of Veterinary Pathology, Veterinary College, Bangalore, for his continuing encouragement, moral support and valuable suggestions during the study. I wish to express profound gratitude and sincere respects for his kind help and co-operation in tissue sectioning for the research work.*

My sincere thanks to ***Mr. Avinash Bhatt,*** *Research Associate, Department of Pharmacology and Toxicology, Veterinary College Bangalore for his technical help, valuable suggestions during my research period.*

I am extremely grateful and indebted to Principal Chief Conservator of Forest (Wild Life) Govt. of Karnataka, Aranya Bhavana, II floor, 18th cross, Malleshwaram, Bangalore-560003, for his kind help and permission in collection of wild animal's skin samples.

I express my sincere thanks to Mr. B. Siddarajaiah, Lab Assistant, Department of Anatomy and Histology, Veterinary College, Hebbal, Bangalore for his constant encouragement and wholehearted support during my study.

It is my privilege to extend sincere thanks to my friends Dr.Vinay Tikare, Dr. T.S. Sridhar Murthy, Dr. K. Ningaraju, Dr. Gowri, Dr. K.G. Sathesh, Dr. Chandranaik, Dr. Sundresh, Dr. Vinod, Dr. Rahila, Dr. Madhu, Dr. Manjunath, Dr. Muthuraj for their affectionate encouragement, inspiration and joyful company during my stay in the campus.

I owe special thanks to my colleague Dr. Santhosh, Baddi, S.Y, Veterinary Officer, Dr. Dhoolappa, Veterinary officer and Dr. Lakshmi Shree, assistant professor Department of Anatomy and Histology for their constant help and collective efforts through out the period of my research.

I am thankful to the non-teaching staff of our department Mr. Pradeep, Mr. Sadappa, Mr. Narayana, and Smt. Girijamma for the help rendered by them during my research.

I feel the inadequacy of words to pay regards to my parents, Brothers, Sister, my wife and my daughters who had sacrificed many things to nurture my ambition.

I would like to express my accreditation to one and all that have helped me directly or indirectly for the completion of this manuscript.

BANGALORE

May 2012 *(G.N. NAGARAJU)*

CONTENTS

LIST OF TABLES

LIST OF FIGURES

LIST OF PLATES

9	Photomicrograph of vertical section through dermis of the skin of leopard showing (a) Nerve fibers penetrating into root of the hair follicle Bielschowsky stain x100	80
10	Photomicrograph of vertical section through epidermis of the skin of Tiger showing, (a) Multiple folds (b) melanin pigments H & E Phloxine x 100	81
11	Photomicrograph of vertical section through epidermis of the skin of Tiger showing, (a) stratum corneum (b) stratum lucidum (c) stratum granulosum (d) stratum spinosum (e) stratum basale Weigerts resorcine fuchsin x 100	81
12	Photomicrograph of horizontal section of the skin of Tiger showing (a) primary hair follicle (b) secondary hair follicles. Weigerts resorcine fuchsin x 100	81
13	Photomicrograph of horizontal section of the skin of Tiger showing (a) Single large primary hair follicle (b) secondary hair follicles. (c) Sebaceous glands. Masson's Trichrome stain x200	82
14	Photomicrograph of horizontal section of the skin of Tiger showing (a) Sweat glands within the compound hair follicle. van Gieson x 100	82
15	Photomicrograph of horizontal section of the skin of Tiger showing (a) Elastic fibers Weigerts resorcine fuchsin x 100	82
16	Photomicrograph of horizontal section of the skin of Tiger showing (a) collagen fibers van Gieson x 200	83
17	Photomicrograph of horizontal section of the skin of leopard showing (a) Reticular fibers between the clusters of hair follicle. Gomori's silver impregnation stain x 40	83

18	Photomicrograph of vertical section through dermis of the skin of Tiger showing (a) Nerve fibers surrounding the primary and secondary hair follicle. Bielschowsky stain x200	83
19	Photomicrograph of vertical section through dermis of the skin of Tiger showing (a) Errector pilli muscle fibers. PTAH x200	84
20	Photomicrograph of vertical section through epidermis of the skin of spotted deer showing, (a) stratum basale (b) stratum granulosum (c) stratum corneum. H & E Phloxine x 100	84
21	Photomicrograph of vertical section through dermis of the skin of spotted deer showing(a) stratum granulosum with round shaped single cell layer Bielschowsky stain x100	84
22	Photomicrograph of vertical section through the skin of spotted deer showing distinct separation of (a) epidermis (b) dermis. H & E Phloxine x 100	85
23	Photomicrograph of horizontal section of the skin of spotted deer showing (a) primary hair follicle (b) secondary hair follicles. Van Gieson x 40	85
24	Photomicrograph of horizontal section of the skin of spotted deer showing hair follicles arranged in a linear fashion. Weigerts resorcine fuchsin x 40	85
25	Photomicrograph of horizontal section of the skin of spotted deer showing (a) Sebaceous glands surround primary hair follicle. van Gieson x 100	86
26	Photomicrograph of horizontal section of the skin of spotted deer showing (a) Merocrine Simple tubular Sweat glands van Gieson x 100	86
27	Photomicrograph of horizontal section of the skin of spotted deer showing (a) Elastic fibers in the dermis. Weigerts resorcine fuchsin x 100	86

38	Photomicrograph of vertical section through dermis of the skin of Goat showing few collagen fibers in both papillary and reticular layers. Van Gieson x 40	90
39	Photomicrograph of vertical section of the skin of Goat showing elastic fibers surrounded the primary hair follicle and sebaceous gland. Weigerts resorcine fuchsin x 200	90
40	Photomicrograph of vertical section of the skin of Goat showing (a) Reticular fibers present in the deeper part of the dermis. Gomori's silver impregnation stain x 200	91
41	Photomicrograph of horizontal section through dermis of the skin of Goat showing paired sebaceous glands located at the base of the hair follicles. H & E Phloxine x 40	91
42	Photomicrograph of horizontal section through dermis of the skin of Goat showing Simple tubular sweat glands below the primary hair follicles. PTAH x40	91
43	Photomicrograph of horizontal section through dermis of the skin of Goat showing Simple tubular sweat glands below the primary hair follicles. PTAH x409	92
44	Photomicrograph of vertical section through epidermis of the skin of Dog showing, (a) Stratum basale (b) stratum spinosum (c) stratum corneum. Masson's Trichrome stain	92
45	Photomicrograph of vertical section through epidermis of the skin of Dog showing Stratum spinosum composed of ten to fifteen cell layers. H & E Phloxine x 100	92
46	Photomicrograph of horizontal section through dermis of the skin of Dog showing (a) Primary hair follicle (b) secondary hair follicles. H & E Phloxine x 100	93

47	Photomicrograph of horizontal section through dermis of the skin of Dog showing (a) Sebaceous glands (b) sweat glands Masson's Trichrome stain x100	93
48	Photomicrograph of horizontal section through dermis of the skin of Dog showing Mixture of (a) nerve fibers (b) reticular fibers (c) collagen fibers (d) elastic fibers. Bielschowsky stain x100	93
49	Photomicrograph of vertical section through epidermis of the skin of Cat showing (a) Stratum basale (b) stratum spinosum (c) stratum granulosum (d) stratum corneum. Gomori's silver impregnation stain x 40	94
50	Photomicrograph of vertical section through epidermis of the skin of Cat showing Stratum spinosum composed of single cell layer, dark with distinct nucleated cells. Masson's Trichrome stain x100	94
51	Photomicrograph of horizontal section through dermis of the skin of Cat showing cluster of compound hair follicle (a) Primary hair follicle (b) secondary hair follicles(c) collagen fibers. van Gieson x 40	94
52	Photomicrograph of horizontal section of the skin of Cat showing irregular elastic fibers distributed around the primary hair follicle and interfollicular space. Weigerts resorcine fuchsin x 200	95
53	Photomicrograph of horizontal section through dermis of the skin of Cat showing (a) Nerve fibers surrounding primary and secondary hair follicle. Bielschowsky stain x10	95
54	Horizontal section through dermis of the skin of Cat showing (a) Skeletal muscle fibers between the (b) adipose cells of dermis and (c) Hypodermis PTAH x 40	95

ABBREVIATIONS

WPSI: Wild Life Protection Society of India

WII: Wildlife Institute of India

HATR: Horizontal attenuated total reflection

FTIR: Fourier transforms infrared

ATR: Attenuated total reflection

%: Percentage

PCA: Principle component analysis

DNA: Deoxyribose nucleic acid.

DRIFT: Diffuse reflectance infrared Fourier transform.

BMP: Bone morphogenic protein.

SF: Splitting factor.

LDA: Linear discriminant analysis.

CVA: Canonical variate analysis.

CLS: Classical least square.

ILS: Inverse least square.

PCR: Principal component regression.

PLS: Partial least square.

PCR: Principal component regression.

Introduction

I INTRODUCTION

India is endowed with a tremendous wealth of flora and fauna including wild animals. According to Wild Life Protection Society of India (WPSI) 2000 census, India harbors 60% of the world's tiger population, 50 per cent of Asiatic elephants, 80 per cent of the Great Indian one horned rhinoceros, entire population of Asiatic lions. According to Wildlife Institute of India (WII) 2003 census, 372 species of mammals with 53 endangered species are present in India.

Illegal trade in wild life and wild life products present serious threats to the long term survival of certain wild animals. such as tiger, leopard and spotted deer which are poached for their bones, skins and visceral organs used in traditional medicine leading to decline in their population. To fulfill the demands of wild animals' skin, sometimes skins from other domestic animals are artificially painted to resemble their counter parts and sold them in grey market at high prices. As a result, the greediness of poachers is threatening the extinction of endangered species (Parij and Bhattacharya, 2001). Forest and police officials are confused and facing difficulties in identifying the confiscated specimens. There is a need for identification of species of confiscated specimens in order to punish the poachers and to save the lives of wild animals.

The identification of skin of wild animals plays an important role in criminal investigations. Understanding the morphological features of the skin of domestic animals is essential to make comparative study with that of wild animals especially tiger, leopard and spotted deer. There is a definite pattern of arrangement of hair follicles in the integument of domestic animals like ox, goat, dog and cat which are species specific

(Evans and Christensen 1967; Trautmann and Fiebiger. 1957; Dellman and Brown. 1981 and Bacha and Bacha 1990). On the other hand no data is available on such morphological features of hair follicle of the wild animals. Thus there is a need for establishing a data base on these features which will serve as a guide in identifying the specific species of animal in disputes of veterolegal origin. Hair is an elastic keratinized structure that develops from the epidermis in the skin. They are distributed on the surface of entire skin except on the palms, soles, dorsal surfaces of the distal phalanges and the region of the anal and urogenital aperture.

Infrared spectroscopy is a novel tool that can be utilized to a great advantage in the analysis of materials virtually in any state. Infrared spectroscopy is based on the principle of vibrations of the atoms in a molecule. An infrared spectrum is commonly obtained by passing infrared radiation through a sample and determining what fraction of the incident radiation is absorbed at a particular energy. The energy at which any peak in an absorption spectrum appears corresponds to the frequency of vibration of a part of a sample molecule.

Infrared spectroscopy is a technique that can be easily adapted for use by untrained personnel in laboratories or on factory floor. A particular attraction is the ease of sample presentation (Marigheto *et al*., 1998). Fourier transform infrared (FTIR) spectroscopy is a fast and non-destructive technique, sensitive, and free of chemical preparation (Wang and Paliwal, 2007 and Xing *et al*., 2007).

Keratins had been studied with various forms of infrared spectroscopy for decades (Ambrose and Elliott 1951). Spectroscopy is now widely used in cultural

heritage conservation to characterize a broad range of artifact classes (Derrick *et al*. 2000 and Bitossi *et al*. 2005). Fourier transform infrared spectroscopy (FT–IR) is an analytical tool that, when used in examining hard biological tissues, stands out for its robustness, ease of sample preparation, simplicity of operation and the ability to make structural elucidations (Rantoul *et al*. 1998; Lyman *et al*. 2001). The resolving power of FT–IR has been applied in such diverse fields as forensic fiber identification (Kirkbride and Tungol, 1999) and bacterial species identification (Timmins *et al*. 1998).

Discriminant analysis (also known as linear discriminant analysis or canonical variates analysis) of vibrational spectra (Raman or infrared) has been successfully used to extend the limitation inherent in vibrational data. Examples include confirmation of edible oils and fats (Beaten and Aparicio 2000), bacterial taxonomy (Amiel *et al*. 2001), sub-typing of nylon polymers (Enlow *et al*. 2005), the forensic characterization of printer toners (Egan *et al*. 2003), geographical sourcing of medicinal plants (Dharmaraj *et al*. 2006), forensic identification of fingernails versus toenails (Widjaja and Seah, 2006) and the forensic identification of fiber blends (Espinoza *et al*. 2006).

Artefacts constructed from Asian elephant, wild boar ivories, spotted deer antlers and ceramics are often encountered in museum collections and in the modern wild life trade. The most common artefacts includes sculptures, statues, bangles, various types of handles, seals, cones, pyramids, buttons, cylinders and toy animals in a wide variety of shapes and sizes. Besides ivory statues, inlay ivory figures are incorporated in chairs, tables, wardrobes, chests, sofas and boxes for keeping gold and jewellary (Sila Tripati and Godfrey, 2007).

Similarly the antlers are used in traditional Chinese medicine for the advancement of health and the prevention of ill health was in direct disagreement with western medical practice, which is more concerned with the treatment of ill health (Fulder 1980a). In fact the entire culture of traditional Eastern medicine is one of the quests for health rather than the treatment of ill health (Brekhman 1980; Kaptchuk and Creacher 1987).

Proper identification of these artefacts is very important, since various ceramic and biological materials are often used as substitute materials. Rigorous and most effective method for identifying the skins and its appendages of wild animals is essential. Hence, the present study was conducted by using histological technique and HATR-FTIR coupled with discriminant analysis to differentiate the elephant ivory, boar ivory, spotted deer antler, leopard hairs, tiger hairs, spotted deer hairs, cattle hairs, goat hairs and their hoofs and claws with the following

Objectives:

1. To study the histological structure of skin and its appendages of wild animals.
2. To compare and differentiate the skin and its appendages of wild animals with the skin and its appendages of domestic animals.
3. To investigate forensic application of FT-IR method in the analysis of hairs of wild and domestic animals.
4. To study the FT-IR analysis of hoof, tusk (Ivory), horns and claws of wild animals.

Review of Literature

II REVIEW OF LITERATURE

2.1. Skin

The integument comprises the skin that covers the entire body, together with certain accessory organs which are derivatives of the skin, such as hairs, claws, horns, hoofs and glands of various kinds. The skin or cutis consists of two main parts; the epidermis, a stratified epithelial layer derived from the ectoderm and the dermis or corium, a connective tissue derivative of the mesoderm. Beneath the dermis is a loose connective tissue layer, the superficial fascia, or hypodermis (Copenhaver *et* al., 1971). The skin is one of the largest organs, making up to 16 % of the body weight (Bloom and Fawcett, 1986).

2.1.1. Epidermis

Trautmann and Fiebiger (1957) described the skin or cutis into epithelial epidermis and connective tissue corium or dermis. The epidermis is a stratified squamous epithelium covered by the stratum corium resting on the papillae of corium. The epithelium is comprises of stratum germinativum and superficial horny layer. The stratum germinativum is divided into stratum cylindricum and stratum spinosum or prickle cell layer (Evans and Christensen, 1967; Bacha and Bacha, 1990). The superficial horny layer is made up of stratum granulosum, stratum lucidum and stratum corneum. Stratum granulosum consist of one to five layers of fusiform, fine serrated cells with keratohyaline granules. Stratum lucidum is a thin acidophilic layer where keratohyaline are replaced by eleidin granules; the stratum corneum is the outermost cornified peripheral layer containing keratins only.

Lovell and Getty (1957) described the epidermis, hair follicle, dermis and skin glands of the dog. The epidermis is composed of three principal layers; stratum cylindricum, stratum spinosum and stratum corneum. The stratum cylindricum consist of one layer of cylindrical cells in which the cells possess little cytoplasm and dark staining nuclei. The stratum spinosum is made up of 10 to 20 layer of diamond shaped, dome shaped or flattened polygonal cells. They have a lighter staining cytoplasm than the cylindrical cells. Stratum corneum is a typical nucleated 4 to 8 cell layers.

Goldsberry and Calhoun (1959) studied the epidermis of the Hereford and Aberdeen Angus cattle where epidermis consisted of five subdivisions as described by (Trautmann and Fiebiger, 1957). The stratum cylindricum, spinosum, granulosum, lucidum and corium were present in the perineal region, the hoof margin and Achilles inertia only. In most cases only two clearly defined subdivision like stratum corneum and stratum granulosum. The stratum corneum consisted of several layers of cornified epithelium, the stratum lucidum was absent, and the stratum granulosum was constant only in the perianal region and extremities and consisted of one to three rows of cells. Stratum spinosum consisted of polygonal cells which become spindle shaped near the surface in areas of more than six layers. The stratum cylindricum consists of single layer of columnar cells which varied in height with the thickness of the epidermis.

Marcarian and Calhoun (1966) studied microscopic integument of adult swine, both the epidermis and dermis of female and male hogs were thicker than the castrated males. The stratum corneum was thickest in the snout and interdigital skin and characterized by sharp epidermal projection, the thinnest stratum corneum was found in

the axilla, eyelid and dorsal area of thorax and abdomen. Stratum lucidum was absent; the stratum granulosum consisted of one to five layers of flat, polygonal cells filled with granules.

Varicak (1941) and Strickland and Calhoun (1963) studied the microscopic structure of cat skin and revealed that epidermis in hairy skin, consisted of four distinct layers with stratum lucidum usually absent.

Sar (1966) reported that epidermis of the goat generally constituted of only four layers, stratum corneum, stratum granulosum, Stratum spinosum and stratum basale. Stratum lucidum was thick in the muzzle, planum nasale and junction of the hoof with the skin. Stratum corneum was prominent in the interdigital skin, hoof and horn margin, muzzle and planum nasale. Stratum lucidum is a shiny with indistinct nuclei and translucent in muzzle, planum nasale and hoof margins. Stratum granulosum consisted of 5 layers of diamond shaped cells containing keratohyaline granules; stratum spinosum consisted of polygonal cells with round nuclei and was prominent in the thick epidermal region.

Copenhaver *et al.* (1971) studied the integument; the thickness which varies considerably in different parts of the body. The relative proportion of the epidermis and dermis vary, the epidermis was composed of stratified squamous epithelium divided into stratum basale (stratum cylindricum), stratum spinosum, stratum granulosum, stratum lucidum and stratum corneum. Stratum basale consisted of columnar or highly cuboidal cells arranged in a single layer (stratum cylindricum) which rested on the basement membrane composed of basal lamina and lamina reticularis. Stratum spinosum is

composed of cells of polygonal shape or prickle cells. Stratum granulosum consisted of two to five rows of flattened, rhombic cells with their long axis parallel with surface of the skin. Stratum lucidum is thin, light staining zone located between the stratum granulosum and the cornified surface layer. Stratum corneum is very thick, composed of clear, dead scale like cells which became more and more flattened towards the free surface.

Talukdar *et al*. (1972) described the microscopic anatomy of skin of the horse, the surface contained grooves and ridges. The average thickness of general body skin is 3.8mm. The epidermis consisted of four layer stratum basale, stratum spinosum, stratum granulosum and stratum corneum. The stratum lucidum is absent. The keratohyaline granules and denritic malanocytes were present in the stratum spinosum and stratum granulosum. Basal process of the cells of the stratum basale anchored the epidermis to the underlying dermis.

Bloom and Fawcett (1986) stated that skin covers the surface of the body and consisted of two main layers, the surface epithelium or epidermis and adjacent connective tissue layer, the corium or dermis. Beneath the dermis is a loose connective tissue layer, the superficial fascia or hypodermis of skin. The skin is one of the largest organ making up some 16 % of the body weight. The free surface of the skin is not smooth but is marked by delicate grooves or flexure lines. The interface of the epidermis and dermis are uneven. The epidermis is composed of cells of two distinct lineages those comprising the bulk of the epithelium undergo keratohyaline granulation and form the dead superficial layer of the skin, they comprising the keratinizing system. The deeper part of

the epidermis doesn't contain keratinizing system but were capable of producing melanin pigment, these are the malanocytes. The epidermis contained four principal layers, but stratum lucidum is seldom seen in the thinner epidermis of general body surface.

Dellmann and Brown (1981) described the skin or integument to be composed of epidermis, dermis (corium), hair follicle, sweat gland and sebaceous gland, other digital organs (claw, hoof) and specialized glands. It is one of the largest organs in the body. Epidermis, the outer most layer of the skin is smooth in some areas but presented ridges or folds reflecting the contour of the underlying superficial layer of dermis. The epidermis of both horny and non horny skin contained the stratum basale, stratum spinosum, stratum granulosum and stratum corneum. The stratum lucidum is found only in non hairy region. In addition to the regular keratohyaline cells of the epidermis there are also melanocytes derived from neural crest and located among the cells of the stratum spinosum and these melanocytes are stellate shaped and their processes extending in the intercellular space of epidermis.

Lloyd and Garthwaite (1982) observed that in canine, the epidermis of skin was composed of three to six cell layers and measured 10.1μm in thickness. The stratum basale**,** stratum spinosum, stratum granulosum and stratum corneum were constantly present (Bacha and Bacha 1990) and stratum granulosum contained basophilic keratohyaline granules in their cytoplasm. In structures with hard keratin such as hooves and claws, stratum granulosum and stratum lucidum were absent with often sloughing off of the dead keratinized cells from the surface (Bacha and Bacha, 1990).

Bhayani *et al*. (1995) found that in lion, the total thickness of epidermis of the skin was maximum in neck region and minimum in lower abdomen.

2.1.2 Dermis

Trautmann and Fiebieger (1957) described in domestic animals that the most superficial layer of the corium consisted of condensed felt work of delicate reticular fibers with an admixture of fibroblast elements. The remainder of the corium consisted of collagenous fibers varying in thickness follow a wavy course and interweave in three dimensions. Some elastic fibers found in between the collagenous bundles.

Lovell and Getty (1957) reported that the dermis of dog composed of reticular, collagenous and elastic fibers, fibroblasts, blood vessels and nerve trunks. The dermis consisted of a mixture of reticular, collagenous and elastic fibers together with fibroblast and nerves. The blood vessels and nerves are largest in the deeper layers of the dermis and sub cutis contained hair follicles, excretory duct of the apocrine gland. Sebaceous gland and arrector pili muscles are present in the dermal layer. The connective tissue of the dermis is finer and directly under the epidermis than in the deeper layers.

Goldsberry and Calhoun (1959) described that the dermis of the Hereford and Aberdeen Angus cattle; the dermis is divided into two layers, the stratum papillaris and stratum reticularis. Both layers of the dermis are present, but were not clearly defined. The papillary layer consisted of loose network of interlacing elastic fibers and small collagenous bundle extending from the base of epidermis to termination of the hair follicle. There were clustering and strands of cell, which were invariably found between

the connective tissue fibers. The dermal papillae varied considerably between areas of thick or thin epidermis. The stratum reticularis consisted of large coarse, interwoven bundles of collagenous fibers generally parallel to the surface. The elastic fibers are present only when associated with supporting areolar tissue, blood vessels and nerve trunks.

Copenhaver (1971) reported that the dermis varied from 0.2 to 0.4 mm in thickness and composed of dense, irregularly arranged connective tissue. It contained all the three types of connective tissue fibers, fibroblasts and histiocytes. Two layers could be distinguished, although they blended without distinct demarcation. The deeper layer is relatively thick and is known as the reticular layer. The superficial layer is thinner and was named the sub epithelial or papillary layer. The reticular layer is characterized by loose collagenous fibers and fiber bundles which often united to form secondary bundles of considerable thickness. The elastic fibers formed complex elastic nets permeating the entire corium. The elastic fibers formed basketlike capsular condensation around the hair bulbs, sweat and sebaceous glands. The papillary or sub epithelial layer is similar in structure to the reticular layer, but the fibers are finer and more closely arranged.

Strickland and Calhoun (1963) observed that the dermis in cat skin composed of collagen, elastic and reticular fibers, nerve fibers, those described by Winkelman (1957). Stratum reticularis was dense, irregularly arranged collagenous fibers approximately 3 times thicker than that of the stratum papillaris, these fiber encircled hair follicles and disappeared at the junction with sub cutis. The elastic fibers increased in amount, extended in all direction and encircled the hair follicles. They appear to adhere to

collagenous fibers in the reticular layer and increasingly abundant near the attachment of the errector pili muscle. The dermis was characterized by definite division between the stratum papillaris and stratum reticularis.

Marcarian and Calhoun (1965) stated that the dermis of the swine contained a prominent panniculus adiposus and are noticed beneath the reticular layer. The elastic fibers ramified throughout the dermis were observed in the trabeculae of the tactile hairs and in the bulbs of follicles; the heaviest concentration of these fibers is in the snout and prepuce. The collagenous bundles of the papillary layer are delicate and thin in contrast to those of the reticular layer.

Sar and Calhoun (1966) stated that in the dermis of goats skin there is no sharp distinction between papillary and reticular layers in most of the body regions, as these layers blended with each other without demarcation. The collagen fibers of the superficial layer of the dermis are fine, loosely arranged, and irregularly distributed. These fibers are thick and densely arranged in the reticular layer. The elastic fibers are abundant in young goats. They are most numerous in the neck and thoracic region, but are scarce in interdigital skin and junctions of hoof and horn with the skin. The superficial layer of dermis is thicker in horse and cattle skin than in that of carnivores where in it encompasses the hair follicles and adjacent sweat glands. The deep layer of the dermis was much more coarse and dense than the superficial layer, and contained large bundles of collagen fibers aligned parallel to the surface (Dellmann and Brown, 1981; Bacha and Bacha1990).

In the dog Evans and Christensen (1967) observed that the individual follicle and hair bulb of the cover-hair or guard-hair is larger and penetrated more deeply in to the subcutaneous tissue than those of the satellite or subsidiary hairs. The canine hair follicle could be defined as apilosebaceous-arrector muscle complex. The sebaceous glands of the individual hair follicles bunch together in clusters and sometimes fuse.

Talukdar *et al.* (1972) reported that the dermis of the horse consisted of two well demarcated layers the superficial or papillary layer contained fine, loosely arranged collagenous fibers bundles. An extensive network of elastic and reticular fibers is seen throughout the dermis, but is more prominent in the superficial layer. The dermis of the lumbar, sacral and gluteal regions are modified by the presence of a third layer of collagenous fibers interwoven with fine elastic and reticular fibers.

Dellmann and Brown (1981) reported that the dermis is made up of collagen, elastic and reticular connective tissue fibers. Hair follicles, sweat and sebaceous gland, blood and lymph vessels and nerves are embedded at various levels throughout the dermis. The dermis is divided into superficial or papillary layer and deep or reticular layer. It is composed of a network of fine collagen, reticular and elastic fibers, fibroblasts, macrophages plasma cells and mast cells. The superficial layer is wider in horse and cattle than that of carnivores and composed of hair follicles and sweat glands. The deep layer is coarse dense contained bundles of collagen fibers. Smooth muscle fibers may be present in the scrotum, teat and penis. The skeletal muscle fibers of the cutaneous muscle (panniculus carnosus) penetrated the dermis and formed the voluntary muscle of the skin. They also observed that the errector pilli muscle contract during cold and caused hair to

become bristle, by which airspaces are created in the medulla, thus serving as an insulator.

Bloom and Fawcett (1986) described that the dermis merged into subcutaneous layer without a sharp boundary. The outer surface of the dermis in contact with the epidermis is usually uneven and is elevated into papillaris that projects into concavities between the ridges on the deep surface of the epidermis. The superficial or papillary layer and the deeper main portion of the dermis or reticular layer without a clear boundary between them. The reticular layer consisted of rather dense connective tissue, its collagenous fibers form a felt work with bundles running in various direction. The papillary layer and its papillae consist of loose connective tissue with much thinner collagenous bundles. The elastic fibers of dermis formed abundant, thick network between the collagenous bundles and are condensed about the hair follicles and the sebaceous and sweat glands.

2.1.3 Hair follicles

Trautmann and Fiebieger (1957) described that the hair follicle; the hair follicle is formed by corium and epidermis. The former furnishes the dermal part of the follicle, while the latter epithelial root sheaths. The connective tissue in the follicle consisted of an outer and inner layer and the glossy membrane, the outer layer is composed of longitudinal bundles of collagenous fibers and delicate elastic fibers. The inner layer is made up of circular collagenous fibers and reached to the net work around the follicle.

Lovell and Getty (1957) described that the hair follicles in the canines developed from a single follicle at birth to a compound follicle at maturity and the compound follicles are arranged in groups of two, three and four with three being most common.

Strickland and Calhoun (1963) Studied hair follicle of dog and observed to consists of clusters of 3 to 5 groups around a central guard hair, follicular folds, corrugation of the inner root sheath, characterized the guard hair.

Marcarian and Calhoun (1966) stated that swine skin consisted of several hair follicles, in which two hairs projected towards the greater volume of the follicle. Follicular folds evident in many of the hair follicle studied formed 1 to 23 corrugation in the inner epithelial root sheath. The hair is arranged in groups of three, where the hair is dense; however single hairs and groups of 2 and 4 were frequently seen. The central hair of triad is usually larger than 2 adjacent hairs.

Sar and Calhoun (1966) studied in goats there are both primary and secondary hair follicles in swine's. Accessory structure, the sweat gland, sebaceous gland and the arrector pili muscle were associated with each primary follicle. Except sebaceous glands accessory structures are not observed in the secondary follicles. The primary follicles are arranged in groups of 3 as reported by (Margolena, 1959), 3 to 6 secondary hair follicle are associated with the trio of primary follicles. A group of secondary hairs are originated from a common follicle and thus formed a compound follicle. Errector Pilli muscle were obliquely attached to the lower third of the primary hair follicles and extended around the sebaceous gland to the papillary layer of the dermis.

Talukdar *et al.* (1972) reported that hair and hair follicle of horse occurred singly and the large rectangular cells of the medulla are characteristic. The larger hair follicles are containing follicular folds below the opening of the sebaceous gland. The structure of the hair follicle conformed to the typical mammalian pattern. The tactile hair follicles are supplied by skeletal muscle and lacked errector Pilli muscle typical of other follicles. The arrector pili muscle extended from the hair follicles to the area just below the epidermis.

Dellmann and Brown (1981) stated that hair follicle is formed by the growth of the ectoderm into underlying mesoderm of the embryo. The follicles are embedded in the dermis. They classified hair follicles into several types. A primary follicle is one with large diameter, is rooted deep in the dermis and usually associated with sebaceous, sweat gland and arrector pili muscle. But a secondary follicle is smaller diameter than the primary follicle; it may have a sebaceous gland and lack of sweat gland and arrector pili muscle. Those follicles with only one hair emerging to the surface are called single or simple follicle, while compound follicle have several hairs emerging from a single opening.

They further described that many differences exist in the arrangement of the hair follicles among the domestic animals. Horse and cattle have single hair follicle distributed evenly, pigs have single follicle grouped in clusters of two to four follicles with three being most common. The compound follicle of dog consisted of single, long primary hair follicle and a group of smaller secondary hair follicles. In cat the arrangement of hair follicle consists of a single, large, primary hair follicle surrounded by

cluster of two to five compound follicles. In sheep usually single follicle are present, where as densely covered wool growing region has large number of compound follicles.

Goldsberry and Calhoun (1986) studied the hair in the Hereford and Aberdeen Angus cattle. They revealed a series of distinct folds invariably present in the wall of the hair follicle. There are 15 to 25 folds which began at the opening of the sebaceous ducts and encircled the middle third of the hair. Hair follicles rarely contained more than one hair, when two occurred, one usually showed signs of degeneration.

Bhayani *et al.* (1995) reported that the skin of lion is similar to that of dog with compound hair follicles. Depth of hair follicles was more in the lower abdomen and less in the thorax region in adult lion. Hair follicles are situated deep in the reticular layer.

Baddi (2009) reported that the skin of lion showed hair follicles densely populated in the dermis of skin. They are made up of bundles of compound hair follicles. Within each bundle there are 1 or 2 large primary hairs surrounded by clusters of compound follicles. Each compound follicle presented 1 or 2 small primary hairs with a few secondary hairs. In the sloth bear skin showed hair follicle bundles sparsely distributed and are elliptical in out line. Each hair follicle bundles consisted of 3-4 primary hair follicles only. There are no secondary hair follicles associated with it. Within the hair bundle clusters of primary hairs are found. In the dermis the dense irregular connective tissue comprised of collagen fibers with sebaceous glands sparsely distributed around the hair follicles.

2.1.4 Sebaceous glands

Epling (1953) described the histological structure of the sebaceous glands of the dog and their compound arrangement and association with the compound follicle. Hansen et al (1954) state that, at the level of the stratum reticularis, sebaceous glands are branched on the sides and lower slope of the follicle at the level of stratum reticularis of dermis.

Sisson and Grossman (1953) stated that sebaceous glands are the best developed in short and rough haired breeds, and that they were largest and most numerous at the lips, anus, dorsal surface of the trunk and the sterna region;

Trautmann and Fiebieger (1957) described that the sebaceous glands that they arise in fetus by proliferation of the outer hair root sheath. They make up of the superficial layer of glands and occur in the corium. They usually open into the neck of a hair follicle. They are simple alveolar holocrine glands and appear as evaginations of the follicle, the glassy membrane of which is continuous with the basement membrane of the gland. They are branched in the horse and dog. Their size and number depended on the species, size of hairs, and the larger the sebaceous glands.

The horse and the dog have the largest glands, while those of the pig were rudimentary. In ungulates two to six glands empty into one hair follicle. In carnivores several hair follicles unite into a group with one common opening, with this follicle complex of about the same number of sebaceous glands. These glands were absent from foot pads, hoofs, claws, horns, the planum nasolabiale and the teats of the ox, and the

planum nasale of sheep, goats and carnivores are devoid of this gland (Trautmann and Fiebieger, 1957).

Lovell and Getty (1957) studied skin glands in the dog that the hair follicles and apocrine sweat glands extended into the subcutaneous adipose tissue. Above this layer the dermis consists of a mixture of reticular, collagenous and elastic fibers together with fibroblast, blood vessels and nerves.

Strickland and Calhoun (1963) studied histological structures of sebaceous glands in cat; the glands are showed a characteristic simple alveolar structure. Differences in size of these glands are varying in certain areas. Two to three of these empty into the upper portion of the hair follicle around which they were clustered. No sebaceous glands are found in the non hairy regions.

Marcarian and Calhoun (1966) stated that the sebaceous glands in adult swine are branched alveolar, and opened, by very short ducts, into the neck of the hair follicles. These glands are composed of a secretary portion and an excretory duct.

Sar and Calhoun (1966) studied in goats that the sebaceous glands were simple or branched alveolar glands distributed throughout all body areas. Large, branched alveolar glands are found at the junctions of the hoof with the skin, base of the ear, base of the horn, and in the perianal region. The horn glands at the base of the horn, described by (Trautmann and Fiebieger, 1957)

Talukdar et al (1972) reported that the sebaceous glands in horse are very large and occurred in all regions there were two glands with each follicle, but multilobulated

glands with eight or more lobules were observed in special areas. Large sebaceous glands are seen in the lips, upper eyelids, submandibular region, udder, teat, vulva, and prepuce. Small glands are encountered in the flank and paralumbar fossa.

Dellmann and Brown (1981) stated that sebaceous glands may be simple, branched or compound alveolar glands that release their secretary product, sebum, by the holocrine mode. Many areas of the body of certain species have especially well-developed accumulations of sebaceous glands, some associated with modified glands. These sites include the infraorbital, inguinal and interdigital regions of sheep, the base of the horn of goats, anal sacs of cats and the prepuce and circumanal regions.

Goldsberry and Calhoun (1959) studied the sebaceous gland structure in the Hereford and Aberdeen Angus cattle revealed that similar to that of other species. The size was inversely proportional to the hair density. They are more highly developed in the perianal region and at the horn, hoof and muzzle regions but were absent in the hair less regions. While the sebaceous glands might entirely surround the hair follicle, they are most frequently located on one side.

2.1.5 Sweat glands

Trautmann and Fiebiger (1957) described in man and other primates that the merocrine tubular glands (sweat glands) are distributed over the entire skin surface, while the apocrine glands are restricted to a few areas, such as the axilla. In domestic animals, on the other hand, the apocrine glands make up the great majority of tubular skin glands. In the sheep, pig, cat, and horse the secretary tubule is wound up, whereas in the ox, goat, and dog it is serpentine. The poorly developed glands of the cat are present in only few

body areas (oral region, anus, lower jaw, and foot pads). The tubular glands of the dog vary greatly in diameter. Although they are distributed over the entire body, they do not function visibly under normal conditions.

Goldsberry and Calhoun (1959) described that the sweat glands of Hereford and Aberdeen Angus cattle into three morphological groups; secular noncoiled, sacular coiled and compound tubular. Most of the glands are characterized by the sacular noncoiled type which had a large lumen, 300 to 400µ in diameter. The lumen often contained granular amorphous material. The sacular coiled type is located in the hock and fetlock regions. The compound tubular glands are found in the nasolabial region.

Strickland and Calhoun (1963) described the sweat glands in cat that the sweat glands are found in all regions except in the planum nasale. Both small and large sacular sweat glands occurred in the cat. These glands are made up of low cuboidal epithelium, reticular tissue and thin layer of smooth muscle. Large the coiled apocrine sweat glands occurred in the upper and lower lips, eye lids, anal sac and prepuce. Coiled merocrine sweat glands situated in the subcutaneous fatty tissue of the metacarpal pads.

Marcarian and Calhoun (1966) studied sweat glands in swine as coiled, tubular, apocrine glands. The latter were found in all areas with the exception of the snout, where tubular merocrine glands were observed.

Sar and Calhoun (1966) described the sweat glands in goat that the glands with exception of the compound tubular sweat glands in the planum nasale, coiled tubular apocrine glands varied in different body regions. Large coiled glands are found mainly in the skin of teats, scrotum, perianum and eyelids. Small coiled apocrine glands

characteristic of other body regions are located deep in the corium below the sebaceous glands and sometimes are clustered around the base of the hair follicles.

Talukdar *et al.* (1972) reported in horse that the sweat glands are apocrine in type, numerous and well developed on the middle of the back, on the limbs and on the upper lips. The lower lip within 1 cm of the mucocutaneous junction and margins of the hoof and ergot lacked glands.

Nickel and Schumer (1981) stated that the sweat glands of sheep are twisted but their ends are not coiled. The apocrine sweat glands are loosely coiled and distributed over the entire skin.

Dellmann and Brown (1981) studied sweat glands based on their morphologic and functional characteristics, sweat (sudoferous) glands are separated into two types; apocrine and merocrine (eccrine).The apocrine is the most extensively developed in the domestic animals. They are simple sacular or tubular glands with a coiled secretary portion and a straight duct. In horse these glands are quite active and produce more visible sweat during exercise and high temperature, in other species the secretion is scanty. In dog and cat the glands were tortuous, in ruminants the lumen is dilated and giving appearance of large saccules. The merocrine glands are also coiled, simple tubular glands found mainly in the pads of the dog and cat, the frog of ungulates, the carpus of pigs and the nasolabial region of ruminants and pigs.

Spectroscopy has emerged as one of the major tools for biomedical, forensic applications and has made significant progress in the field of analytical techniques. Research has been carried out on a number of natural tissues using spectroscopic

techniques, including FTIR spectroscopy. These vibrational spectroscopic techniques are relatively simple, reproducible, nondestructive to the tissue, and only small amounts of material (micrograms to nanograms) with a minimum sample preparation are required. In addition, these techniques also provide molecular-level information allowing investigation of functional groups, bonding types, and molecular conformations. Spectral bands in vibrational spectra are molecule specific and provide direct information about the biochemical composition. These bands are relatively narrow, easy to resolve, and sensitive to molecular structure, conformation, and environment (Movasaghi.*et al*., 2007)

A considerably wide field of medical and biological studies has been covered by spectroscopic methods in recent years. It is strongly believed that in studies related to spectroscopic techniques, both the reliable experimental procedure and characterization of spectral peak positions and their assignment along with accurate peak detection and definition are of crucial importance. Although a number of scientists have used different techniques, it seems that there is a marked similarity in their spectral interpretation of comparable areas in their collected spectra (Movasaghi. *et al.,* 2007).

2.2.1 Electromagnetic Radiation

The visible part of the electromagnetic spectrum is, by definition, radiation visible to the human eye. Other detection systems reveal radiation beyond the visible regions of the spectrum and these are classified as radio wave, microwave, infrared, ultraviolet, X-ray and γ-ray. The electromagnetic spectrum and the varied interactions between these radiations and many forms of matter can be considered in terms of either classical or quantum theories.

The nature of the various radiations has been interpreted by Maxwell's classical theory of electro- and magneto-dynamics – hence, the term electromagnetic radiation. According to this theory, radiation is considered as two mutually perpendicular electric and magnetic fields, oscillating in single planes at right angles to each other. These fields are in phase and are being propagated as a sine wave. The magnitudes of the electric and magnetic vectors are represented by *E* and *B*, respectively (Stuart, 2004).

A significant discovery made about electromagnetic radiation was that the velocity of propagation in a vacuum was constant for all regions of the spectrum. This is known as the velocity of light, *c*, and has the value 2.997 925 × 108 m s^{-1}. If one complete wave travelling a fixed distance each cycle is visualized, it may be observed that the velocity of this wave is the product of the *w*avelength, λ (the distance between adjacent peaks), and the frequency, ν (the number of cycles per second). Therefore: The presentation of spectral regions may be in terms of wavelength as meters or sub-multiples of a meter (Stuart, 2004).

2.2.2 Infrared Absorptions

For a molecule to show infrared absorptions it must possess a specific feature, i.e. an electric dipole moment of the molecule must change during the vibration. This is the selection rule for infrared spectroscopy.

2.2.3 Normal Modes of Vibration

The interactions of infrared radiation with matter may be understood in terms of changes in molecular dipoles associated with vibrations and rotations. In order to begin

with a basic model, a molecule can be looked upon as a system of masses joined by bonds with spring-like properties. Taking first the simple case of diatomic molecules, such molecules have three degrees of translational freedom and two degrees of rotational freedom. The atoms in the molecules can also move relative to one other, that is, bond lengths can vary or one atom can move out of its present plane. This is a description of stretching and bending movements that are collectively referred to as vibrations. For a diatomic molecule, only one vibration that corresponds to the stretching and compression of the bond is possible. This accounts for one degree of vibrational freedom (Stuart, 2004).

Vibrations can involve either a change in bond length (stretching) or bond angle (bending). Some bonds can stretch in-phase (symmetrical stretching) or out-of-phase (asymmetric stretching). If a molecule has different terminal atoms such as HCN, ClCN or ONCl, then the two stretching modes are no longer symmetric and asymmetric vibrations of similar bonds, but will have varying proportions of the stretching motion of each group. In other words, the amount of coupling will vary.

Bending vibrations also contribute to infrared spectra. It is best to consider the molecule being cut by a plane through the hydrogen atoms and the carbon atom. The hydrogen's can move in the same direction or in opposite directions in this plane, here the plane of the page. For more complex molecules, the analysis becomes simpler since hydrogen atoms may be considered in isolation because they are usually attached to more massive, and therefore, more rigid parts of the molecule. This results in in-plane and out-of-plane bending vibrations (Stuart, 2004).

2.2.4 FTIR SPECTROSCOPY

FTIR spectroscopy is a vibrational spectroscopic technique that can be used to optically probe the molecular changes associated with biological tissues. The method is employed to find more conservative ways of analysis to measure characteristics within molicules that would allow accurate and precise assignment of the functional groups, bonding types, and molecular conformations. Spectral bands in vibrational spectra are molecule specific and provide direct information about the biochemical composition.

FTIR peaks are relatively narrow and in many cases can be associated with the vibration of a particular chemical bond (or a single functional group) in the molecule. It is based on interference of radiation between two beams to yield an interferogram. The latter is a signal produced as a function of the change of path length between the two beams. The two domains of distance and frequency are interconvertible by the mathematical method of Fourier-transformation. The radiation emerging from the source is passed through an interferometer to the sample before reaching a detector. Upon amplification of the signal, in which high-frequency contributions have been eliminated by a filter, the data are converted to digital form by an analog-to-digital converter and transferred to the computer for Fourier-transformation (Stuart, 2004).

2.2.5 Spectra

Early infrared instruments recorded percentage transmittance over a linear wavelength range. It is now unusual to use wavelength for routine samples and the wave number scale is commonly used. The output from the instrument is referred to as a spectrum. Most commercial instruments present a spectrum with the wave number

decreasing from left to right. The infrared spectrum can be divided into three main regions: the far infrared (<400 cm^{-1}), the mid-infrared (4000–400 cm^{-1}) and the near-infrared (13000–4000 cm^{-1}). Many infrared applications employ the mid-infrared region, but the near- and far-infrared regions also provide important information about certain materials. Generally, there are less infrared bands in the 4000–1800 cm^{-1} region with many bands between 1800 and 400 cm^{-1}. Sometimes, the scale is changed so that the region between 4000 and 1800 cm^{-1} is contracted and the region between 1800 and 400 cm^{-1} is expanded to emphasize features of interest. The ordinate scale may be presented in % transmittance with 100% at the top of the spectrum. It is commonplace to have a choice of absorbance or transmittance as a measure of band intensity, the relationship between these two quantities transmittance spectra. It almost comes down to personal preference which of the two modes to use, but the transmittance is traditionally used for spectral interpretation, while absorbance is used for quantitative work (Stuart, 2004).

2.2.6 Attenuated Total Reflectance Spectroscopy

Attenuated total reflectance (ATR) spectroscopy utilizes the phenomenon of total internal reflection .A beam of radiation entering a crystal will undergo total internal reflection when the angle of incidence at the interface between the sample and crystal is greater than the critical angle, where the latter is a function of the refractive indices of the two surfaces. The beam penetrates a fraction of a wavelength beyond the reflecting surface and when a material that selectively absorbs radiation is in close contact with the reflecting surface, the beam loses energy at the wavelength where the material absorbs. The resultant attenuated radiation is measured and plotted as a function of wavelength by

the spectrometer and gives rise to the absorption spectral characteristics of the sample (Stuart, 2004).

2.2.7 Spectral Analysis

Once an infrared spectrum has been recorded, the next stage of this experimental technique is interpretation. Fortunately, spectrum interpretation is simplified by the fact that the bands that appear can usually be assigned to particular parts of a molecule, producing what are known as group frequencies. The characteristic group frequencies observed in the mid-infrared region is discussed.

2.2.8 Mid-Infrared Region

The mid-infrared spectrum (4000–400 cm^{-1}) can be approximately divided into four regions and the nature of a group frequency may generally be determined by the region in which it is located. The regions are generalized as follows: the X–H stretching region (4000–2500 cm^{-1}), the triple-bond region (2500–2000 cm^{-1}), the double-bond region (2000–1500 cm^{-1}) and the fingerprint region (1500–600 cm^{-1}). The fundamental vibrations in the 4000–2500 cm^{-1} region are generally due to O–H, C–H and N–H stretching. O–H stretching produces a broad band that occurs in the range 3700–3600 cm^{-1}. By comparison, N–H stretching is usually observed between 3400 and 3300 cm^{-1}.

This absorption is generally much sharper than O–H stretching and may, therefore, be differentiated. C–H stretching bands from aliphatic compounds occur in the range 3000–2850 cm^{-1}. If the C–H bond is adjacent to a double bond or aromatic ring, the C–H stretching wave number increases and absorbs between 3100 and 3000 cm^{-1}.

Triple-bond stretching absorptions fall in the 2500–2000 cm^{-1} regions because of the high force constants of the bonds. C≡C bonds absorb between 2300 and 2050 cm^{-1}, while the nitrile group (C≡N) occurs between 2300 and 2200 cm^{-1}. These groups may be distinguished since C≡C stretching is normally very weak, while C≡N stretching is of medium intensity. These are the most common absorptions in this region, but you may come across some X–H stretching absorptions (Stuart, 2004).

These absorptions usually occur near 2400 and 2200 cm^{-1}, respectively. The principal bands in the 2000–1500 cm^{-1} region are due to C=C and C=O stretching. Carbonyl stretching is one of the easiest absorptions to recognize in an infrared spectrum. It is usually the most intense band in the spectrum and depending on the type of C=O bond, occurs in the 1830–1650 cm^{-1} region. Note also that metal carbonyls may absorb above 2000 cm^{-1}. C=C stretching is much weaker and occurs at around 1650 cm^{-1}, but this band is often absent for symmetry or dipole moment reasons. C=N stretching also occurs in this region and is usually stronger (Stuart, 2004).

It has been assumed so far that each band in an infrared spectrum can be assigned to a particular deformation of the molecule, the movement of a group of atoms, or the bending or stretching of a particular bond. This is possible for many bands, particularly stretching vibrations of multiple bonds that are ‘well behaved’. However, many vibrations are not so well behaved and may vary by hundreds of wave numbers, even for similar molecules. This applies to most bending and skeletal vibrations, which absorb in the 1500–650 cm^{-1} regions, for which small steric or electronic effects in the molecule lead to large shifts. A spectrum of a molecule may have a hundred or more absorption

bands present, but there is no need to assign the vast majority. The spectrum can be regarded as a ‘fingerprint’ of the molecule and so this region is referred to as the fingerprint region (Stuart, 2004).

2.2.9 Derivatives

Spectra may also be differentiated. A single absorption peak have first and second derivative. The benefits of derivative techniques are twofold. Resolution is enhanced in the first derivative since changes in the gradient are examined. The second derivative gives a negative peak for each band and shoulder in the absorption spectrum

2.3. Biological Applications

Biological systems, including lipids, proteins, peptides, biomembranes, nucleic acids, animal tissues, microbial cells, plants and clinical samples, have all been successfully studied by using infrared spectroscopy. This technique has been employed for a number of decades for the characterization of isolated biological molecules, particularly proteins and lipids. However, the last decade has seen a rapid rise in the number of studies of more complex systems, such as diseased tissues. Microscopic techniques, combined with other sophisticated analytical methods, allow for complex samples of micron size to be investigated

2.3.1. Chemometric analysis of FTIR spectra

The improvement in technology associated with spectroscopy has led to the expansion of quantitative and qualitative infrared spectroscopy. The application of statistical methods to the analysis of experimental data is known as Chemo metric

analysis (stuart.2004). The most commonly used analytical methods in infrared spectroscopy are classical least square (CLS), inverse least square (ILS), partial least square (PLS) and principal component regression (PCR).

There are two major types of pattern recognition methods. The methods like principle component analysis (PCA) and cluster analysis do not use information related to predefined classes of objects are classified under unsupervised pattern recognition method. On the other hand method like linear discriminant analysis requires a priori information. On the set of samples that is used for classification purpose and it is placed in the category of supervised pattern recognition method (Ballabio and Todeschini, 2009).

2.3.2. Keratin biochemistry

Keratins are structural proteins found in hairs, skin, nails etc. the three polypeptides of keratin form alpha helical structure and hold together by disulfide bonds. The toughness and strength of keratins are directly related to the number of disulfide bonds. Thus, the harder keratins possess more disulfide bonds. The mechanical strength of the hair is attributed to disulfide bonds (Lehninger, 1982)

Elliott (1956) reported that for the folded form the amide I band occurs at 1655cm-1 and the amide II band occurs at 1540cm-1, whereas for the extended form the corresponding bands are at 1630 and 1520 cm-1 respectively. The possibility that differences between folded and extended polypeptide chain conformations could be detected by infrared spectroscopy was first shown by Elliott & Ambrose (1950). Subsequent studies on synthetic polypeptides (Ambrose & Elliott, 1951a*;* Elliott, 1953)

and on fibrous proteins (Ambrose & Elliott, 1951b*)* and Elliott (1956) are established this fact.

Alexander *et al.,* (1968) and Marshal *et al.,* (1991) have reported an intrinsic difference in vertebrate keratins was that mammals including elephants and giraffe produce only alpha keratins while reptiles and birds produce both alpha and beta keratins.

Lehninger (1982) described the keratins including hairs into a broad class of fibrous protein, which has been divided into two major classes' alpha keratins and beta keratins.

Solomon *et al.,* (1986) described that alpha keratins are characterized by a helical structure whereas beta keratins have a beta pleated structure, either form of keratinization produces extremely hard keratin (sea turtle shell scutes, horn sheath, hoof ungus,claw angus) which provide external protection to mammals and reptiles.

Griebenow *et al.* (1992) reported that the spectra of wool fiber which displayed the characteristic absorption bands of proteins at $1630cm^{-1}$ (amide I) $1515cm^{-1}$ (amide II) and $1230cm^{-1}$ (amide III). Amide I primarily a C=O stretching vibration while amide II and amide III are heavily mixed vibrational modes. In particular, amide III results from N-H bending and C-N stretching vibrations. Amide III is a very complex range resulting from in phase combination of C-N stretching and N-H in plane bending with some contribution from C-C stretching and C=O bending vibrations. Amide I, II and III are very important bands because from their position and shape information about protein structure and conformation can be derived. In fact hydrogen bonding steric situation and

environment properties is known to influence the frequencies of the amide vibrations. However, amide II and III are vibrational modes and correlation between bands shape and the structure of proteins may become rather questionable. For this, it has been decided to study the shifts and shape of amide I.

Gallagher (1992) studied FTIR spectroscopy which provides information about the secondary structure content of proteins, unlike X-ray crystallography and NMR spectroscopy which provide information about the tertiary structure. FTIR spectroscopy works by shining infrared radiation on a sample and seeing which wavelengths of radiation in the infrared region of the spectrum are absorbed by the sample. Each compound has a characteristic set of absorption bands in its infrared spectrum. Characteristic bands found in the infrared spectra of proteins and polypeptides include the Amide I and Amide II. These arise from the amide bonds that link the amino acids.

The absorption associated with the Amide I band leads to stretching vibrations of the C=O bond of the amide, absorption associated with the Amide II band leads primarily to bending vibrations of the N—H bond .Because both the C=O and the N—H bonds are involved in the hydrogen bonding that takes place between the different elements of secondary structure, the locations of both the Amide I and Amide II bands are sensitive to the secondary structure content of a protein. Studies with proteins of known structure have been used to correlate systematically the shape of the Amide I band to secondary structure content. The Amide II band, though sensitive to secondary structure content, is not as good a predictor for quantitating the secondary structure of proteins. One difficulty with analyzing the Amide I band for secondary structure is that the shifts in the Amide I

band are small compared to the intrinsic width of the band. Instead of a series of nicely resolved peaks for each type of secondary structure, one broad lumpy peak is observed several numerical methods are used to increase the apparent resolution of the Amide I band so that estimates can be made of the secondary structure content (Gallagher, 1992)

Rintoul *et al*., (1998) and Lyman *et al*., (2001) used HATR-FTIR in examining hard biological tissues, which stands out for its robustness, ease of sample preparation, simplicity of operation and the ability to make structural elucidations. The resolving power of FT–IR has been applied in such diverse fields as forensic fiber identification (Kirkbride and Tungol 1999) and bacterial species identification (Timmins *et al* 1998). Discriminant analysis (also known as linear discriminant analysis or canonical variates analysis) of vibrational spectra (Raman or infrared) has been successfully used to extend the limitation inherent in vibrational data. Examples include confirmation of edible oils and fats (Beaten and Aparicio, 2000), bacterial taxonomy (Amiel *et al*. 2001), sub-typing of nylon polymers (Enlow *et al*. 2005), the forensic characterization of printer toners (Egan *et al*. 2003), geographical sourcing of medicinal plants (Dharmaraj *et al*. 2006), forensic identification of fingernails versus toenails (Widjaja and Seah, 2006) and the forensic identification of fiber blends (Espinoza *et al*. 2006).

Alibardi (2000a, 2003b, 2003c) has revived the selective advantage of inheriting alpha keratins verses beta keratins.

Pielesz *et al*. (2000) studied the identification of structural changes in the keratin of wool fibre with an azo dye using Raman and Fourier transform Infrared spectroscopy methods. They found Changes were observed in the region of Amides I and II and the

fingerprint region. For FT-Raman Spectroscopy, changes were observed in the region of S–S bonds, tyrosine and methionine regions and the fingerprint region (1100–900 cm^{-1}). The percentage of share of particular conformational forms of keratin (a-helix, disordered, b-sheet) was observed. the amide I mode was resolved into three Gauss-shaped bands corresponding to a-helix (1654 cm^{-1}), b-sheet (1680 cm^{-1}) and undefined (1667 cm^{-1}) structure .The phenylalanine peak at 1003 cm^{-1} was chosen as a reference band. A frequently compared FT-IR measured region is the 1650–1550 cm^{-1} range, i.e. the region of Amide I and Amide II vibrations.

The Amide I mode is predominantly the peptide carbonyl stretching vibration of the CONH unit together with an out-of-phase CN stretching component and a small contribution from the CCN deformation. The Amide II mode is predominantly NH in-plane bending plus CN stretching contribution, but it always has a significant contribution from CC stretching and smaller contributions from the CO in-plane bend and NC stretch. For the untreated sample a clear band of the a-helical structure, a disordered structure, is visible, for vibrations of both Amide I (1652 cm^{-1}) and Amide II (1541 cm^{-1}).

Panayiotou (2004) described the spectral analysis of cat fur, parrot feather, human hair, horse hair, cow hair, sheep wool and dog hair by using FTIR spectroscopy followed by chemometrics analysis. She stated that amide A and amide B were found in the 3300-3050 cm^{-1}. Spectral features in these regions are assigned to the stretching modes of the C-H lipid alkyl chains. The methyl (CH_3) assignment and symmetric modes are observed at 2955cm^{-1} and 2933cm^{-1} respectively and methylene (CH_2) asymmetric and symmetric modes at 2875 cm^{-1} and 2855cm^{-1}.

The wave number region between 1700-1500cm^{-1} contained the most intensive feature in the IR spectra arising from the –CONH grouping, predominantly from protein structure such as amide I and amide II band at 1657cm^{-1} and 1537cm^{-1} respectively. The region in between 1200-400cm^{-1} contains one of the most important bands, which was attributed to the cystic acid vibration at 1040cm^{-1}.

Movasaghi *et al.*, (2007) studied the biochemical compounds (lipids, proteins, nucleic acids) and the chemical structure of these compounds can be evaluated using peak frequencies at 2956 cm^{-1} (asymmetric stretching vibration of CH_3 of acyl chains), 2922 cm^{-1} (asymmetric stretching vibration of CH_2 of acyl chains), 2874 cm^{-1} (symmetric stretching vibration of CH_3 of acyl chains), 2852 cm^{-1} (Symmetric stretching vibration of CH_2 of acyl chains), and 1600–1800 cm^{-1} (C=O stretching).

The specifications of protein contents of biological samples can also be understood from 1717 cm^{-1} (amide I, arising from C=O stretching vibration), 1500–600 cm^{-1} (amide II, N-H bending vibration coupled to C-N stretching), and 1220–1350 cm^{-1} (amide III, C-N stretching and N-H in plane bending, often with significant contributions from CH_2 wagging vibrations). The peaks related to nucleic acids are as follows: 1717 cm^{-1}(C=O stretching vibration of purine base), 1666 cm-1 (C=O stretching vibration of pyrimidinic base), and 1220–1240 cm21 (asymmetric $PO_2^{\ 2}$ stretching), 1117 cm^{-1} (C-O stretching vibration of C-OH group of ribose), 1040–100 cm^{-1}

Jalkanen *et al.*, (2005) used vibrational spectroscopy to study protein and DNA structure, hydration, and binding of bimolecular, as a combined theoretical and experimental approach. The system studied systematically was the amino acids, peptides,

and a variety of small molecules. The goal was to interpret the experimentally measured vibrational spectra for these molecules to the greatest extent possible and to understand the structure, function, and electronic properties of these molecules in their various environments. It was also believed that the application of different spectroscopic methods to biophysical and environmental assays is expanding, and therefore a true understanding of the phenomenon from a rigorous theoretical basis is required.

Fabian (**2000)** and **Bandekar (1992)** have described the infrared spectra of proteins exhibit absorption bands associated with their characteristic amide group. In-plane modes are due to C=O stretching, C–N stretching, N–H stretching and O–C–N bending, while an out-of-plane mode is due to C–N torsion. The characteristic bands of the amide groups of protein Chains are similar to the absorption bands exhibited by secondary amides in general, and are labeled as amide bands. There are nine such bands, called amide A, amide B and amides I–VII, in order of decreasing wave number.

The amide II band represents mainly (60%) N–H bending, with some C–N stretching (40%) and it is possible to split the amide II band into components depending on the secondary structure of the protein. The position of the amide II band is sensitive to deuteration, shifting from around 1550 cm^{-1} to a wave number of 1450 cm^{-1}. The amide II band of the deuterated protein overlaps with the H–O–D bending vibration, so making it difficult to obtain information about the conformation of this band. However, the remainder of the amide II band at 1550 cm^{-1} may provide information about the accessibility of solvent to the polypeptide backbone (Fabian, 2000; Bandekar**,** 1992)

Hydrophobic environments or tightly ordered structures, such as α-helices or β-sheets, reduce the chance of exchange of the amide N–H proton. The most useful infrared band for the analysis of the secondary structure of proteins in aqueous media is the amide I band, occurring between approximately 1700 and 1600 cm^{-1} (Barth, 2000). The amide I band represents 80% of the C=O stretching vibration of the amide group coupled to the in-plane N–H bending and C–N stretching modes.

The exact wave number of this vibration depends on the nature of hydrogen bonding involving the C=O and N–H groups and this is determined by the particular secondary structure adopted by the protein being considered. Proteins generally contain a variety of domains containing polypeptide fragments in different conformations. As a consequence, the observed amide I band is usually a complex composite, consisting of a number of overlapping component bands representing helices, β-structures, turns and random structures.

Frazier (2005) stated that hawk bill scutes are typically thicker than those of other sea turtle species and are more conducive to use as a raw material source. Green sea turtles raised in captivity with high protein diets have produced relatively thick scutes that can be used in the same manner as hawk bill scutes.

Paries *et al*., (2005) used attenuated total reflectance infrared spectroscopy to differentiate hard keratin (tortoise shell and horn) from natural synthetic imitation (galalith or bakelite) though they analyzed only artifacts and did not compare their results with vouchered specimens of original species.

Espinoza *et al.*, (2006) studied broad range of sea turtle and bovidae keratins using diffuse reflectance infrared Fourier transform spectroscopy (DRIFT) combined with discriminant analysis. They analyzed the absorption of the amide I, amide II and amide III peaks occurring over a broad range. The amide II moiety of the spectrum showed an intense absorption at 1516 cm^{-1}, which is characteristic of β-keratins in reptilian origin. In the Cheloniidae family, the 1516 cm^{-1} absorption was present in all individuals tested but, surprisingly, this peak was also present in the bovidae sampled. Conversely, the amide II absorption at 1543 cm^{-1} has been described as diagnostic for α-keratins, and thus mammals. However, they reported it was present in the bovidae tested. When analyzing the keratin, the higher resolution of Raman spectroscopy allows one to differentiate between the 1543 cm^{-1} and 1516 cm^{-1} absorptions.

Mathematical post processing of the spectra employing discriminant analysis provided a useful statistical tool to differentiate tortoise shell from bovid horn keratin. All keratin standards used in their study were correctly classified with the discriminant analysis. A resulting performance index of 95.7% shows that DRIFTS, combined with discriminant analysis, is a powerful quantitative technique for distinguishing sea turtle and bovid keratins commonly encountered in museum collections and the modern wildlife trade.

Renata zemaityte (2006) have studied the modern technology of Fourier Transform Infrared Spectroscopy (FTIR) allows textile fiber constitution and sometimes the former colors identification. The comparison of various wool fibers in FTIR spectra showed the possibility of distinguishing some animal breed wool fibers and even fibers

colors (the difference in natural white and black wool fiber's spectra was obvious The sharper inclination and deflection for black wool spectrum in the frequencies region from 2900 cm^{-1} to 2400 cm^{-1} is noticed. The black wool spectrum has no visible peak at 3100 cm^{-1} meanwhile in the case of white wool spectrum the peak in the similar frequency zone is obvious.

In the case of Cameroon sheep wool (in the frequencies region from 3500 cm^{-1} to 2850 cm^{-1} and from 1700 cm^{-1} to 1050 cm^{-1}). The analogous investigations were carried out with flax, hemp, nettle cellulose fibers and cellulose archaeological fabric It is known that cellulose fibers are more vulnerable under than protein fibers. So the analysis contains a lot of discrepancies as well. Flax, hemp and nettle fiber's spectra have a rise peak in the frequencies about 3000 cm^{-1} and a descent peak in the frequencies about 2900 cm^{-1}. In the case of archaeological textile in the frequencies region from 3200 cm^{-1} to 2600 cm^{-1} the spectrum gradually rises (no well-defined peaks are obtained). Peak presence in archaeological textile spectrum in the frequencies region about 1700 cm^{-1}, 1650 cm^{-1} and 900 cm^{-1} show similarity to flax fiber, but in the frequencies regions 1700 cm^{-1}, and from 1300 cm^{-1} to 1000 cm^{-1} show similarity to nettle fiber.

Espinoza *et al.*, (2007) investigated the utility of horizontal-attenuated total-reflection Fourier transform infrared (HATR FTIR) spectroscopy for the analysis and identification of tail hair of reputed elephant and giraffe origin, commonly used to manufacture indigenous artifacts (e.g. bracelets, earrings, finger rings, etc.) in the wildlife trade. They described a prominent peak at 1032 cm^{-1}, seen extensively in proboscidean standards and absent in giraffe samples. This absorption appears to be related to surface

cystine oxides and suggests that cysteic acid is one of the compounds useful for distinguishing elephant and giraffe hairs.

An examination of the second order derivative of the proboscidean spectra revealed that cysteic acid stretching [SO] at 1040 cm^{-1} and 1170 cm^{-1}) is present in the African and Asian elephant samples, which was absent in the giraffe hairs. While spectral libraries are helpful in determining the material class represented by suspected hair artifacts (i.e. keratin vs. plastic vs. botanical), mathematical post-processing of the spectra employing discriminant analysis provided a more useful statistical tool for differentiating elephant and giraffe hairs than relying on visual inspection of spectral peaks alone. A resulting performance index of 91.8% showed that HATR FTIR, combined with discriminant analysis is a reliable tool for differentiating elephant hairs from giraffe hairs.

Edward G. Batrick (2002) according to them vibrational spectroscopy is applicable to a wide range of physical evidence. Because polymers are so common, they frequently play an evidentiary role in criminal cases. Polymeric materials such as fibers, paints and adhesive tapes are frequently analyzed to identify characteristic information regarding their composition. Physical and chemical information on these materials is stored in computer databases to help determine the manufacturer or, supplier, or simply to discriminate between many similar samples of material. The material was heavily filled with calcite ($CaCO_3$), identified by the intense, broad C–O antisymmetric stretch near 1450 cm1, and narrow out-of-plane and in-plane bends near 880 and 710 cm^{-1} respectively.

The IR spectrum clearly shows the resin binder features. The N–H stretch near 3350 cm^{-1}, the C–H stretches near 3000 cm^{-1}, the C=O stretch near 1730 cm^{-1}, the C–N stretch near 1540 cm^{-1}, and the typical C–O envelope from 1300 to 1000 cm^{-1} are observed in the IR. Of particular interest to paint analysis are any contributions by pigments. The weak, broad band at 868 cm^{-1} appears to be contributed by chrome yellow, as shown in the reference spectrum. However, because of the band's comparatively low intensity and lack of detail in the paint spectrum, it would be difficult to positively identify chrome yellow by this method alone.

The peaks labeled at 659, 425 and 357 cm^{-1} are rutile, a crystal form of titanium dioxide) is the Raman spectrum of the yellow auto paint. The major peaks at 843 and 365 cm^{-1} match up with the Raman spectrum of chrome yellow Peaks at 611 and 446 cm^{-1} are contributed by rutile, as shown in an atypical duct tape backing spectrum containing calcium carbonate (calcite). The calcite filler has a lattice band21 near 315 cm^{-1} that would not have been observed without the extended frequency range capabilities. The C–O asymmetric stretching band near 1450 cm^{-1} underlies the C–H bending band near 1460 cm^{-1}. The C–O out-of-plane bend can be observed near 880 cm^{-1}

Shengqing *et al*. (2011) have made work on identification of Rhinoceros horn and its substitutes by using FTIR spectroscopy. The chemical components of rhinoceros horn are made up of amino acids, cholesterol, taurine, hexosamine, phospholipids, and so on (Wang *et al*. 2007)

Amino acid: 1650 cm^{-1} belongs to C=O stretching vibration; 3050 cm^{-1} belongs to N-H stretching vibration. Cholesterol: 3270 cm^{-1} belongs to O-H stretching vibration;

1540 cm^{-1} belongs to C=C stretching vibration. Taurine: 1116 cm^{-1} belongs to S=O asymmetric stretching vibration; 1040 cm^{-1} belongs to S=O symmetric stretching vibration; 881 cm^{-1} belongs to S-O stretching vibration. Hexosamine: 1733 cm^{-1} belongs to C=O stretching vibration. Phospholipids: 2355, 2300 cm^{-1} belongs to P-H stretching vibration; 1240 cm^{-1} double peaks belong to P=O stretching vibration. Other saturated hydrocarbons: 2920 cm^{-1} belongs to C-H asymmetric stretching vibration; 2850 cm^{-1} belongs to C-H symmetric stretching vibration; 1450 cm^{-1} belongs to C-H bending vibration.

The absorption peaks of the cattle horn's infrared spectrum at 2907 cm^{-1}, 2850 cm^{-1}, 1446 cm^{-1} are obviously weaker than those of the rhinoceros horn, which are respectively C-H asymmetric stretching, C-H symmetric stretching vibration, C-H bending vibration. And the weaker absorption peak intensity means the content of saturation hydrocarbon is lower. The cattle horn's infrared spectrum has only one absorption peak at 2350 cm^{-1}, yet the rhinoceros horn's infrared spectrum has two absorption peaks, which is P-H stretching vibration region of phospholipids; And the absorption peak intensity at1076 $cm^{-1}$of cattle horn is weaker obviously than that of rhinoceros horn, which is the S=O stretching vibration. Furthermore, there is no C=O stretching vibration absorption peaks of hexosamine at 1733 $cm^{-1}$and no S-O stretching vibration peak of taurine at 881 cm-1 in the cattle horn's infrared spectrum.

In the yak horn's infrared spectrum, compared to that of rhinoceros horn, there are out-of-plane bending N-H vibration at 634 cm^{-1} of amino acid and NC=O symmetric stretching vibration at 1583 cm^{-1} of amino acids, and there is no P-H stretching vibration

absorption peaks of phospholipids at 2350 cm^{-1} and no S-O stretching vibration absorption peaks of taurine at 881 cm^{-1}. The absorption peaks of the goat horn's infrared spectrum at 2920 cm^{-1}, 2850 cm^{-1}, 2450 cm^{-1} are obviously weaker than those of the rhinoceros horn, which are respectively C-H asymmetric stretching, C-H symmetric stretching vibration, C-H bending vibration.

This explains the saturated hydrocarbon content of the goat horn is less. Compared to the rhinoceros horn's infrared spectrum, there is no P-H stretching vibration absorption peaks of phospholipids at 2350 cm^{-1}, no C=O stretching vibration absorption peaks of hexosamine at 1733 cm^{-1} and no S-O stretching vibration absorption peaks of taurine at 881 cm^{-1} in the goat horn's infrared spectrum.

Sheep horn's O-H stretching vibration absorption peaks at 3295 cm^{-1}, 3259 cm^{-1},3206 cm^{-1}, 3060 cm^{-1} are much more than those of rhinoceros horn, meaning sheep horn's cholesterol content is high. The sheep horn's infrared spectrum has only one absorption peak at 2352 cm^{-1}, no S-O stretching vibration absorption peaks of taurine at 881 cm^{-1} in the sheep horn's infrared spectrum.

2.3.3. BONE

Mature compact bone contains about 2% of its volume as cells, the remainder being extracellular matrix. Of this matrix 70% is occupied by mineral, about 20% is organic, and the remainder is water. Of the organic material 90% is collagen, about 1% is proteoglycans and the rest is a series of matrix proteins. The collagen of bone is almost all type I. The proteoglycans of bone are all of the small no aggregating Type (decorin and biglycan) and contain only chondroitin sulfate. The matrix proteins are characterized

by their anionic nature, being rich in phosphate (phosphoproteins, e.g. osteonectin), sialic acid (sialoproteins, e.g. osteopontin) or gamma-carboxyglutamic acid (Gla proteins, e.g. Osteocalcin). Growth factors such as TGF-β and BMP (bone morphogenic protein) are also stored within the bone matrix (Roughly and Lee, 1994)

Paschalis *et al.*, (1997) described mineral to matrix ratios from the ratio of integrated areas of the phosphate band at 900-1200cm^{-1}, amide I band at 1585-1725 and carbonate band at 850-900cm^{-1}. The frequencies for apatite and acid phosphate contains calcium phosphate band at 1020cm^{-1} and 1030cm^{-1}.

Fourier transform infrared spectroscopy **(**FTIR) has been used previously to analyze collagen secondary structure. Many vibrational bands characteristic of peptide groups and side chains provide information on protein structures. Among these, the amide I band (peptide bond C=O stretch, 1650 cm^{-1}) is especially sensitive to secondary structures. Thus, information on protein structure is obtained from analysis of broad peaks consisting of overlapped component bands. This is accomplished by applying techniques such as Fourier self deconvolution, second-derivative spectroscopy and difference among the various underlying bands making up the amide I spectral peak, two are of particular interest in the study of collagen: one at ;1660 cm^{-1} and one at ;1690cm^{-1}.

Stiner *et al.*, (2001) described the FTIR analysis of bone using four infra-red peak Indexes: the dahllite crystallinity index called splitting factor (SF); and the carbonate (876 cm^{-1}), water (3500 cm^{-1}) and calcite (712 cm^{-1}) peaks, each standardized to the 563 cm^{-1} phosphate peak. They were used the 874 cm^{-1} carbonate adsorption rather than the

1415 cm^{-1} adsorption, because the latter was affected by the presence of organic matrix absorption bands in the relatively well-preserved bones.

2.3.4. Ivory: Morphology and internal structure

The word "ivory was traditionally applied only to the tusks of elephants. However, the chemical structure of the teeth and tusks of mammals is the same regardless of the species of origin, and the trade in certain teeth and tusks other than elephant is well established and widespread. Therefore, "ivory" can correctly be used to describe any mammalian tooth or tusk of commercial interest. Teeth and tusks have the same origins. Teeth are specialized structures adapted for food mastication. Tusks, which are extremely large teeth projecting beyond the lips, have evolved from teeth and give certain species an evolutionary advantage. The teeth of most mammals consist of a root, a neck and a crown (Banerjee, and Bortolaso, 2004)

Tusk consists of a root and the tusk proper. Teeth and tusks have the same physical structures: pulp cavity, dentine, cementum and enamel. The innermost area is the pulp cavity. The pulp cavity is an empty space within the tooth that conforms to the shape of the pulp. Elephant and mammoth tusk ivory comes from the two modified upper incisors of extant and extinct members of the same order (Proboscides). The tusks of an elephant are deeply implanted into the long cylindrical sockets which are located in the bones in the anterior portion of its upper jaw. The tusk of an elephant has three distinct regions: pulp cavity in the centre, dentine in the middle and cementum in the outmost border. Odontoblastic cells line the pulp cavity and are responsible for the production of dentine. Dentine, which is the main component of ivory, forms a layer of consistent

thickness around the pulp cavity and comprises the bulk of the tusk. Dentine is a mineralized tissue with an organic matrix of collagenous proteins. The inorganic component of dentine is dahllite, a phosphate mineral. Dentine contains a microscopic structure called dentinal tubules which are micro-canals that radiate outward through the dentine from the pulp cavity to the exterior of the cementum border. These canals have different configurations in different ivories and their diameter ranges between 0.8 and 2.2 microns. Their length is dictated by the radius of the tusk. The three dimensional configuration of the dental tubules is under genetic control and is therefore a characteristic unique to the order. The configurations of the dental tubules are observed on the polished cross sections of elephant tusks and are called Schreger line.

Banerjee *et al.*, (2008) carried out the spectral analysis of the crystallinity of carbonate hydroxyapatite, the mineral composing mammoth ivory, can be measured by evaluating its splitting factor (SF). SF is based on the increasing separation of the FTIR absorption band at 565 and 605 cm-1. The relative retention of organic material and the incorporation of carbonate, relative to phosphate were determined by comparing the heights of amide and the phosphate peaks (1640/1035 cm^{-1}) and the carbonate and phosphate ones (1420/1035 cm^{-1})

FTIR spectra were collected and described that the amide I peak (1650–1620 cm^{-1}) and the phosphate peak (PO_3^{-4}), centered at approximately 1035 cm^{-1}, were used as the respective reference absorptions for the organic and mineral components of ivory, while the peak centered at 1420 cm^{-1} was used as the carbonate (CO_2^{-3}) reference peak. The intensity ratios $I1640/I1035$ and $I1420/I1035$ were calculated for all duplicate

samples to quantify the relative retention of organic material and the incorporation of carbonate, relative to phosphate, in the inorganic matrix respectively. Absorptions at approximately 1035 and 960 cm^{-1}, typical of phosphate and at 1460, 1420 and 873 cm^{-1}, typical of carbonate in un-degraded biological apatites, indicate that the carbonate-containing hydroxyapatite structure has been substantially retained in these materials. Interestingly, high carbonate/phosphate ratios (*I*1420/*I*1035) for all samples indicate that carbonate substitution for phosphate has been a significant part of the overall digenesis of the ivory found off Goa (Silatripati1 *et al.*, 2007)

2.3.5. Velvet Antler Composition

A major non-collagenous protein, proteoglycan, a protein substituted with glycosaminoglycan chains, occurs in the cartilaginous tissue of antler. Glycosaminoglycan (GAGs) and specifically, chondroitin sulfate (CS), are of particular interest to physicians and pharmacists, made from units of amino sugar, including D-glucosamine and D galactosamine, GAGs bond to core proteins and form proteoglycans. Cartilage proteoglycans regulate water retention and are integral to the differentiation and proliferation of chondocytes. Other significant types of GAG in velvet antler include keratin sulfate, hyaluronic acid, dermatan sulfate; chondroitin sulfate proteoglycan and decorin Glycosaminoglycans were isolated from the tip, upper, middle and base of growing antlers. Using cellulose acetate electrophoresis, chondroitin sulfate was determined to be the major glycosaminoglycan occurring densely in the cartilaginous tip and upper sections of the antler, along with small amounts of hyaluronic acid. The bone and bone-marrow containing middle and base antler sections also contain these compounds, and, in addition, chondroitinase-ACI resistant materials. Chondroitin sulfate

in the middle and base sections of antler are of larger molecular weight than CS found in the upper section and tip of the antler The average molecular size is greater in 40% ethanol, versus 50% ethanol, fraction. Finally, bone tissue, as opposed to cartilage, contains CS with larger molecular size (Sunwoo *et al*., 1997).

Church (1999) studied the Velvet antler is soft growing antler tissue which is cast off every year and re-grown by Cervus spp (deer). In Latin, the word from which antler is derived, anteoculae, means "in front of the eyes," and this is where they grow, from thick, bony cores that rise from skin covered pedicals. Antlers differ from horns in that horns are permanent. Dried velvet antler is composed of approximately 34% ash, 12% moisture, 54% organic material, of which 10% is nitrogen and 3% fat. Composition varies from species to species and with antler maturity and region of antler studies (tip, upper, middle, base).

The growing antler contains a number of necessary cells, including fibroblasts, chondroblasts, chondocytes and osteocytes. The tips of the antlers begin as undifferentiated mesenchymal cells which are transformed into cartilage. Later, the cartilage is turned to bone, due to the effects of testosterone. Velvet antler is antler that is still in its cartilaginous stage. So far, it has been rather difficult to ensure the cartilage-versus-bone content of harvested antlers. Food, climate, time of year, age of stag and the various concentrations of substances in different regions of the antler itself are factors that have yet to be harnessed with assurance.

Heavy calcification means that the antlers had begun maturing into bone, and products made from these are downgraded pharmaceutically. Lipid levels in the velvet

antler are also an important consideration in velvet antler quality, and change as the antlers mature and on the region of the antler that is under evaluation. The tip section, or wax piece, contains higher lipid, uronic acid, sulfated glycosaminoglycan, and sialic acid levels than other regions of the antler. These levels decrease moving down the antler to the middle region, which is also called the blood piece, to the bottom (bone or base) region. .

In velvet antler, type II collagen is the primary collagen type involved in the formation of cartilaginous antler. It contains high levels of hydroxylysine and also has a high glucosylation rate. (Yasui and Nimni., 1988) Types I and X collagen also occur in velvet antler, but as with the cartilage of most vertebrates, type II is the major type (Price, et al., 1996). It is important to note that the heat involved with drying the antlers destroys velvet antler cartilage.

2.3.6. Clay minerals

Clay minerals may be differentiated by their infrared spectra through a study of the bands due to the O–H and Si–O groups. In the O–H stretching region, 3800–3400 cm^{-1} for clay minerals, there are a number of bands observed. The inner hydroxyl groups between the tetrahedral and octahedral sheets result in a band near 3620 cm^{-1}. The other three O–H groups at the octahedral surface form weak hydrogen bonds with the oxygen's of the Si–O–Si bonds in the next layer and these results in stretching bands at 3669 and 3653 cm^{-1}. Where clays have most of their octahedral sites occupied by divalent central atoms such as Mg (II) or Fe (II), a single band in the O–H stretching region is often observed. In the 1300–400 cm^{-1} regions, clay minerals show Si–O stretching and bending

and O–H bending bands. The shape and position of the bands depend very much on the arrangement within the layers. For example, for kaolinite or dickite, which mainly have Al (III) in the octahedral position, several well-resolved strong Inorganic Molecules 109 bands in the 1120–1000 cm^{-1} region are observed. In comparison, for crysotile, which mainly contains Mg (II) in the octahedral sites, the main Si–O band is observed at 960 cm^{-1}. The O–H bending bands are strongly influenced by the layering in clays. Where the octahedral sheets are mainly occupied by trivalent Central atoms, the O–H bending bands occur in the 950–800 cm^{-1} region. Where most of the octahedral sites are occupied by divalent central atoms, the O–H bending bands are shifted to lower wave numbers in the 700–600 cm^{-1} range (Stuart, 2004).

Materials and Methods

III MATERIALS AND METHODS

3.1. Morphological studies:

The differentiation of morphological features of the skin of Tiger, Leopard, Cat, Dog, spotted deer, cattle and goat were undertaken in the Department of Anatomy and Histology, Veterinary College, Bangalore. The Tiger, Leopard, spotted deer skin specimens were obtained from confiscated skins received from forest and police officials and also from Zoos and National parks of Karnataka. Cattle and goat skins were procured from the Bangalore slaughter house. Dog and Cat skin were obtained from the Department of Surgery and Pathology. The ivory and spotted deer antler samples were belonging to the laboratory collections of Department of Anatomy, Veterinary College, Bangalore. A total of 8 ivory samples from elephant tusks, 4 ivory samples from boar Canines and 6 antler samples were used for the study and considered as standard material. An ivory sample from elephant tusk and a tusk artifact confiscated by police were used as test samples. Skin specimens were stored in 10% buffer formalin for 2-3 days. Further, they were processed for the routine histological techniques. A minimum of six samples from each species (Tiger, Leopard, Cat, Dog, spotted deer, cattle and goat) were used for this study. Skin samples from the lateral abdominal region were collected and cut into 2×2 cm size and fixed in 10% Neutral buffered formalin for a minimum of 48 hours.

The skin samples were processed for paraffin embedding and 6 µm thick horizontal and vertical sections were cut. The horizontal and vertical sections were stained with H&E Phloxine (Singh & Sulochana, 1996) for morphological studies ,

Weigerts resorcine fuchsin (Culling,1981) for elastic fibers, Van Gieson stain (Culling, 1981) for collagen fibers, Masson's Trichrome (Luna,1968) for keratin granules, PTAH (Luna, 1968) for skeletal muscle fibers, Bielschowsky stain (Culling,1981) for nerve cell and their process, Gomori's silver impregnation (Culling, 1981) for reticular fibers and the results were recorded.

3.2. FT-IR analysis

A total of 10 Leopard hair samples, 10 spotted deer hair samples, 10 cattle hair samples, 10 goat hair samples and 8 tiger hair samples were used for hair analysis and same number of hoof, horn, and claw samples for other appendages. The samples were collected from the Bannerghatta national park, KVAFSU dairy farm and local goat farm. All samples were first sonicated for 10 minutes in water followed by 10 minutes in isopropyl alcohol and then samples were allowed to air dry and micro waved for 30 seconds prior to analysis in order to reduce the contamination.

The hair samples were analyzed using Nicolet 6700 FTIR spectrometer ((Thermo Fisher Scientific Inc., Madison, WI, USA 2009). controlled by OMNIC^{TM} 8.1.11 software with Smart Orbit ^{TM}. A horizontal single reflection ATR accessory with type IIA diamond crystal mounted in a tungsten carbide plate was used for collecting the sample spectra. The Spectrometer was consisting of a DTGS KBr detector and KBr beam splitter. After cleaning the sample it was placed on the diamond crystal of Smart Orbit and uniformly pressed by turning pressure knob (45 pounds) of swivel pressure tower connected with a powder tip accessory.

A background scan was recorded prior to first sample spectral acquisition. Further background scans were recorded for every 30 minutes time interval. All the sample and back ground spectra were acquired by scanning 32 times with the resolution of 4.0 cm^{-1} and data spacing of 1.928 cm^{1}. All spectra were acquired by setting the instrument for automatic atmosphere suppression. No other corrections were applied during spectral acquisition. The final format of the spectra was absorbance vs. wave number (cm^{-1}) with the spectral range from 400 to 4000 cm^{-1}. The acquired spectra were subjected to automatic base line correction. The auto base line corrected spectra were used for further analysis. Each standard was properly labeled and minimum of 8 spectra for each standard was acquired.

Different spectral measurements were calculated by using TQ Analyst EZ^{TM} 8.0 Edition (Thermo Fisher Scientific Inc., Madison, WI, USA 2009). The spectral measurements of keratinous tissues calculated were

1. Area under curve at 11 different regions of the spectra – 3400-3100 cm^{-1}, 3100-3000 cm^{-1}, 3000-2800 cm^{-1}, 1770-1585 cm^{-1}, 1585-1480 cm^{-1}, 1480-1423 cm^{-1}, 1423-1360 cm^{-1}, 1360-1205 cm^{-1}, 1205-1140 cm^{-1}, 1140-970 cm^{-1}, 970-900 cm^{-1}.

2. Maximal height measurements at 12 different regions – 940-955 cm^{-1}, 1060-1080 cm^{-1}, 1090-1105 cm^{-1}, 1158-1172 cm^{-1}, 1185-1200 cm^{-1}, 1225-1245 cm^{-1}, 1268-1278 cm^{-1}, 1305-1327 cm^{-1}, 1385-1405 cm^{-1}, 1440-1460 cm^{-1}, 1515-1535 cm^{-1} and 1625-1645 cm^{-1}.

3. Fixed location height measurements at 28 fixed wave numbers of the spectra – 832, 876, 1009, 1043, 1076, 1101, 1126, 1156, 1173, 1230, 1311, 1343, 1368, 1386, 1402, 1450, 1497, , 1512, 1534, 1548, 1609, 1622, 1636, 1641, 1648, 1668, 1678 and 1690 cm^{-1}.

The spectral measurements of bony tissues calculated were Area under curve at 15 different regions of the spectra – 3100-3000 cm^{-1}, 3000-2850 $cm^{-1,}$ 1700-1590 cm^{-1}, 1590-1485 cm^{-1}, 1485-1430cm^{-1} ,1430-1350cm^{-1},1350-1300 cm^{-1},1300-1260 cm^{-1}, 1260-1215 $cm^{-1,}$ 1215-1180 cm^{-1}, 1150-890 cm^{-1}, 890-825 $cm^{-1,}$ 800-630 cm^{-1}, 630-585 cm^{-1} and 585-450 $cm^{-1.}$

1. Maximal height measurements at 13 different regions – 546-562 cm^{-1}, 588-606 cm^{-1}, 650-669 cm^{-1}, 860-883 cm^{-1}, 999-1022 cm^{-1}, 1190-1211 cm^{-1}, 1230-1255 $cm^{-1,}$ 1271-1296 cm^{-1}, 1330-1348 cm^{-1}, 1396-1423 cm^{-1}, 1441-1462 $cm^{-1,}$ 1535-1560 cm^{-1} and 1620-1651 $cm^{-1.}$

2. Minimal height measurements at 12 different regions – 577-594 cm^{-1},629-660 cm^{-1}, 802-835 cm^{-1}, 879-903 $cm^{-1,}$ 1174-1194 $cm^{-1,}$ 1205-1225 cm^{-1}, 1263-1281 $cm^{-1,}$ 1288-1309 $cm^{-1,}$ 1340-1367 $cm^{-1,}$ 1419-1439 $cm^{-1,}$ 1473-1493 cm^{-1} and 1574-1597 $cm^{-1.}$

3. Fixed location height measurements at 31 fixed wave numbers of the spectra – 467, 521, 556, 583, 599, 655, 667, 827, 874, 890, 958, 1012, 1111, 1181, 1202, 1217, 1240, 1265, 1285, 1300, 1338, 1361, 1401, 1430, 1453, 1485, 1544, 1553, 1590, 1629 and 1674 $cm^{-1.}$

All spectral measurements were made by applying Savitzky-Golay 9 point smoothing filter with polynomial order of 3.

All spectral measures were first copied into Microsoft Excel spread sheet. The Area measurements of each spectrum were first normalized by dividing each area measurement by corresponding spectral area measurement at 1150-890 cm^{-1}. The maximal and minimal height measurement data were normalized by dividing each corresponding spectral data by maximal height measure at 1010 cm^{-1}. The fixed location height measurement data were normalized by dividing each corresponding spectral data by data at 1012 cm^{-1}.

3.3. Wilks' Lambda: Is the ratio of the within sum of squares to the total sum of squares for the entire set of variables in analysis. Wilks' Lambda varies between 0 to 1. It is also Called U statistics.

Values close to zero indicate more accuracy, while values close to one indicate less accuracy.

3.4. Classification matrix: is a matrix that contains the number of correctly classified and misclassified cases.

3.5. **Performance index**: is a measure of how well a discriminant analysis method can categorize spectra from calibration standard.

Results

IV RESULTS

4.1. SKIN

The function of skin is to protect the body and to serve as an organ of heat regulation, excretion and sensation. It consists of an epithelial part, the epidermis and a connective tissue part, the dermis and other structure, such as hair follicle, sebaceous glands, sweat glands, nerve fibers and blood vessels. The hair, the horny portion of the hoof, nails or claws on the digits, the horns and antlers are also derived from the skin, by special modification and development.

4.1.1. LEOPARD SKIN:

The vertical section of the skin of the leopard (*Panthera pardus*) showed that the epidermis was thin, not smooth and pin point projections were seen at the opening of the hair follicles. The epidermis consisted of four layers namely stratum corneum, stratum granulosum, stratum spinosum and stratum basale (plate 1). The stratum basale and stratum corneum were distinct, and they were made up of one to two epithelial cell layers. The degenerated keratohyaline granules were observed in the stratum granulosum. There was clear demarcation between papillary layer and reticular layer of the dermis. In the papillary layer hair bundles were supported by the smooth muscle fibers (plate 2). The dense irregular connective tissue consisting of plenty of collagen fibers along with branched alveolar sebaceous glands were observed in the dermis (plate 3).

Horizontal section of the skin consisted of single large primary hair follicle associated with clusters of compound hair follicles (plate 4). In each compound follicle

there were six to eight secondary hair follicles located at one side along with one or two indistinct sebaceous glands. Sweat glands were observed at the superficial part of the dermis (plate2, 5). The merocrine sweat glands were coiled in a manner and devoid of reticular fibers (plate 6). There were fine elastic fibers seen around the hair follicles, not associated with sebaceous and sweat glands (plate 7). Reticular fibers were seen between the each hair follicle bundles (plate 8). The nerve fibers were penetrated into the primary hair follicle and also encircled the cluster of secondary follicles (plate 9).

4. 1.2.BENGAL TIGER SKIN:

The vertical section of the skin of tiger (*Panthera tigris tigris*) showed irregular, multiple folds of epidermis. The epidermis consisted of five layers namely stratum corneum, stratum lucidum, stratum granulosum, stratum spinosum and stratum basale (plate 10). The stratum corneum consisted of five to six epithelial cell layers which were dead cornified cells; the stratum lucidum was thin and a translucent layer. The stratum granulosum consisted of two to three layers of round nucleated cells with keratohyaline granules. The stratum spinosum consisted of elongated nucleated cell layer resting on with the stratum basale (plate 11). There were few darkly stained melanin pigments observed in the deeper cell layers of the epidermis (plate 10).

The horizontal section of the skin of the tiger showed clusters of compound hair follicles, which consisted of one primary hair follicle along with two to three or four secondary hair follicles (plate 12), attached to the clusters of hair follicles. The sebaceous glands were observed (plate 13) and within the compound hair follicles few sweat glands were observed (plate 14).

The fine elastic fibers encircled the primary hair follicle, sebaceous glands and inter follicular space (plate 15); the collagen fibers were associated with both primary hair follicle, secondary hair follicle and between the interfollicular regions (plate 16).

There were plenty of fine, irregular reticular fibers located between the clusters of hair follicles (plate 17). Nerve fibers surrounded both primary and secondary hair follicles (plate 18), and erector pili muscles were observed parallel to the clusters of compound hair follicles (plate 19).

4.1.3. SPOTTED DEER SKIN

The epidermis of the spotted deer (*Axis Axis*) consisted of only three layers namely stratum corneum, stratum granulosum and stratum basale (plate 20). The stratum corneum consisted of smooth, thin epithelial layer. The stratum lucidum and stratum spinosum layers were not observed and there was stratum granulosum with round shaped single cell layer with very thin basement membrane (plate 21). There was distinct separation of epidermis and dermis, which consists of loose connective tissue (plate 22).

The horizontal section of the skin showed the primary hair follicles associated with two to three secondary hair follicles (plate 23).These columns of hair follicles were arranged in a parallel fashion to each other (plate 24). The sebaceous glands surrounded the primary hair follicle (plate 25). There was sparse distribution of collagen fibers. The sweat glands were located at the junction of dermis and hypodermis which were merocrine simple tubular glands (plate 26). The interfollicular spaces were predominantly occupied by the elastic tissues. There were elastic fibers surrounding the hair follicle and sebaceous glands. Dermal connective tissue was occupied by the plenty of elastic fiber

(plate 27). The erector pilli muscle distribution was scanty, reticular fibers were present in the dermis of the skin but present only at the basement membrane. The nerve fibers were penetrating and encircling the primary hair follicle and secondary hair follicles (plate 28). The sweat glands were more predominantly innervated than the sebaceous glands.

4.1.4. CATTLE SKIN

The skin of cattle (*Bos indicus*) showed all five layers namely stratum basale, stratum granulosum, stratum spinosum, stratum lucidum and stratum corneum. The stratum corneum was prominent, nuclei were absent. Stratum lucidum was a shiny, translucent, homogenous layer. Stratum granulosum consisted of three layers of round shaped cells containing keratohyaline granules. Stratum spinosum consisted of oval shaped nuclei with four to six cell layers. The stratum basale contained single layer of columnar cells (plate 29)

Horizontal section showed that there was no sharp distinction between papillary and reticular layers in the dermis. The papillary layer consisted of a loose network of interlacing elastic fiber (plate 30) and few collagen bundles (plate 31). The elastic fiber was more frequent at the insertion of the arrector pili muscle close to the hair follicle. The distribution of hair follicle was species specific arranged in a single row of primary hair follicles. These follicles were associated with sebaceous gland (plate 32). The coiled tubular sweat glands were surrounded by reticular fibers; there were no secondary hair follicles (plate 33). The outer hair root sheath was covered by collagen fiber and between the hair follicle there was plenty of collagen fiber present. At the base of the hair follicle

sebaceous glands were appreciated. The glandular body was filled with epithelial tissue and the stroma was covered with thin collagen fiber. The cortex of the hair follicle showed elongated oval shaped pigments (plate 34) .Between the hair follicles there were simple tubular sweat gland lined with simple columnar cells (plate 33). Nerve fibers were also seen surrounding the hair follicle and also penetrating into the hair follicle (plate 35).

4.1.5. GOAT SKIN

In case of the goat (*Capra hircus*) skin the epidermal layer generally consisted of four layers namely stratum corneum, stratum granulosum, stratum spinosum and stratum basale (plate 36). The stratum corneum was a thick layer made up of two to three epithelial cell layers. The stratum granulosum consisted of single layered oval shaped cells with keratohyaline granules. The stratum spinosum consisted of three to eight nucleated cell layers. The stratum basale consisted of cuboidal cell layer (plate 37).

There was no distinction between papillary and reticular layer in the dermis. However dermal papillae were more prominent. Collagenous fibers were thick and densely arranged in both papillary and reticular part (plate 38). The elastic fibers were less and branched, these elastic fibers surrounded the primary hair follicle and sebaceous gland (plate 39). The reticular fibers were present in the deeper part of the dermis (plate 40).

The horizontal section of skin showed uniformly distributed primary follicles in a linear fashion without secondary hair follicles and paired sebaceous glands were located at the base (plate 41). Each follicle was surrounded by collagen fibers. The sebaceous glands were located between the primary hair follicles along with arrector pili muscle;

whereas the simple tubular sweat glands were located below the primary hair follicle (plate 42). The nerve fibers were innervated primary hair root (plate 43).

4.1.6. DOG SKIN

The vertical section of the dog (*Canis lupus familiaris*) skin did not show epidermal pegs. The epidermis consisted of three layers namely stratum corneum, stratum spinosum and stratum basale (plate 44). The corneum consisted of a thick layer of keratinized, non nucleated cells. The stratum basale was made up of single layer of low columnar cells. The stratum spinosum composed of elongated cells containing lightly stained nuclei (plate 45).

The horizontal section showed that the compound follicles arranged in a capsular form, each compound follicle consisted of one large primary follicle with six to eight secondary follicles (plate 46).The compound follicles were encapsulated with fibrous connective tissue. The hair follicles were associated with sebaceous and apocrine sweat glands extended into the subcutaneous adipose tissue (plate 47) above this layer the dermis consisted of a mixture of reticular, collagenous and elastic fibers together with fibroblast, blood vessels and nerves (plate 48).

4.1.7. CAT SKIN

The vertical section of the skin of cat (*Felis domesticus cattus*) showed that epidermis consisted of four distinct layers with stratum lucidum being absent (plate 49). The stratum corneum was thicker; stratum granulosum consisted of two layers of round

dark nucleated cells. The stratum spinosum consisted of single cell layer, dark with distinct nucleated cells. Melanin pigments were not observed (plate 50).

The horizontal section of the skin showed that the cluster of compound follicles, In each compound hair follicle there were six to eight secondary follicles with one large primary follicle were observed (plate 51). These compound follicles were associated with the sebaceous gland but were lacking in sweat glands. Few simple tubular sweat glands were observed between the reticular layer and adipose tissue of the dermis (plate 50). The dense collagen fibers were located between the clusters of the compound hair follicles (plate 51). Irregular, scattered, prominent elastic fibers were distributed around the primary hair follicle and interfollicular space (plate 52). Reticular fibers were not observed; nerve fibers were penetrating into the root of the primary hair follicle and encircling both primary and secondary follicles (plate 53).skeletal muscle fibers were seen between adipose cells of the dermis and hypodermis. Deep part of the dermis blood vessels and muscles fibers were observed (plate 54).large quantity of adipose tissue was observed at the bottom of dermis.

4.2. FT-IR analysis

Infrared spectroscopy is a technique that can be easily adapted for spectral analysis of hairs of endangered species such as tiger, leopard, spotted deer, along with domesticated animals such as cattle and goats.

In the present study the results for differentiating the hair keratin of herbivorous animals from those of feline groups by HATR-FTIR followed by discriminant analysis was undertaken.

A detailed spectral analysis was carried out by using primary and second derivative spectra, the peaks of secondary derivatives spectra were assigned to the their standard detailed peak assignments as indicated in the tables A and B.

4.2.1. Spectral analysis of hairs

Fig (1) represents the composite spectra of cattle, goat, spotted deer, leopard and tiger hairs. A thorough examination of these spectra reveals the presence of frequencies characteristics of keratin as assigned in Table A (Hopkins et al 1991, Joy and Lewis 1991, Akhtar and Edwards et. al., 1998).

Fig1 (a) represents the average primary spectrum of cattle hairs. In cattle hairs Amide A band was observed at 3272cm^{-1}. Amide B band was observed at 3080cm-1, weak CH_3 vibration modes occurred at 2961cm^{-1} and at 2930cm^{-1}. C-H stretching band at 1628cm^{-}1 was due to Amide I band. Amide II band was seen at 1525cm^{-1}.A sharp asymmetric CH_3 bands of methyl group found at 1450cm^{-1},weak peak of aliphatic side groups of amino acid residues seen at 1394cm^{-1}. Amide III bands was represented by a weak peak found at 1311cm^{-1}and medium peak at 1237cm-1. A shoulder at 1158cm^{-1}was assigned to C-O stretching. S-O stretching of cystine monoxide occurred at 1076cm^{-1}, 1042cm^{-1} and 952cm^{-1}.

Fig1 (b) represents the average primary spectrum of goat hairs. Amide A band was observed at 3273cm^{-1}, Amide B band was observed at 3080cm^{-1}, a medium CH_3 vibration modes occurred at 2964cm^{-1}, the C-H stretching band at 2931cm^{-1}. Amide I band occurred at 1629cm-1.Amide II peak was observed at 1521cm^{-1} due to C=N, C-C stretching. Sharp peaks were observed at 1450cm^{-1}, 1399cm^{-1} due to asymmetric CH_3

bending modes of methyl groups, Amide III bands were observed at 1311cm^{-1} and 1241cm^{-1}. A prominent peak was observed at 1161cm^{-1} due to C-O stretching. There were multiple peaks at 1124cm^{-1},1105cm^{-1}, 1076^{-1}and 1042cm^{-1} were due to strong intensity of (S=O) cystine monoxide interaction.

Fig 1(c) represents the average primary spectrum of leopard hairs. Amide A peak was observed at 3272cm^{-1}, Amide B band was observed at 3069cm^{-1}, weak peak observed at 2961cm^{-1}due to vibration of CH_3 modes, the C-H stretching band was seen at 2931cm^{-1}. Amide I band was observed at 1628$cm^{-1}$the functional group responsible for this is C=O,C=C stretching. Amide II band occurred at 1519cm^{-1}due to tyrosine chain stretching. The asymmetric CH_3 bending modes of the methyl groups of protein was observed at 1450cm^{-1}, A medium and flat peak was observed at 1403cm^{-1} and a weak peak observed at 1341cm^{-1} which was due to CH_2 wagging. Prominent Amide III peak was observed at 1236cm^{-1}, and a shoulder seen at 1159cm^{-1}, Symmetric (S-O) stretching of cystine monoxide peaks were observed at 1076cm^{-1} and 1042$cm^{-1}$and mild peak observed at 954cm^{-1}.

Fig1 (d) showed the average infrared primary spectrum of spotted deer hairs. An examination of these spectra showed the absorption of Amide A bands at 3272cm^{-1}, Amide B band stretching at 3076cm^{-1}, 2962cm^{-1} resulting due to CH_3 stretching. C-H stretching occurred at 2931cm^{-1}. The characteristic absorption bands of protein (keratins) at 1626cm^{-1} (amide I) 1520cm^{-1} (amideII). The asymmetric CH_3 bending modes of the methyl groups of protein was observed at 1450cm^{-1}, A medium peak observed at 1390 cm^{-1}. amide III peaks observed at 1314cm^{-1}, 1236cm^{-1}, the functional group responsible

for these absorption at each frequencies C=O stretching vibration, while amide II was due to N-H bending and C-H stretching. Amide III band was a combination of C-H stretching, N-H bending, C-C stretching and C-O bending vibration. The symmetric stretching was found at 1076cm-1 and 1042cm^{-1}. The functional group responsible for these peaks is S-O stretching which indicate the more quantity of cystine amino acids.

Fig 1(e) represents the average primary spectrum of tiger hairs. The spectrum showed the characteristic absorption Amide A bands, the assigned peak was 3272cm^{-1}, Amide B peak was observed at 3070cm^{-1}.The functional group responsible for the absorption was due to asymmetrical stretching vibration of CH_3 which causes a medium peak at 2966cm^{-1} where as symmetrical vibration of methylene band was observed at 2929cm^{-1}.Amide I band was observed at 1627cm^{-1} and a prominent peak of Amide II was seen at 1520cm^{-1}.A flat peak of methylene deformation observed at 1399cm^{-1}, weak amide III peak observed at 1306cm^{-1} and prominent peak of Amide III band observed at 1236cm-1.The absorption of carbonyl (C=O) group seen at 1160cm-1,1125cm^{-1} and 1102cm^{-1}. An absorption band at frequencies of 1076cm-1 and no visible peak at 1043cm^{-1} related to bending vibration of (S=O) cystine monoxide groups and finally a sharp, prominent peak observed at 951cm^{-1} was due to rocking of methylene group.

4.3. Discriminant analysis

Discriminant analysis is a multivariate statistical method that assists in the classification of data into distinct groups. In the present study the discriminant function was used to classify keratin materials of uncertain origin. Spectral data was utilized for the discriminant analysis. Each known standard is validated by determining the

mahalanobis distance of the sample from the average spectrum. The closer a sample is to a particular centroid class, the higher the likelihood that it will be classified with that particular sample. The performance index is a measure of how well a discriminant analysis method can categorize spectrum from calibration standard. When the performance index exceeds more than 90% and the wilks's lambda lies closer to zero indicates that the unknown samples were correctly assessed against a normal distribution of known samples.

4.3.1. Discriminant analysis of Hairs

The linear Discriminant analysis was carried out using spectral measurement data of cattle (n=145), goat (n=88), leopard (n=111), spotted deer (n=57) and tiger (n=60). The results were depicted in the form of canonical score plots given in Figs from 6 to 15 and tables from 5 to 9.

Fig 6 represents the canonical score plot of cattle, spotted deer and leopard. The performance index of the discriminant analysis was 100% accuracy and the Wilks's lambda was 0.022(Table 5).

Fig 7 represents the canonical score plot of tiger, leopard and spotted deer. The performance index of the discriminant analysis of these three species was 99% and the Wilks's lambda was 0.03(Table 5)

Fig 8 represents the canonical score plot of cattle, goat and tiger, the performance index of the discriminant analysis of these three species was 100% and the Wilks's lambda was 0.025(Table 6).

Fig 9 represents the canonical score plot of cattle, leopard and spotted deer, the performance index of the discriminant analysis was 99% for cattle while it was 100% for leopard and spotted deer and the Wilks's lambda was 0.03(Table 6).

Fig 10 represents the canonical score plot of cattle, leopard and tiger; the performance index of the discriminant analysis of these three species was 100%, and the Wilks' lambda was 0.015(Table 7).

Fig 11 represents the canonical score plot of cattle, tiger and spotted deer, the performance index of the discriminant analysis for spotted deer was 98%, while it was 100% for cattle and tiger, and the Wilks's lambda was 0.021(Table 7).

Fig 12 represents the canonical score plot of goat, leopard and spotted deer, the performance index of the discriminant analysis of spotted deer was 95%, goat was 99% and leopard was 100%, and the Wilks's lambda was 0.025(Table 8).

Fig 13 represents the canonical score plot of goat, leopard and tiger, the performance index of the discriminant analysis for tiger was 100%, and 99% for goat and leopard. The Wilks's lambda was 0.015 (Table 8).

Fig 14 represents the canonical score plot of goat, tiger and spotted deer; the performance index of the discriminant analysis for spotted deer was 98%, goat was 99% and tiger was 100%. The Wilks's lambda was 0.016 (Table 9).

Fig 15 represents the canonical score plot of spotted deer, leopard and tiger; the performance index of the discriminant analysis for all these three species was 100%.The Wilks's lambda was 0.013 (Table 9).

4.4.1. Spectral analysis of hoof, claws and horns

Fig 2 represents the composite spectra of species studied. The top (a) represents the average spectrum of cattle (*Bos indicus*), 2 (b) represents the average spectrum of goat (*capra hircus*),

2 (c) represents average spectra of, leopard (*Panthera pardus*) 2(d) represents the average spectrum of spotted deer (*Axis axis*) and 2(e) represents average spectra of Bengal tiger (*Panthera tigris tigris*) An analysis of these spectra allows us to confirm the presence of frequencies characteristics of keratins as assigned in (Table A).

Fig 2(a) represents the average primary spectrum of cattle hoof. Amide A exhibits absorption of peak at 3273cm-1, Amide B peak was observed at 3069cm^{-1},CH_3 mode and C-H stretching observed 2962cm^{-1} and 2934cm^{-1}.The Amide I peak seen at 1631cm^{-1} and prominent Amide II peak was observed at 1514cm^{-1}. Asymmetric CH_3 bending modes of the methyl group of protein and methylene deformation was observed at 1451cm-1. Sharp peak observed at 1392cm^{-1}, the functional group responsible for these frequencies was aliphatic side groups of the amino acid residues. Amide III band components of proteins observed at 1312cm^{-1} as a weak peak and wide prominent peak at 1237cm^{-1}. There was shoulder at1156cm^{-1} is due to C-O stretching. And broad peak was seen at 1078 cm^{-1} wave number due to S-O stretching vibration of cystine monoxide residues.

Fig 2(b) represents the average primary spectrum of goat hoof. Amide A exhibited absorption of peak at 3271cm-1, Amide B stretching observed at 3069cm^{-1},CH_3 mode and C-H stretching observed 2962cm^{-1} and 2935cm^{-1}.The Amide I peak seen at 1631cm^{-1} and prominent Amide II peak observed at 1515cm^{-1}. Asymmetric CH_3 bending modes of the methyl group of protein and methylene deformation was observed at 1451cm-1. Sharp peak was observed at 1393cm^{-1}, the functional group responsible for these frequencies was aliphatic side groups of the amino acid residues. Amide III band components of proteins observed at 1313cm^{-1} as a weak peak and wide prominent peak at 1238cm^{-1}. There was shoulder at1156cm^{-1} is due to C-O stretching. And there was a wide stretching seen at 1077 cm^{-1} wave number, due to S-O stretching vibration of cystine monoxide residues.

Fig 2(c) represents the average primary spectrum of leopard claws. Amide A exhibited absorption of peak at 3271cm-1, Amide B stretching was observed at 3068cm^{-1},CH_3 mode and C-H stretching observed 2960cm^{-1} and 2929cm^{-1}.The Amide I peak seen at 1633cm^{-1} and prominent Amide II peak was observed at 1514cm^{-1}respectively. Asymmetric CH_3 bending modes of the methyl group of protein and methylene deformation observed at 1450cm-1. Medium peak observed at 1403cm^{-1}, the functional group responsible for these frequencies was aliphatic side groups of the amino acid residues. Amide III band components of proteins was observed at 1309cm^{-1} as a weak peak and more prominent peak at 1236cm^{-1}. There was shoulder at 1163cm^{-1} is due to C-O stretching. And there was wide stretching seen at 1078cm^{-1} wave number, due to S-O stretching vibration of cystine monoxide residues.

Fig 2(d) represents the average primary spectrum of spotted deer hoof. Amide A exhibited absorption of peak at 3273cm-1, Amide B stretching was observed at 3073cm^{-1}, CH_3 mode and C-H stretching observed 2962cm^{-1} and 2933cm^{-1}.The Amide I peak seen at 1632cm^{-1} and prominent Amide II peak observed at 1515cm^{-1}. Asymmetric CH_3 bending modes of the methyl group of protein and methylene deformation observed at 1450cm-1. Sharp peak observed at 1393cm^{-1}, the functional group responsible for these frequencies was aliphatic side groups of the amino acid residues. Amide III band components of proteins was observed at 1312cm^{-1} as a weak peak and wide prominent peak at 1237cm^{-1}. There was shoulder at1156cm^{-1} due to C-O stretching. And there was wide stretching seen at 1076 cm^{-1} wave number due to S-O stretching vibration of cystine monoxide residues.

Fig 2(e) represents the average primary spectrum of tiger claws. Amide A exhibits absorption of peak at 3271cm-1, Amide B band was observed at 3069cm^{-1},CH_3 mode and C-H stretching observed 2961cm^{-1} and 2934cm^{-1}.The Amide I peak seen at 1633cm^{-1} and prominent Amide II peak observed at 1514cm^{-1}. Asymmetric CH_3 bending modes of the methyl group of protein and methylene deformation observed at 1450cm-1. Medium peak observed at 1400cm^{-1}, the functional group responsible for these frequencies was aliphatic side groups of the amino acid residues. Amide III band components of proteins observed at 1310cm^{-1} as a weak peak and more prominent peak at 1236cm^{-1}. There was shoulder at 1166cm^{-1} is due to C-O stretching. And there were twin peaks seen at 1106 and 1078cm^{-1} wave number, due to S-O stretching vibration of cystine monoxide residues.

Fig 3 (a) represents the average primary spectrum of cattle horn. Amide A exhibits absorption of peak at 3272cm-1, Amide B band was observed at 3068cm^{-1},CH_3 mode and prominent C-H stretching observed 2961cm^{-1} and 2930cm^{-1}.The Amide I peak seen at 1632cm^{-1} and prominent Amide II peak observed at 1515cm^{-1}. Asymmetric CH_3 bending modes of the methyl group of protein and methylene deformation observed at 1450cm-1. Medium peak observed at 1392cm^{-1}, the functional group responsible for these frequencies was aliphatic side groups of the amino acid residues. Amide III band components of proteins observed at 1312cm^{-1} as a weak peak and more prominent peak at 1237cm^{-1}. There was shoulder at 1156cm^{-1} is due to C-O stretching. And there was broad peak seen at 1077cm^{-1} wave number, due to S-O stretching vibration of cystine monoxide residues.

Fig 3 (b) represents the average primary spectrum of goat horn. Amide A exhibits absorption of peak at 3272cm-1, Amide B stretching observed at 3069cm^{-1},CH_3 mode and C-H stretching observed 2962cm^{-1} and 2933cm^{-1}.The Amide I peak seen at 1631cm^{-1} and prominent Amide II peak observed at 1515cm^{-1}. Asymmetric CH_3 bending modes of the methyl group of protein and methylene deformation observed at 1451cm-1. Medium peak observed at 1393cm^{-1}, the functional group responsible for these frequencies was aliphatic side groups of the amino acid residues. Amide III band components of proteins observed at 1312cm^{-1} as a weak peak and more prominent peak at 1239cm^{-1}. There was shoulder at 1156cm^{-1} is due to C-O stretching. And there was broad peak seen at 1077 cm^{-1} wave number, due to S-O stretching vibration of cystine monoxide residues.

Fig 3 (c) represents the average primary spectrum of spotted deer antlers, the observations were described in the bony structures.

4.4.2. Discriminant analysis of hoof, claws and horns

The linear Discriminant analysis was carried out using spectral measurement data of cattle hoofs (n=50), goat hoofs (n=60), leopard claws (n=70), spotted deer hoofs (n=10), tiger claws (n=70), cattle horn (n=60) and goat horn (n=49). The results were depicted in the form of canonical score plot of (fig 16-25) and Tables 10 to15.

Fig 16 represents the canonical score plot of cattle hoof, goat hoof and spotted deer hoof, the performance index of the discriminant analysis for spotted deer hoof was 90% and 100% for cattle and goat hoofs, the Wilks's lambda was 0.031(Table 10).

Fig 17 represents the canonical score plot of cattle hoofs, goat hoofs and leopard claws, the performance index of the discriminant analysis of all these three species was 100% and the Wilks's lambda was 0.003(Table 10).

Fig 18 represents the canonical score plot of cattle hoofs, goat hoofs and tiger claws, the performance index of the discriminant analysis of all these three species was 100% and the Wilks's lambda was 0.006 (Table 11).

Fig 19 represents the canonical score plot of cattle hoofs, spotted deer hoofs and leopard claws, the performance index of the discriminant analysis of all these three species was 100%, and the Wilks' lambda calculated was 0.001(Table 11).

Fig 20 represents the canonical score plot of cattle hoofs, spotted deer hoofs and tiger claws, the performance index of the discriminant analysis of cattle, leopard claws was 100%, and spotted deer hoof was 90%, the Wilks's lambda calculated was 0.029(Table 12).

Fig 21 represents the canonical score plot of spotted deer hoofs, goat hoofs and leopard claws, the performance index of the discriminant analysis of all these three species was 100%, and the Wilks's lambda calculated was 0.007 (Table 12).

Fig 22 represents the canonical score plot of goat hoofs, spotted deer hoofs and tiger claws, the performance index of the discriminant analysis of all these three species was 100% and the Wilks's lambda calculated was 0.007(Table 13).

Fig 23 represents the canonical score plot of cattle hoofs, leopard claws and tiger claws, the performance index of the discriminant analysis of cattle and tiger claws was 100%, while leopard claws was 93% and the Wilks's lambda calculated was 0.011(Table 13).

Fig 24 represents the canonical score plot of goat hoofs, leopard claws and tiger claws the performance index of the discriminant analysis of cattle was 100%, tiger claws was 99%%, and leopard claws was 97%, and the Wilks's lambda calculated was 0.005(Table 14).

Fig 25 represents the canonical score plot of spotted deer hoofs, leopard claws and tiger claws, the performance index of the discriminant analysis of spotted deer hoofs was

100%, tiger claws was 99%, and leopard claws was 97%, the Wilks's lambda calculated was 0.017(Table 14).

The performance index of the discriminant analysis was 100% accuracy with that of cattle horn, goat horn and spotted deer antlers (fig 26).and Wilks's lambda calculated was 0.001(Table 15)

4.5.1. Spectral analysis of ivories, antlers

Fig 4 represents composite spectra of boar ivory, elephant ivory and spotted deer antler

4.5.2. Spectral analysis of boar ivory

Fig 4 (a) represents the average primary spectrum of boar ivory. The results showed that Amide A peak observed at 3275cm^{-1}wave number due to O-H stretching vibration. Amide B peak was found at 3105cm^{-1}. Very weak CH_3 stretching band peak was observed at 2981cm^{-1} Amide I peak observed at 1635cm^{-1}. Amide II peak was found at 1546cm^{-1}. The peak at 1450$cm^{-1}$was assigned to asymmetric CH_3bending mode of proteins. The peak at 1413$cm^{-1}$was assigned C-H deformation. The weak peak at 1244$cm^{-1}$was assigned to amide III. The highest peak at 1009cm^{-1} was assigned to PO_4^{3-} III stretching. The medium peak at 872 $cm^{-1}$was assigned to CO_3^{2-}II stretching vibration. The broad peak at 701$cm^{-1}$was assigned to CO_3^{2-}IV band. The peaks at 598 and 555cm^{-1} were assigned to PO_4^{3-}IV.

4.5.3. Spectral analysis of elephant ivory

Fig 4 (b) represents the average primary spectrum of elephant ivory. The results showed that Amide A peak observed at 3274cm^{-1}wave number due to O-H stretching vibration. Amide B peak was found at 3102cm^{-1}. Very weak CH_3 stretching band peak was observed at 2980cm^{-1} Amide I peak observed at 1634cm^{-1}. Amide II peak was found at 1545cm^{-1}. The prominent peak at 1451$cm^{-1}$was assigned to asymmetric CH_3bending mode of proteins. The weak peak at 1420$cm^{-1}$was assigned C-H deformation. The medium peak at 1243$cm^{-1}$was assigned to amide III. The highest peak at 1011cm^{-1} was assigned to PO_4^{3-} III stretching. The medium peak at 872 $cm^{-1}$was assigned to CO_3^{2-}II stretching vibration. The broad peak at 687$cm^{-1}$was assigned to CO_3^{2-}IV band. The peaks at 597 and 555cm^{-1} were assigned to PO_4^{3-}IV.

4.5.4. Spectral analysis of antlers

Fig 4 (c) represents the average primary spectrum of spotted deer antler. The results showed that Amide A peak observed at 3277cm^{-1}wave number due to O-H stretching vibration. Amide B peak was found at 3100cm^{-1}. Very weak CH_3 stretching band peak was observed at 2959cm^{-1} Amide I peak observed at 1634cm^{-1}. Amide II peak was found at 1545cm^{-1}. The weak peak at 1449$cm^{-1}$was assigned to asymmetric CH_3bending mode of proteins. The prominent peak at 1412$cm^{-1}$was assigned C-H deformation. The medium peak at 1243$cm^{-1}$was assigned to amide III. The highest peak at 1011cm^{-1} was assigned to PO_4^{3-} III stretching. The medium peak at 872 $cm^{-1}$was assigned to CO_3^{2-}II stretching vibration. The broad peak at 671$cm^{-1}$was assigned to CO_3^{2-} IV band. The peaks at 598 and 556cm^{-1} were assigned to PO_4^{3-}IV.

4.5.5. Spectral analysis of artifacts

Fig 5 represents the average primary spectra of artifacts showed that there was no O-H stretching vibration absorption peak between 3500-3000cm^{-1} the functional group responsible for this peak was amide A band. Amide I and amide II bands stretching were not visible at 1632cm^{-1} and 1515 cm^{-1}. More prominent peak found at 1720cm^{-1}, 1412cm^{-1}, 1263cm^{-1}, 1118cm^{-1}, and 872cm^{-1}. The functional responsible group is due to M-H stretching, and M-O bending of inorganic metal and halogen ions.

4.5.6. Discriminant analysis of ivories, antlers:

The linear Discriminant analysis was carried out using spectral measurement data of elephant ivory (n=30), boar ivory (n=20) and spotted deer antler (n=48). The results were depicted in the form of canonical score plot of (fig 27) and Table 16 to 17.

Fig 27 represents the geographical representation of spotted deer antler, wild boar ivory and elephant ivory the classical classification matrix was 100% and wilks's lambda was 0.003 (Table 16) it was clear indication of differentiate between boar ivory, elephant ivory and spotted deer antlers and fig (28) represents the canonical score plot of wild boar ivory, elephant ivory and artefact was 100% and Wilks lambda was 0.019 (Table 17).

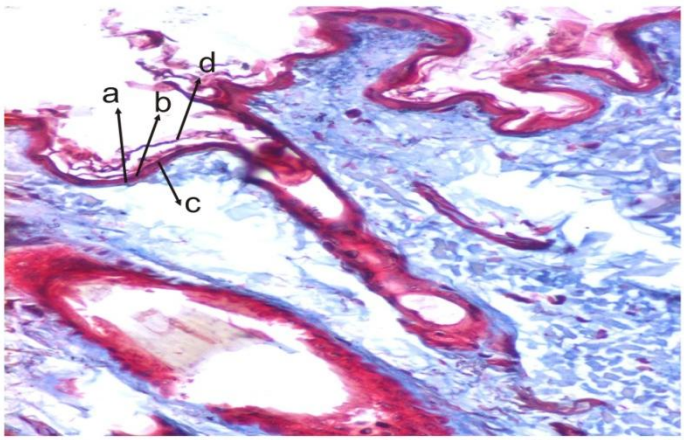

Plate 1- Vertical section through epidermis of the skin of leopard showing, (a) Stratum basale (b) Stratum spinosum (c) Stratum granulosum (d) Stratum corneum.
Masson's Trichrome stain x 200

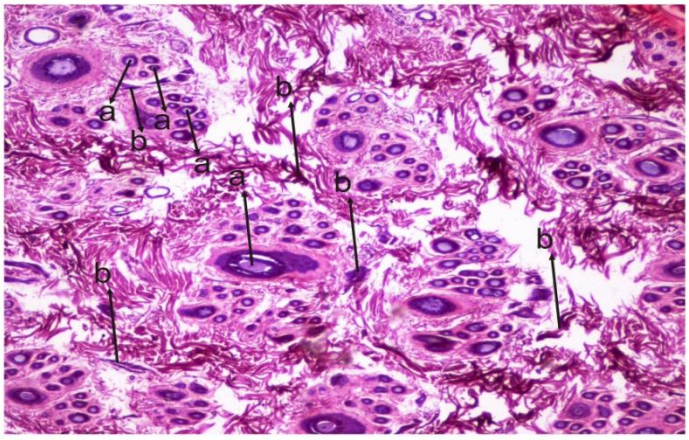

Plate 2- Vertical section through dermis of the skin of leopard showing (a)Hair follicles were supported by the (b) smooth muscle fibers.
PTAH x40

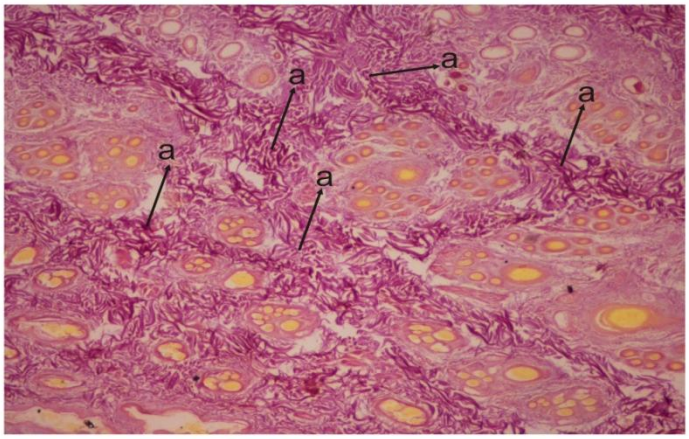

Plate 3- Vertical section through dermis of the skin of leopard showing (a)collagen fibers
Van Gieson x 40

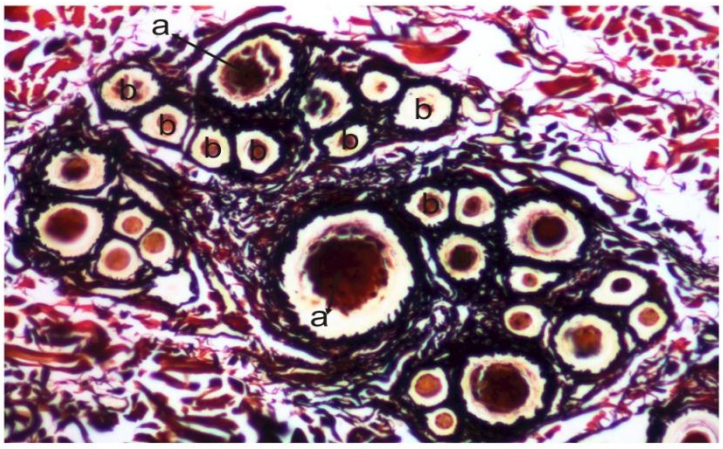

Plate 4- Horizontal section of the skin of leopard showing (a) Single large primary hair follicle (b) Secondary hair follicles.
Gomori's silver impregnation stain x 200

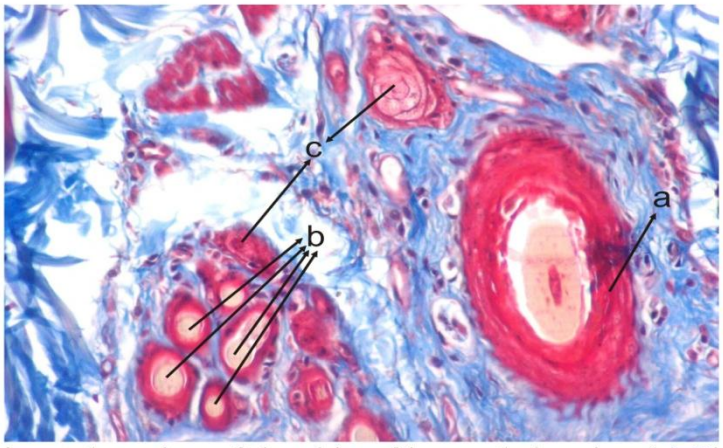

Plate 5-Horizontal section of the skin of leopard showing (a) Single large primary hair follicle (b) secondary hair follicles. (c) Sebaceous glands.
Masson's Trichrome stain x200

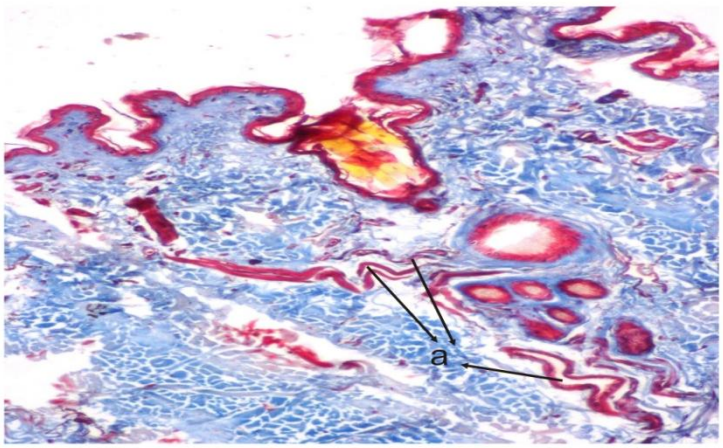

Plate 6- Horizontal section of the skin of leopard showing (a) Serpentine type of Sweat glands
Masson's Trichrome stain x200

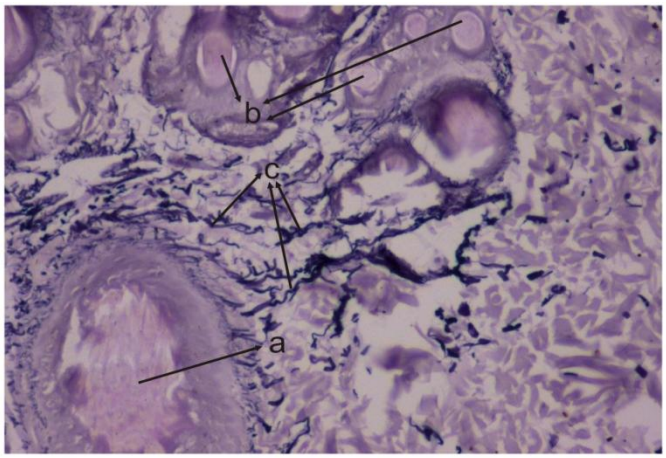

Plate 7- Horizontal section of the skin of leopard showing (a) Primary hair follicle (b) Secondary hair follicles (c) Elastic fibers.
Weigerts resorcine fuchsin x 200

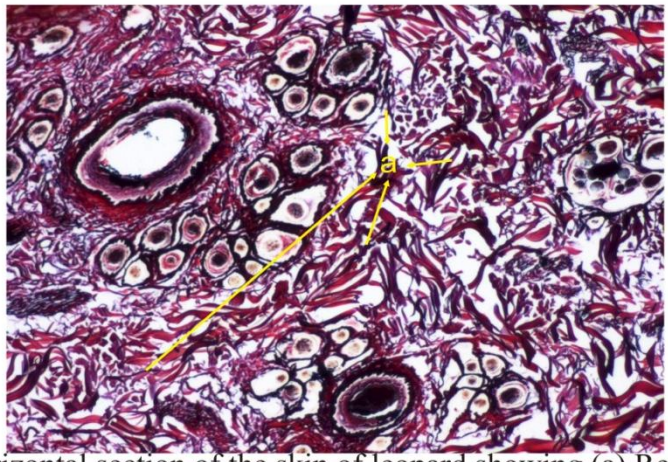

Plate 8- Horizontal section of the skin of leopard showing (a) Reticular fibers between the each hair follicle.
Gomori's silver impregnation stain x 100

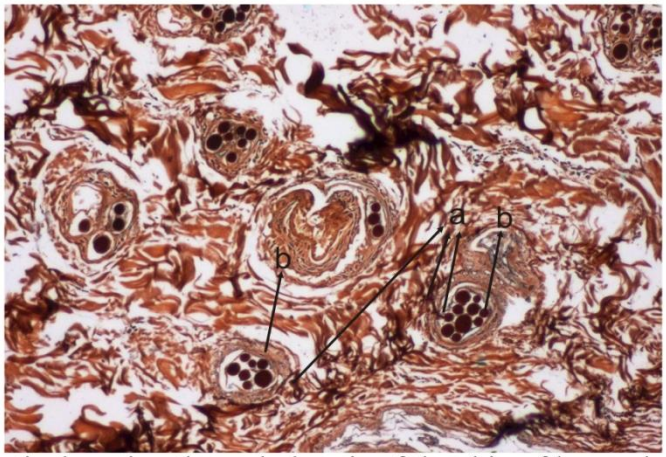

Plate 9- Vertical section through dermis of the skin of leopard showing (a) Nerve fibers penetrating into root of the (b)hair follicle.
Bielschowsky stain x100

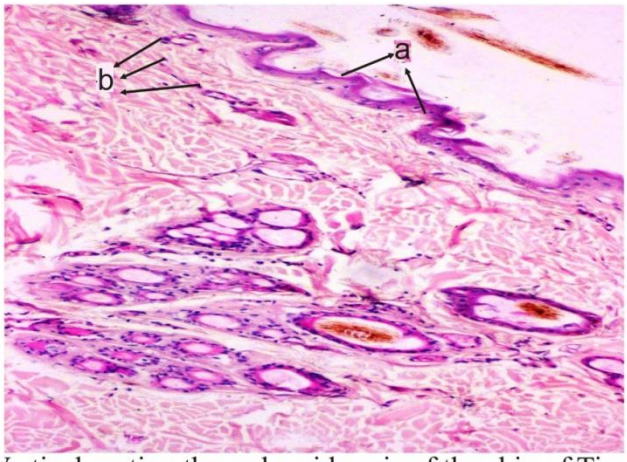

Plate 10- Vertical section through epidermis of the skin of Tiger showing, (a) Multiple irregular folds (b) Melanin pigment
H & E Phloxine x 100

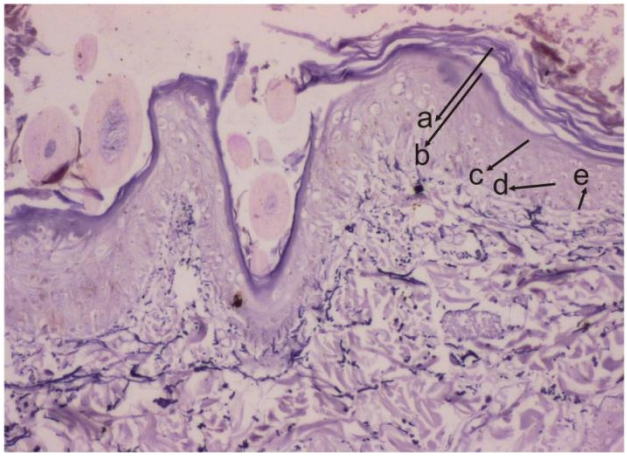

Plate 11- Vertical section through epidermis of the skin of Tiger showing, (a) stratum corneum (b) stratum lucidum (c) stratum granulosum (d) stratum spinosum (e) stratum basale Weigerts resorcine fuchsin x 100

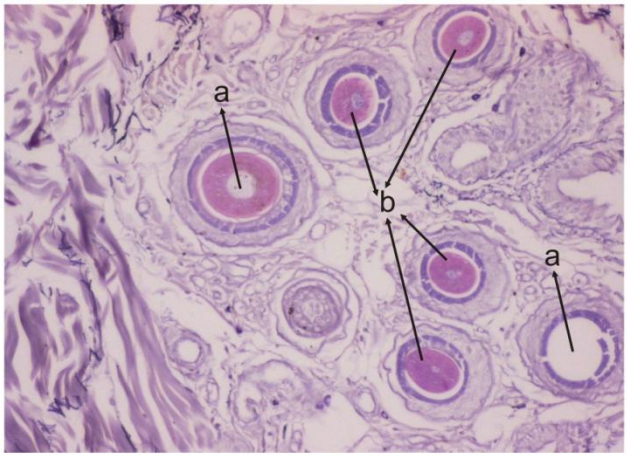

Plate 12- Horizontal section of the skin of Tiger showing (a) primary hair follicle (b) secondary hair follicles.
Weigerts resorcine fuchsin x 100

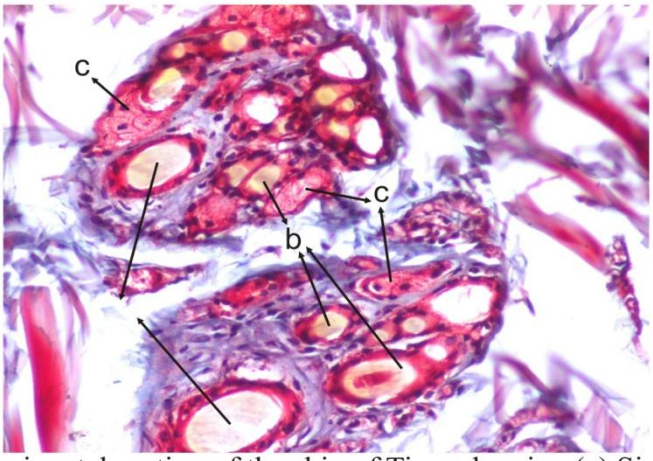

Plate 13- Horizontal section of the skin of Tiger showing (a) Single large primary hair follicle (b) Secondary hair follicles. (c) Sebaceous glands.
Masson's Trichrome stain x200

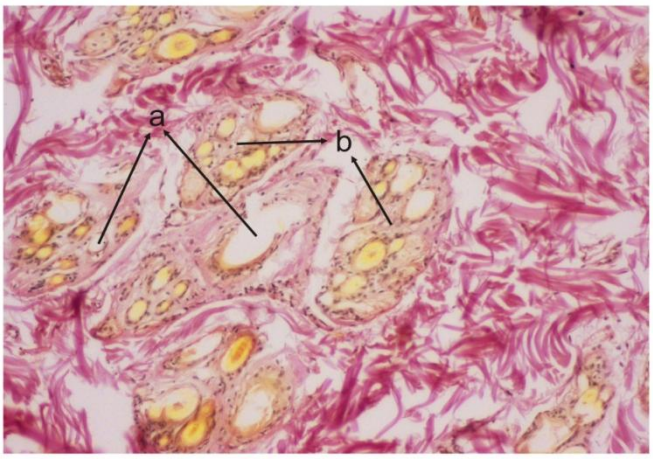

Plate 14- Horizontal section of the skin of Tiger showing (a) Sweat glands within the (b)compound hair follicles.
van Gieson x 100

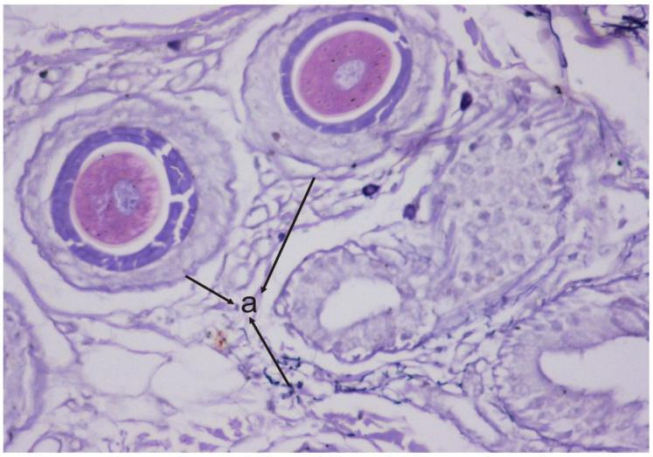

Plate 15- Horizontal section of the skin of Tiger showing (a) Elastic fibers
Weigerts resorcine fuchsin x 100

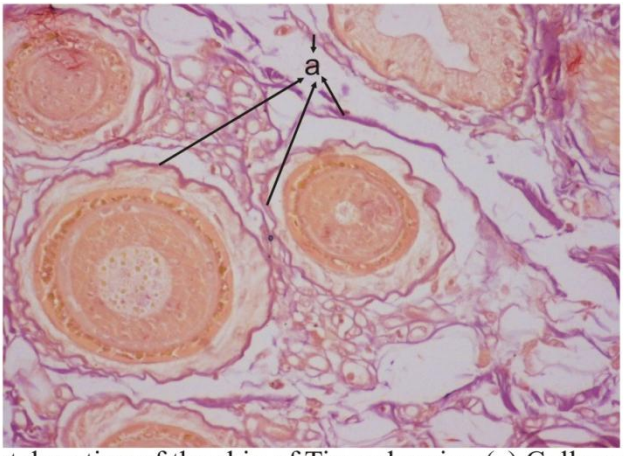

Plate 16- Horizontal section of the skin of Tiger showing (a) Collagen fibers in dermis.
van Gieson x 200

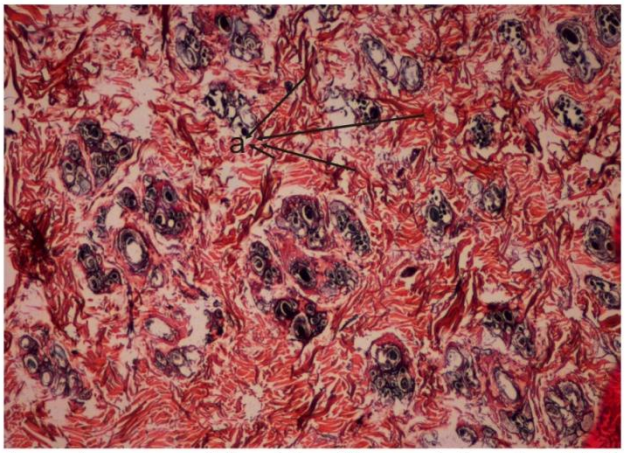

Plate 17- Horizontal section of the skin of leopard showing (a) Reticular fibers between the clusters of hair follicle.
Gomori's silver impregnation stain x 40

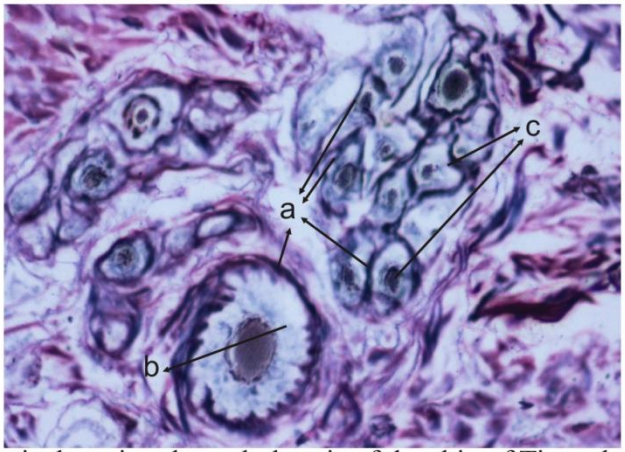

Plate 18- Vertical section through dermis of the skin of Tiger showing (a) Nerve fibers surrounding the (b) Primary and (c) Secondary hair follicle.
Bielschowsky stain x200

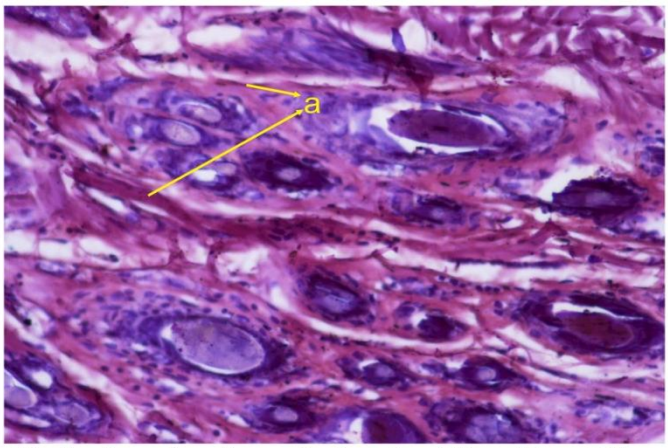

Plate 19- Vertical section through dermis of the skin of Tiger showing (a)Errector pilli muscle fibers.

PTAH x200

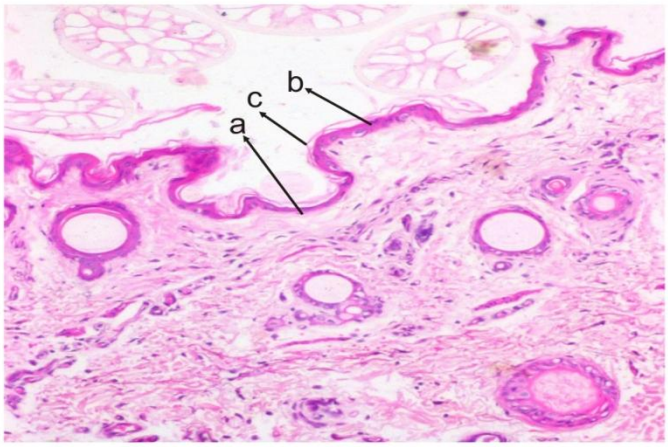

Plate 20- Vertical section through epidermis of the skin of spotted deer showing, (a) stratum basale (b) stratum granulosum (c) stratum corneum.

H & E Phloxine x 100

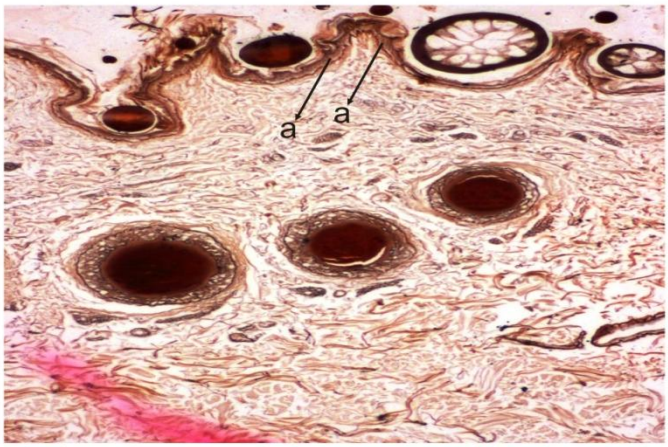

Plate 21- Vertical section through dermis of the skin of spotted deer showing (a) stratum granulosum with round shaped single cell layer

Bielschowsky stain x100

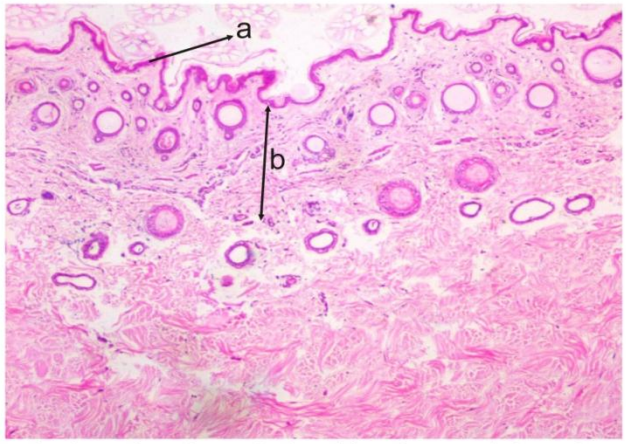

Plate 22- Vertical section through the skin of spotted deer showing distinct separation of (a) Epidermis (b) Dermis.

H & E Phloxine x 100

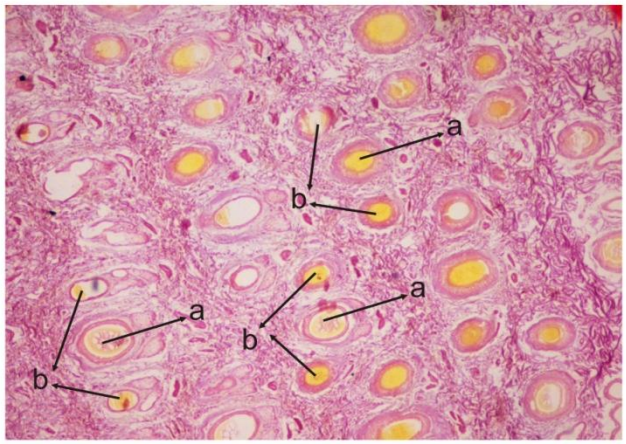

Plate 23- Horizontal section of the skin of spotted deer showing (a) primary hair follicle (b) secondary hair follicles.

Van Gieson x 40

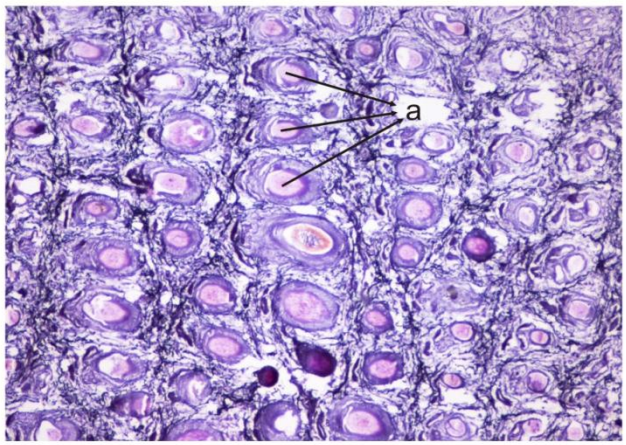

Plate 24- Horizontal section of the skin of spotted deer showing (a)hair follicles arranged in a linear fashion.

Weigerts resorcine fuchsin x 40

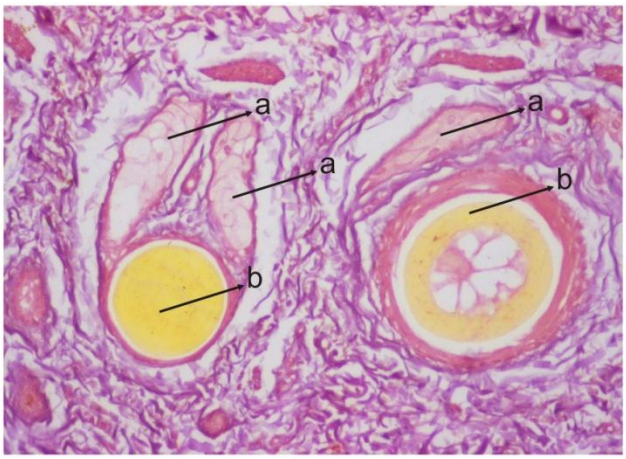

Plate 25- Horizontal section of the skin of spotted deer showing (a) Sebaceous glands surrounds the (b)Primary hair follicle.

van Gieson x 100

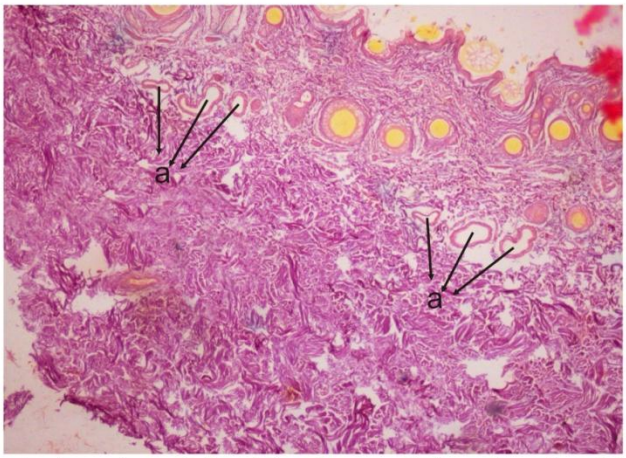

Plate 26- Vertical section of the skin of spotted deer showing (a) Merocrine Simple tubular Sweat glands

van Gieson x 100

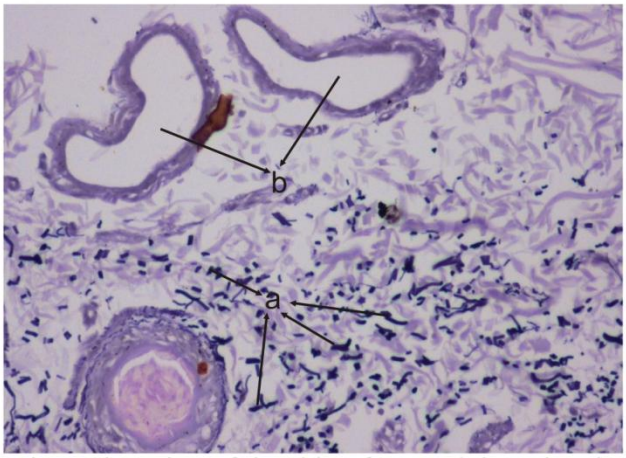

Plate 27- Horizontal section of the skin of spotted deer showing (a) Elastic fibers and (b) Sweat glands in the dermis.

Weigerts resorcine fuchsin x 100

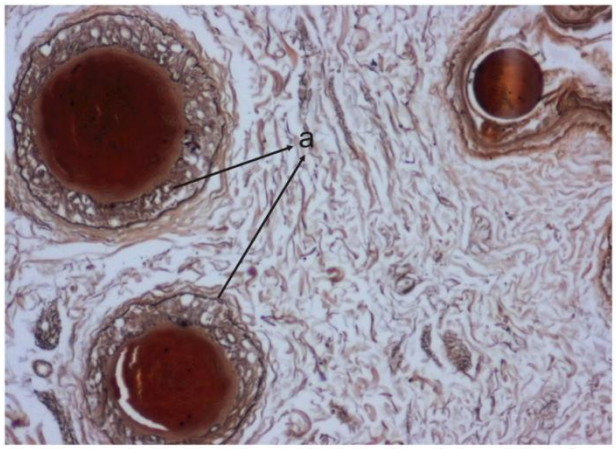

Plate 28- Horizontal section through dermis of the skin of Spotted deer showing (a) Nerve fibers encircling the primary and secondary hair follicle. Bielschowsky stain x200

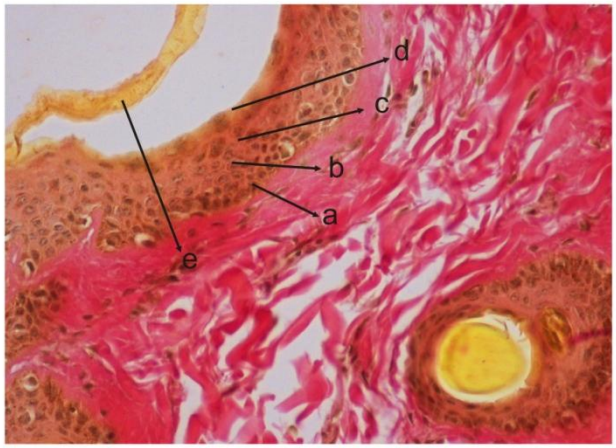

Plate 29- Vertical section through epidermis of the skin of Cattle showing, (a) stratum basale (b) stratum spinosum (c) stratum granulosum (d) stratum lucidum (e) stratum corneum. van Gieson x 200

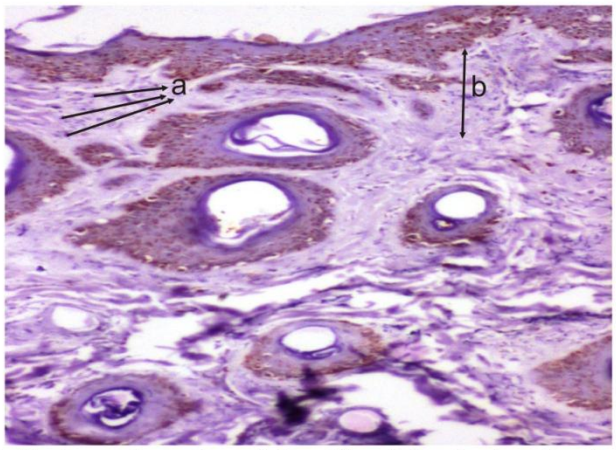

Plate 30- Horizontal section of the skin of Cattle showing (a) Elastic fibers in the (b)papillary layer of dermis. Weigerts resorcine fuchsin x 100

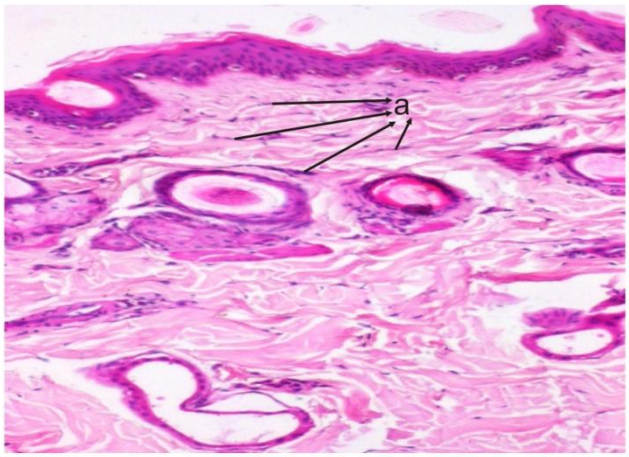

Plate 31- Vertical section through dermis of the skin of Cattle showing few (a)Collagen fibers

H & E Phloxine x 100

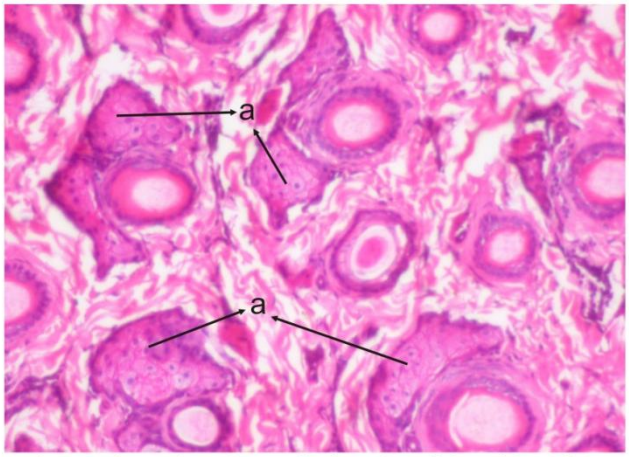

Plate 32- Horizontal section through dermis of the skin of Cattle showing (a)Sebaceous glands

H & E Phloxine x 100

Plate 33- Horizontal section of the skin of Cattle showing (a) Coiled tubular Sweat glands

van Gieson x 100

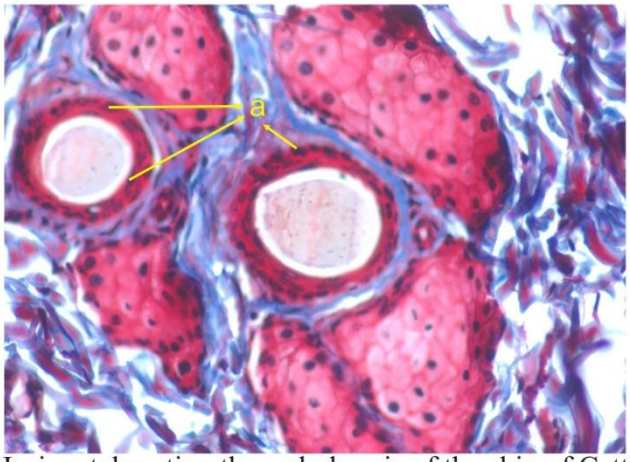

Plate 34- Horizontal section through dermis of the skin of Cattle showing hair follicle showed elongated oval shaped pigments.
Masson's Trichrome stain x200

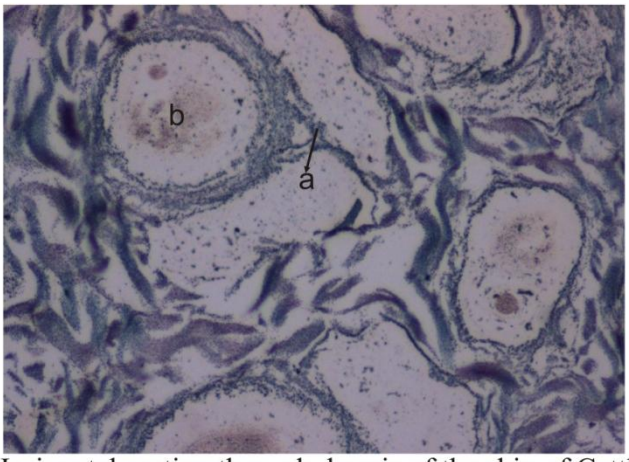

Plate 35- Horizontal section through dermis of the skin of Cattle showing (a) Nerve fibers encircling and penetrating the (b) hair follicle.
Bielschowsky stain x200

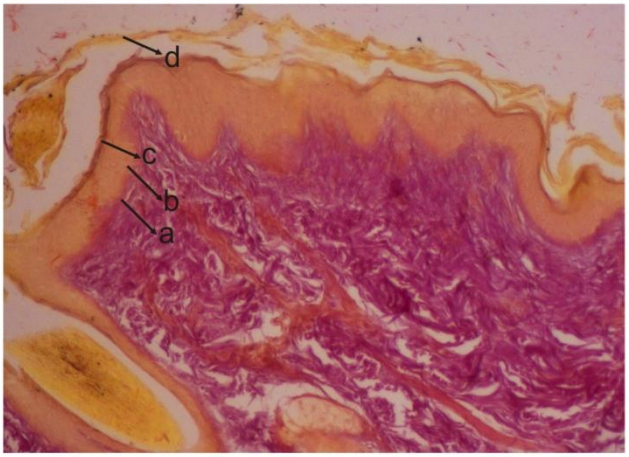

Plate 36 - Vertical section through epidermis of the skin of Goat showing (a) Stratum basale (b) stratum spinosum (c) stratum granulosum (d) stratum corneum.
van Gieson x 100

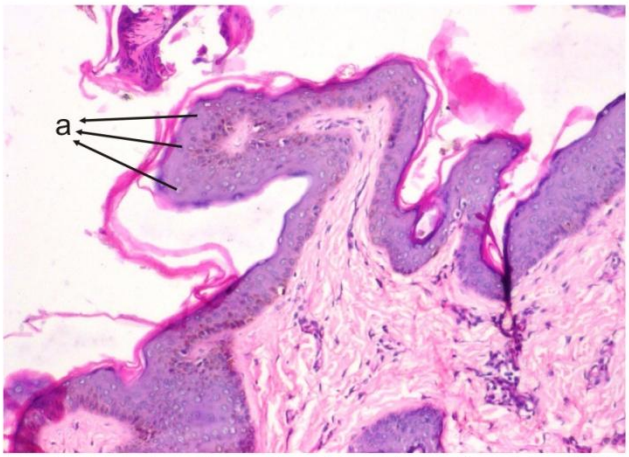

Plate 37 - Vertical section through epidermis of the skin of Goat showing (a)Keratohyaline granules in the stratum granulosum.
H & E Phloxine x 100

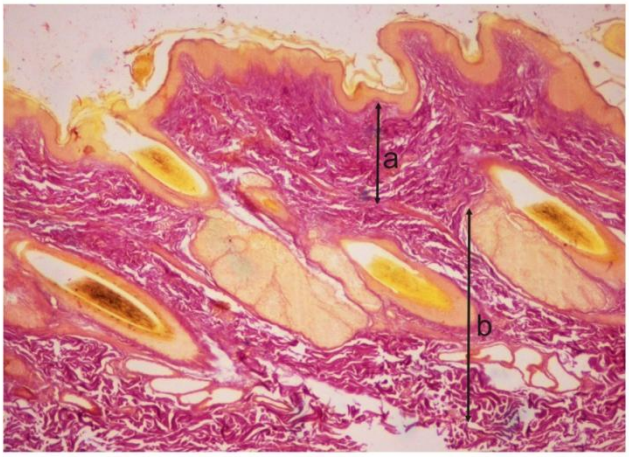

Plate 38- Vertical section through dermis of the skin of Goat showing few collagen fibers in both (a)Papillary and (b)Reticular layers.
Van Gieson x 40

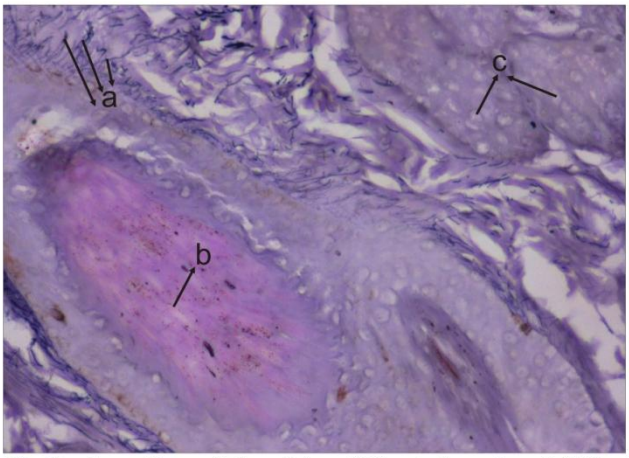

Plate 39- Vertical section of the skin of Goat showing (a)Elastic fibers surrounded the (b)Primary hair follicle and (c)Sebaceous gland.
Weigerts resorcine fuchsin x 200

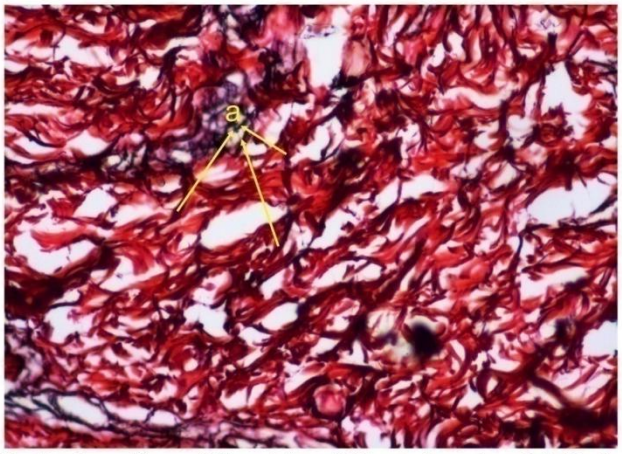

Plate 40- Vertical section of the skin of Goat showing (a) Reticular fibers present in the deeper part of the dermis.
Gomori's silver impregnation stain x 200

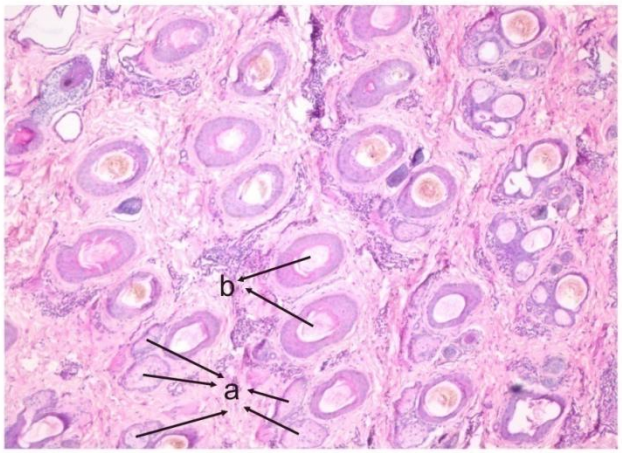

Plate 41- Horizontal section through dermis of the skin of Goat showing paired (a)Sebaceous glands located at the base of the (b)Hair follicles.
H & E Phloxine x 40

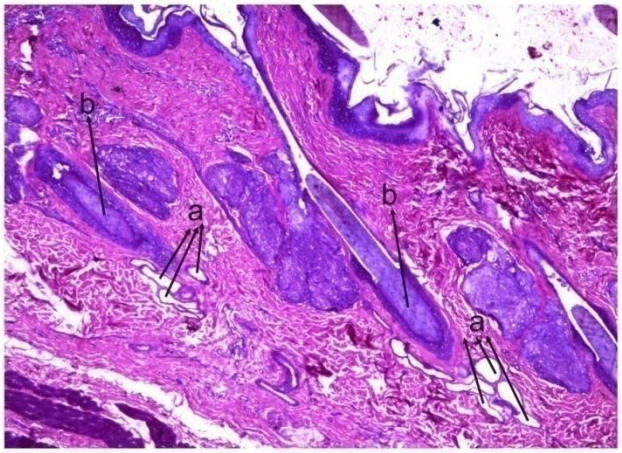

Plate 42- Horizontal section through dermis of the skin of Goat showing (a)Simple tubular sweat glands below the (b)Primary hair follicles.
PTAH x40

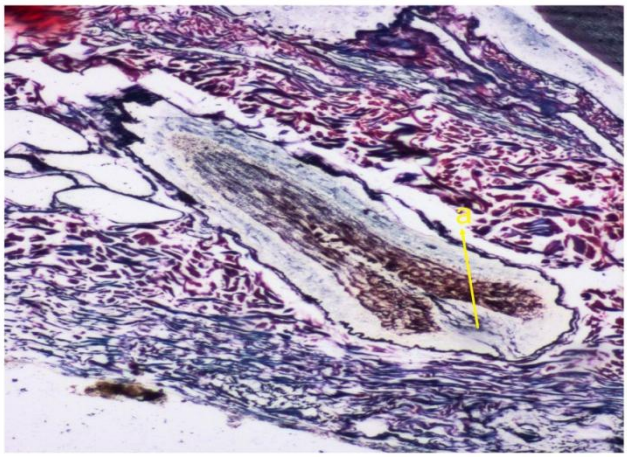

Plate 43- Horizontal section through dermis of the skin of Goat showing (a) Nerve fibers penetrating into the hair follicle.
Bielschowsky stain x100

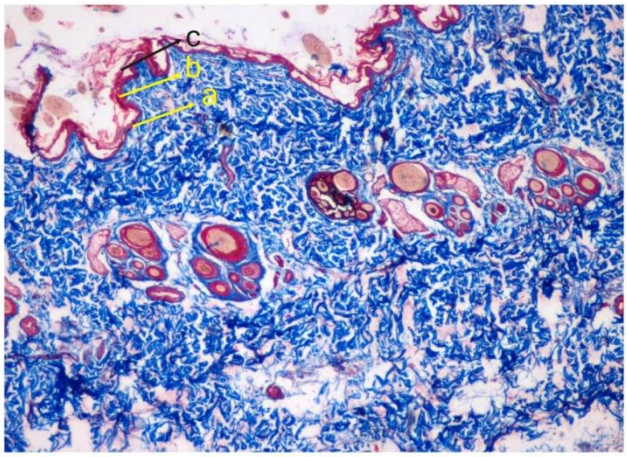

Plate 44- Vertical section through epidermis of the skin of Dog showing, (a) Stratum basale (b) Stratum spinosum © Stratum corneum.
Masson's Trichrome stain x40

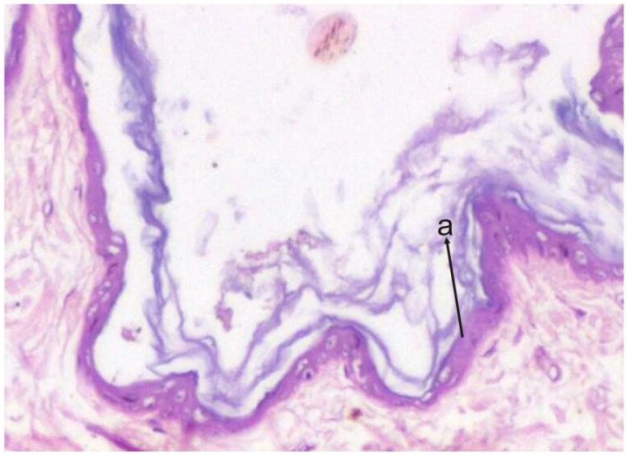

Plate 45 - Vertical section through epidermis of the skin of Dog showing (a)Stratum spinosum composed of ten to fifteen cell layers.
H & E Phloxine x 100

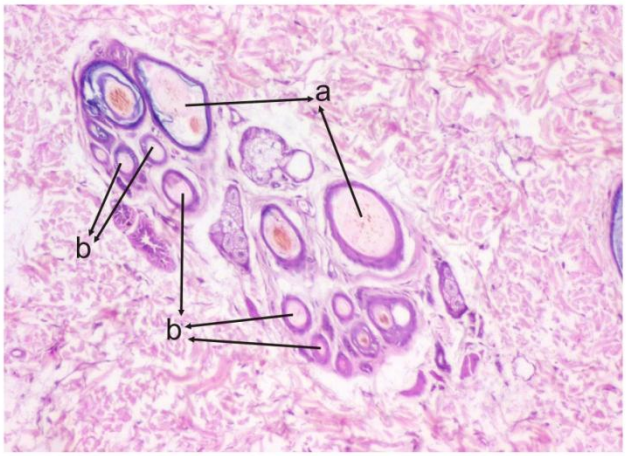

Plate 46- Horizontal section through dermis of the skin of Dog showing (a)Primary hair follicle (b) Secondary hair follicles.
H & E Phloxine x 100

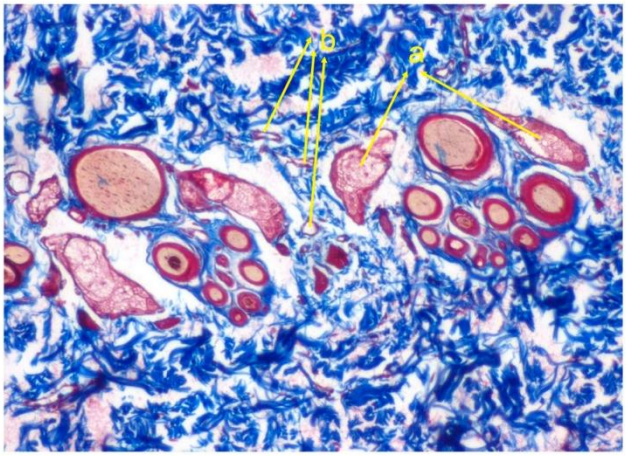

Plate 47- Horizontal section through dermis of the skin of Dog showing (a) Sebaceous glands (b) Sweat glands
Masson's Trichrome stain x100

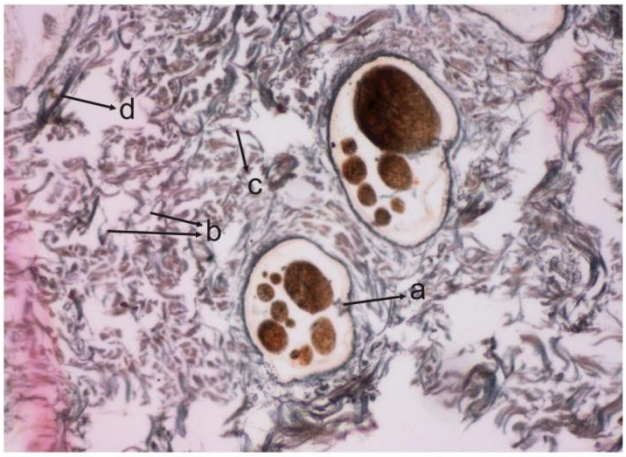

Plate 48- Horizontal section through dermis of the skin of Dog showing mixture of (a) Nerve fibers (b) Reticular fibers (c) Collagen fibers (d) Elastic fibers.
Bielschowsky stain x100

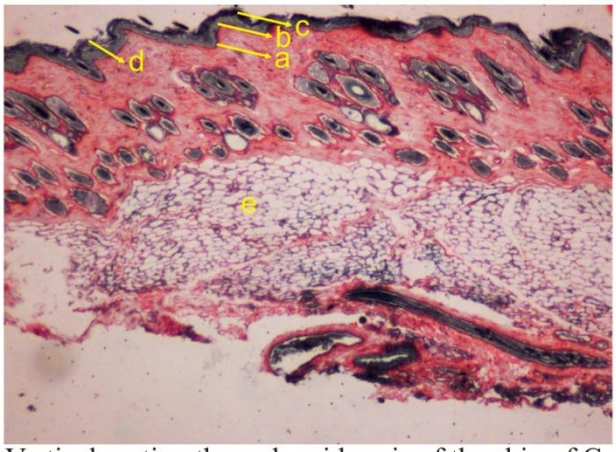

Plate 49- Vertical section through epidermis of the skin of Cat showing
(a) Stratum basale (b) Stratum spinosum (c) Stratum granulosum (d) Stratum corneum.
(e) Adipose tissue

Gomori's silver impregnation stain x 40

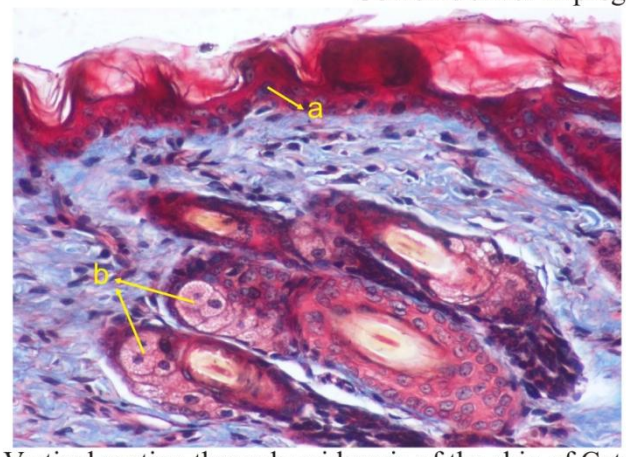

Plat 50 -Vertical section through epidermis of the skin of Cat showing
(a)Stratum spinosum composed of single cell layer, dark with distinct nucleated cells.
(b) Sebaceous glands

Masson's Trichrome stain x100

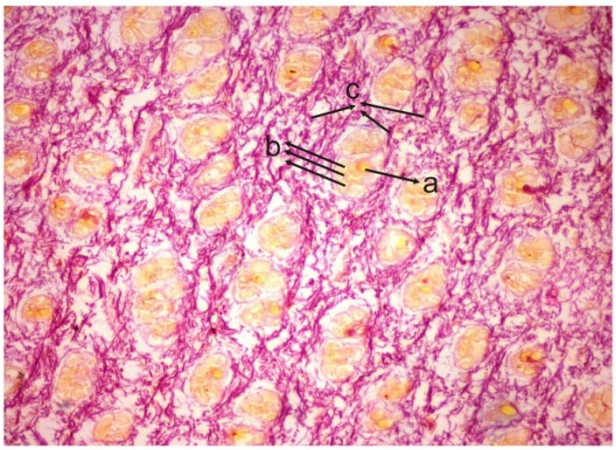

Plate 51- Horizontal section through dermis of the skin of Cat showing cluster of compound hair follicle (a) Primary hair follicle (b) Secondary hair follicles(c)Collagen fibers.

van Gieson x 40

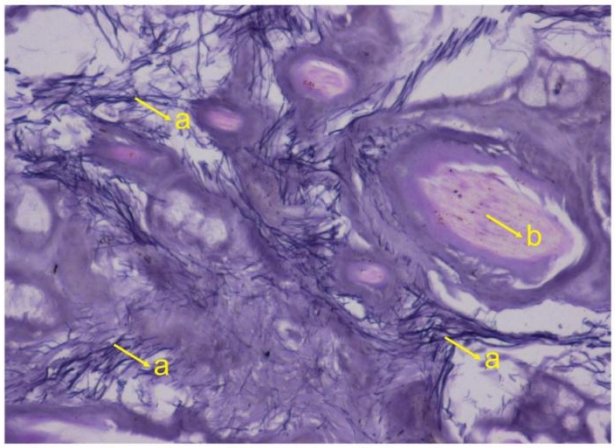

Plate 52- Horizontal section of the skin of Cat showing irregular (a)Elastic fibers distributed around the (b)Primary hair follicle and interfollicular space.
Weigerts resorcine fuchsin x 200

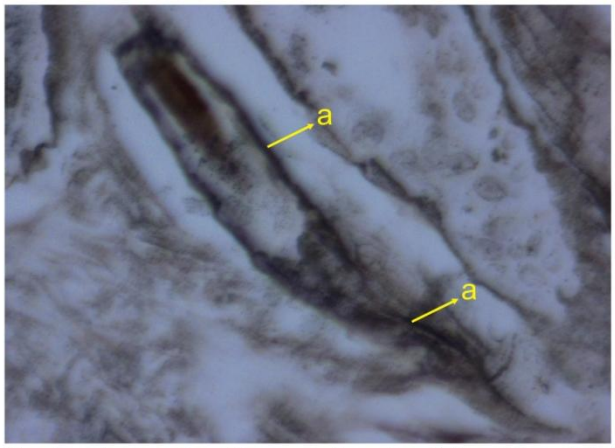

Plate 53- Horizontal section through dermis of the skin of Cat showing (a) Nerve fibers surrounding primary and secondary hair follicle.
Bielschowsky stain x100

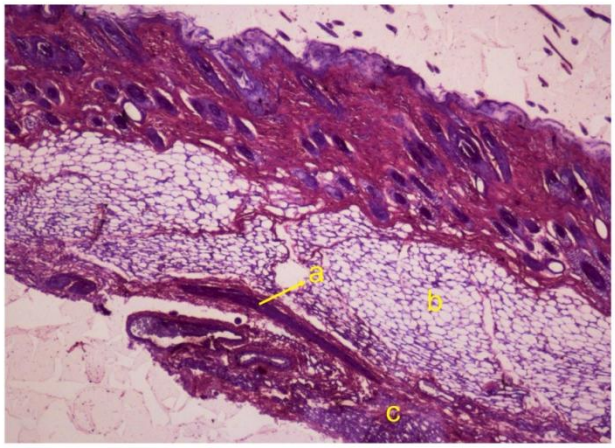

Plate 54- Horizontal section through dermis of the skin of Cat showing (a) Skeletal muscle fibers between the (b)Adipose cells of dermis and (c) Hypodermis.
PTAH x40

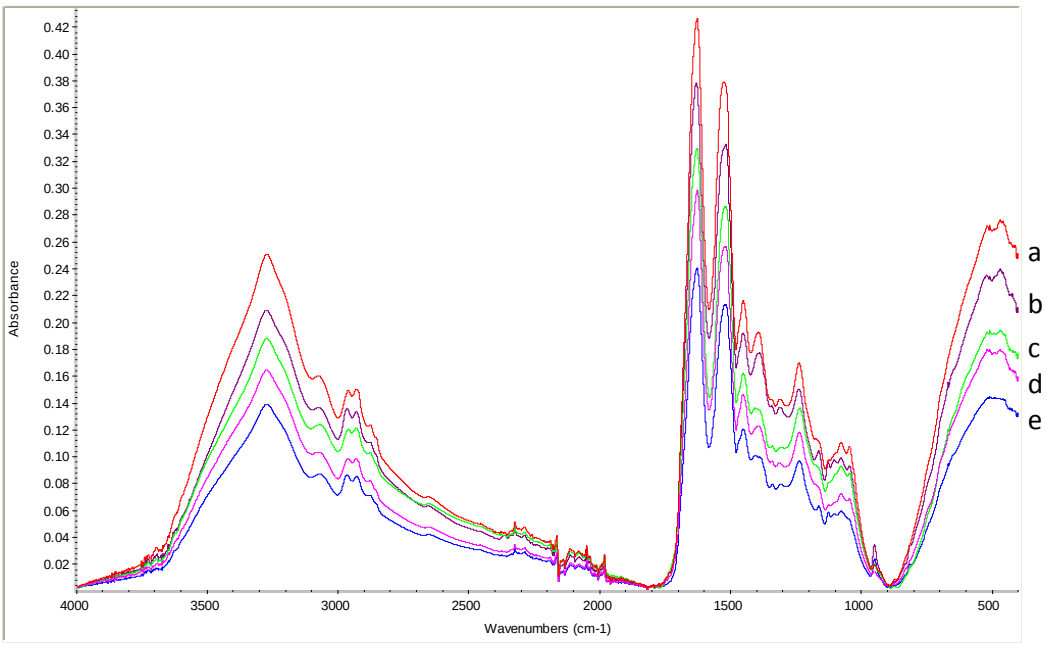

Fig 1 : Showing composite FTIR Spectra of Hairs __a__: Cattle __b__ : Goat __c_ : Leopard _d__ : Spotted Deer __e__ : Tiger

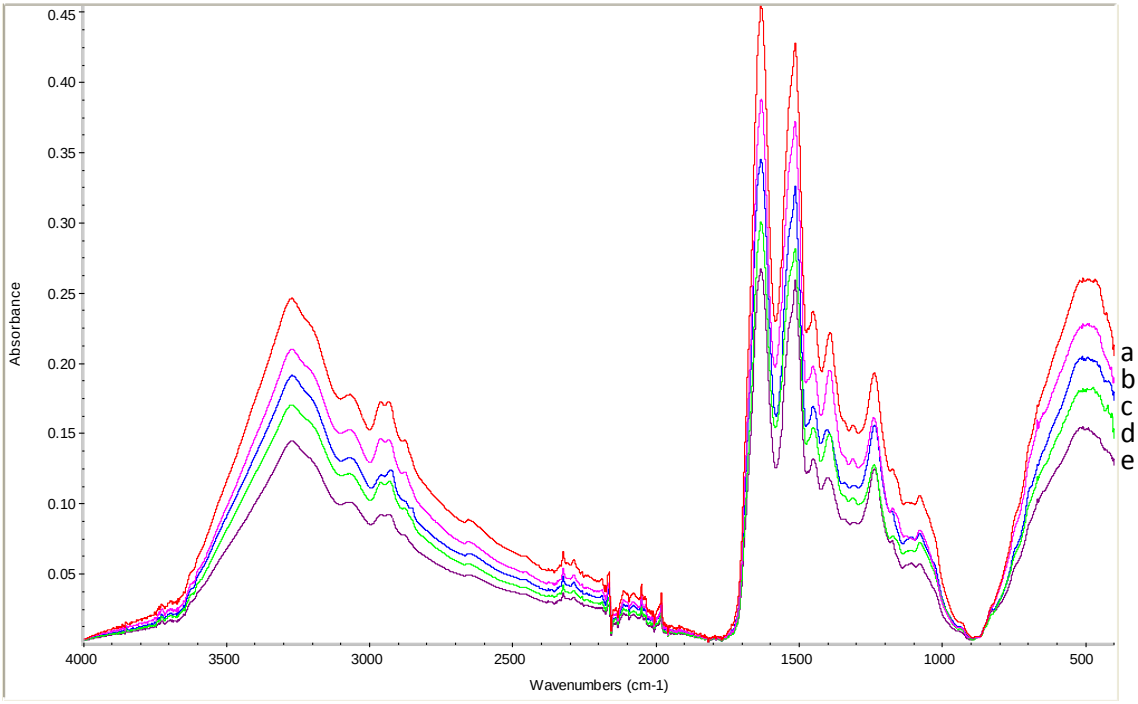

Fig 2 : Showing composite FTIR Spectra of hoofs and claws __a__: Cattle __b_: Goat __c__: Leopard __d_: Spotted Deer __e__: Tiger

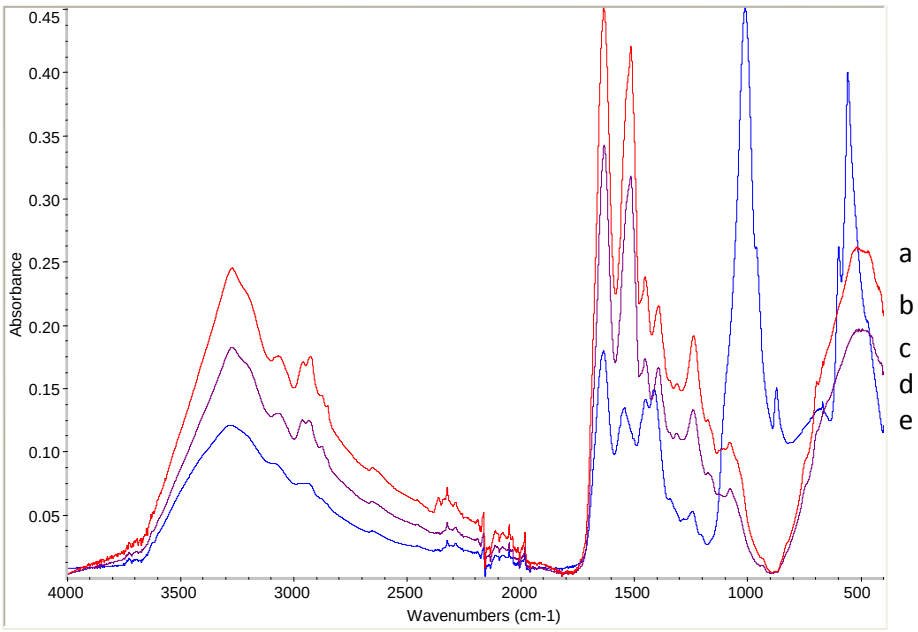

Fig 3 : Showing composite FTIR Spectra of horns and Antler__a__: Cattle __b__ : Goat __c__: Spotted Deer.

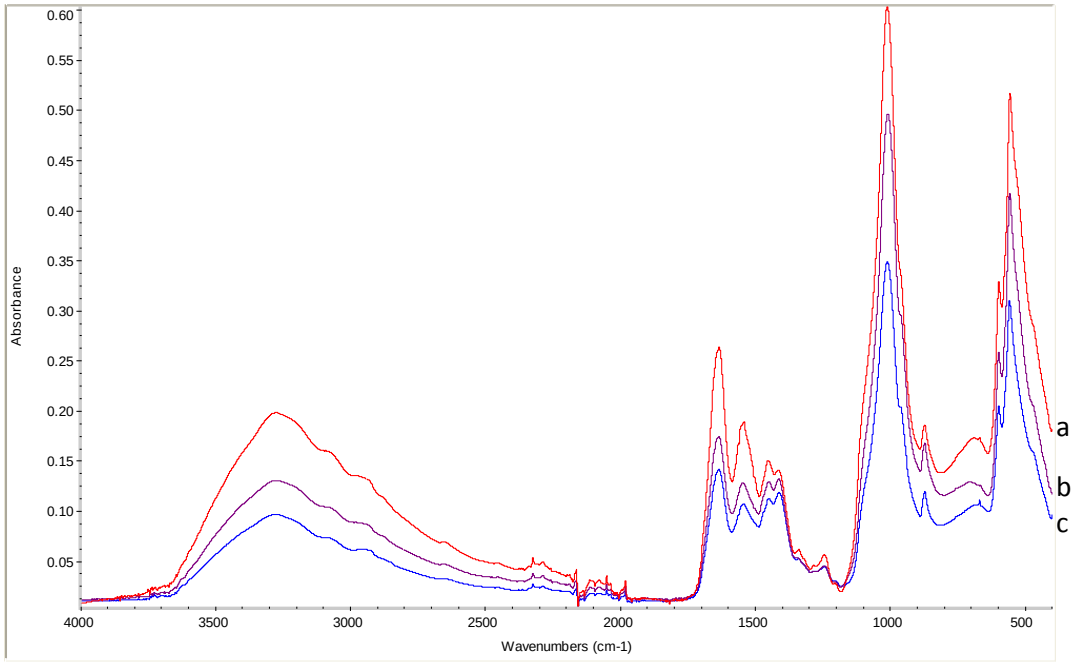

Fig 4 : Showing composite spectra of _a___: Elephant ivory __b__: wild Boar ivory __c__: Spotted Deer antler.

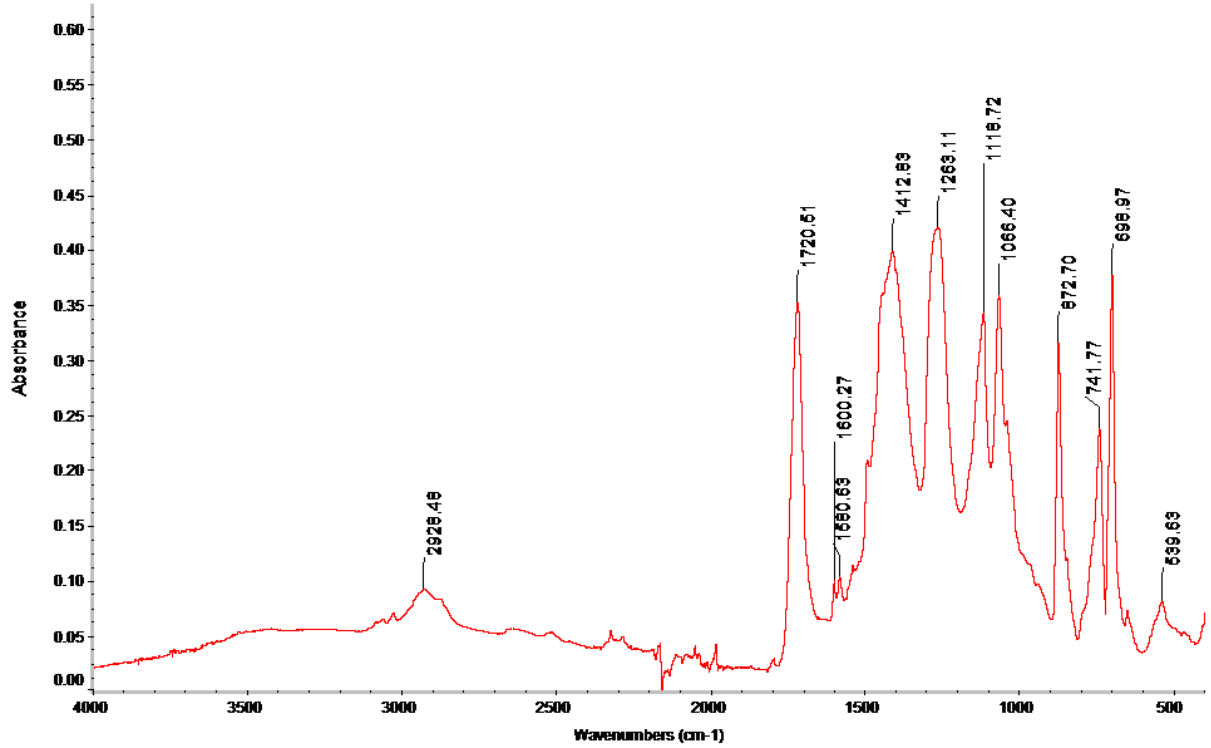

Fig 5: showing primary FTIR Spectrum of artifacts.

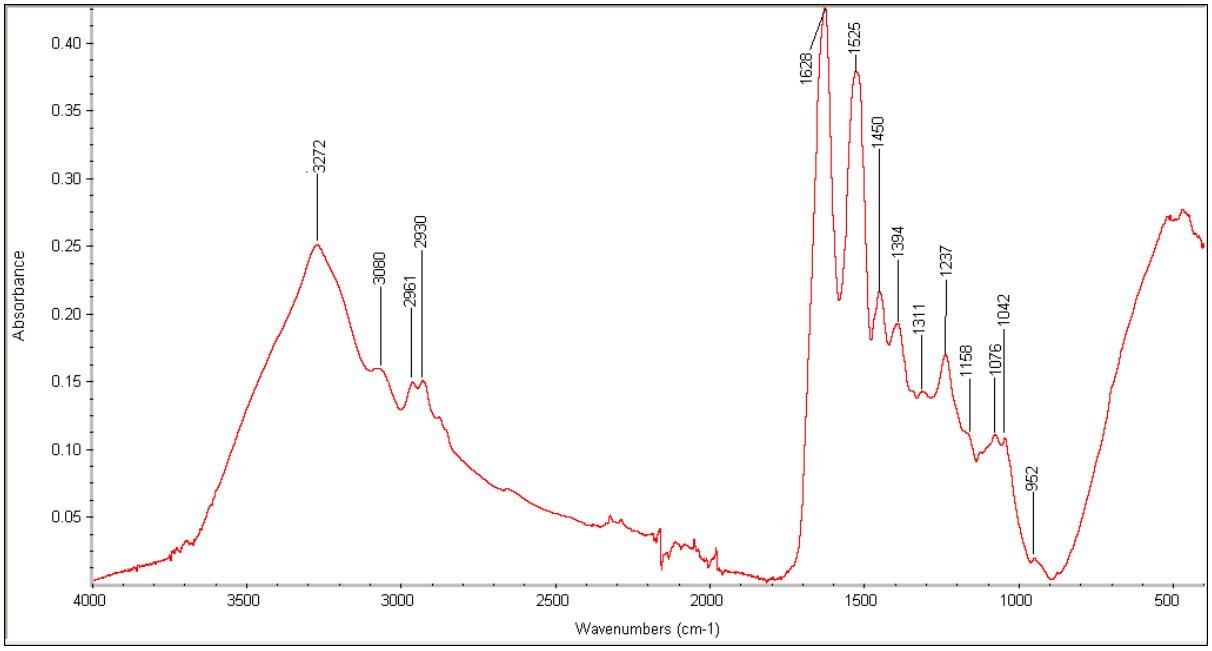

Fig 1(a) Average primary spectrum of cattle hairs

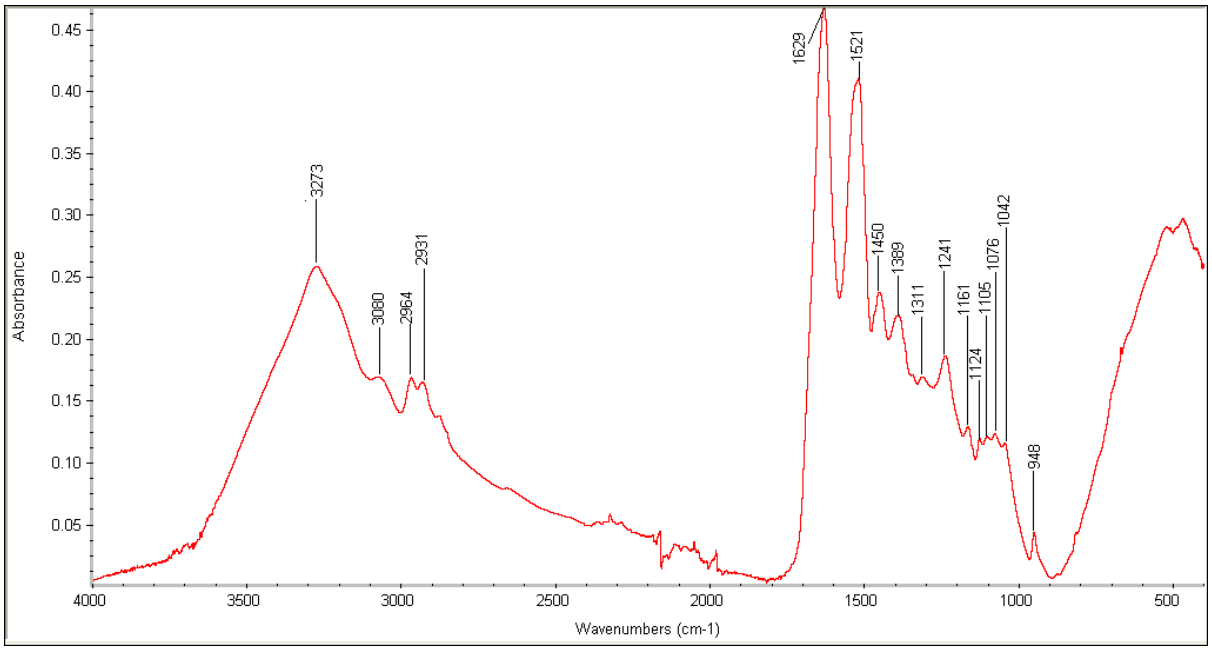

Fig 1(b) Average primary spectrum of goat hairs

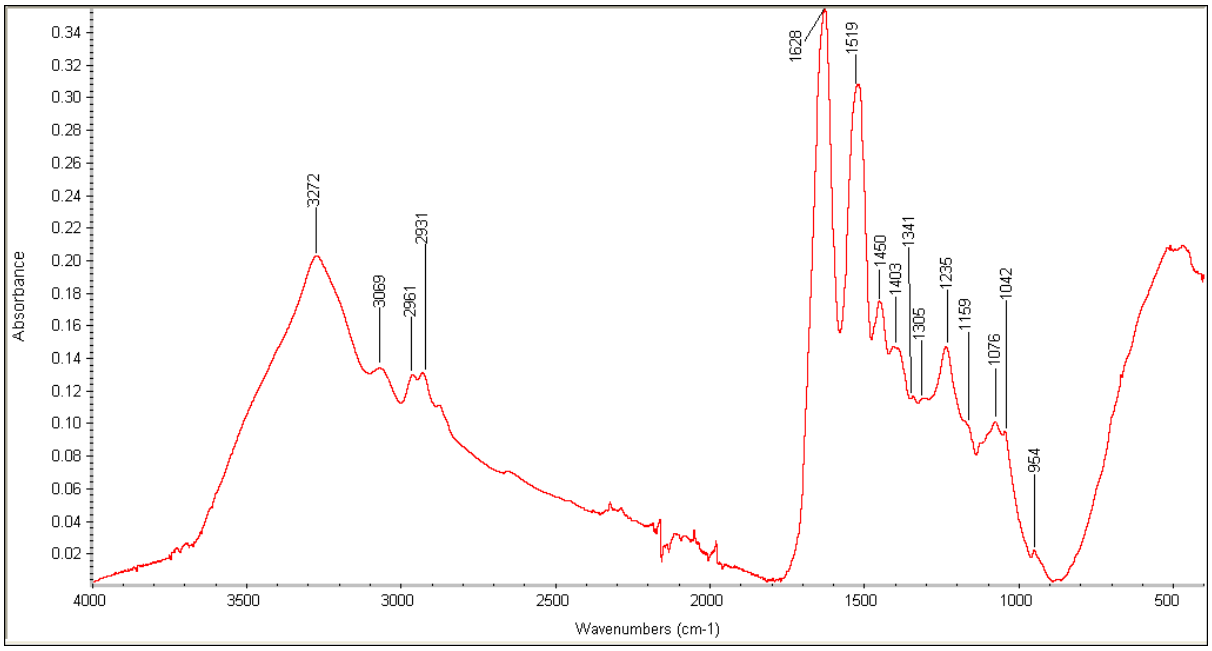

Fig 1(c) Average primary spectrum of leopard hairs

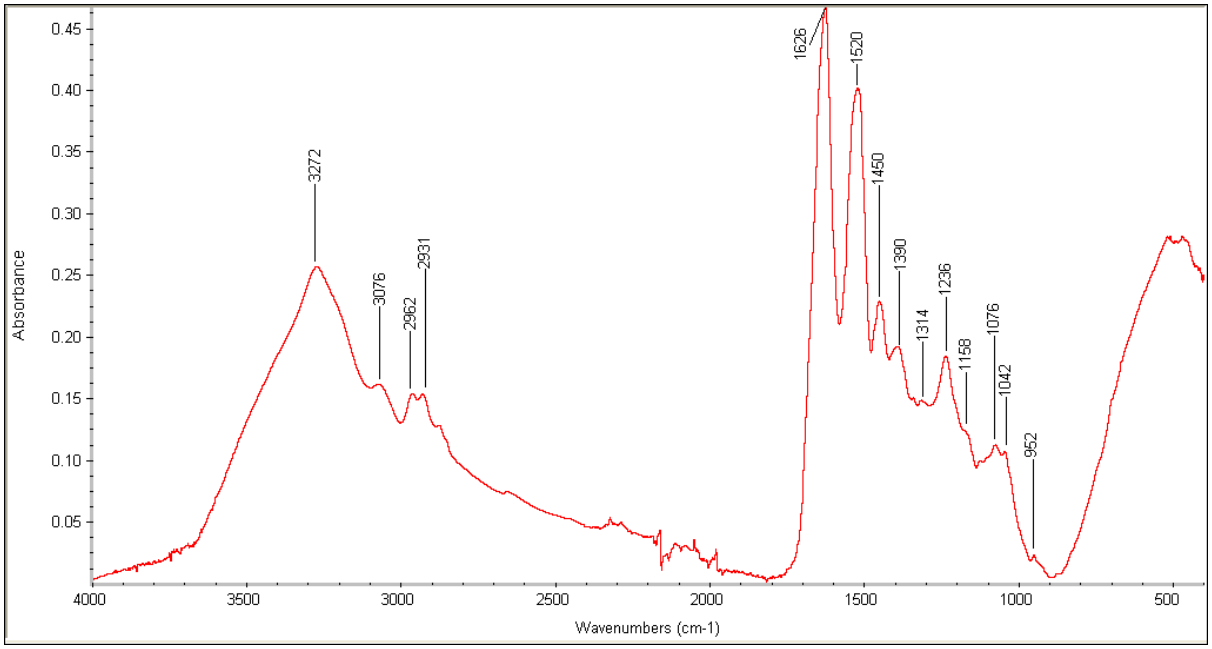

Fig 1(d) Average primary spectrum of spotted deer hair

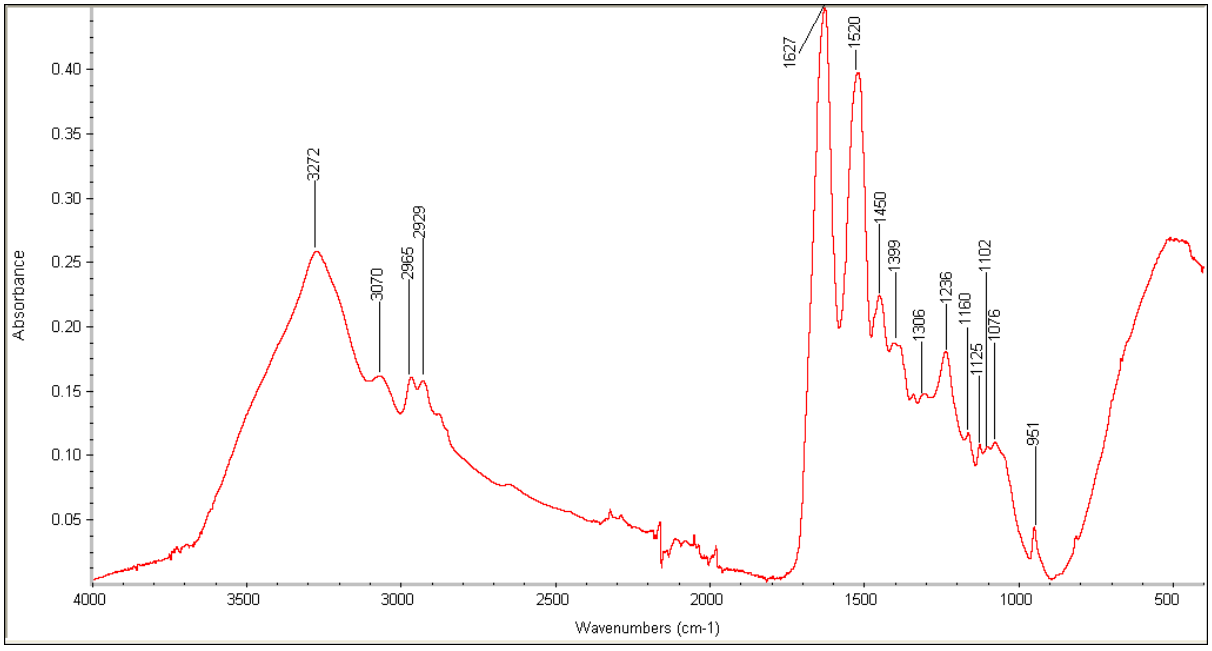

Fig 1(e) Average primary spectrum of tiger hairs

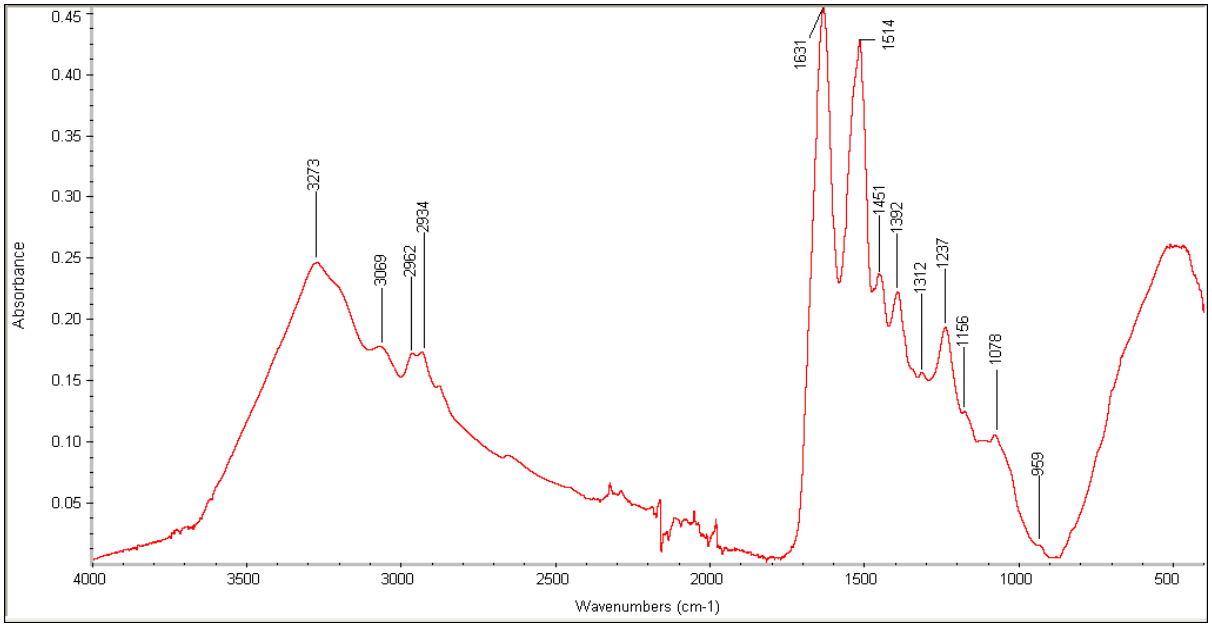

Fig 2(a) Average primary spectrum of cattle hoofs.

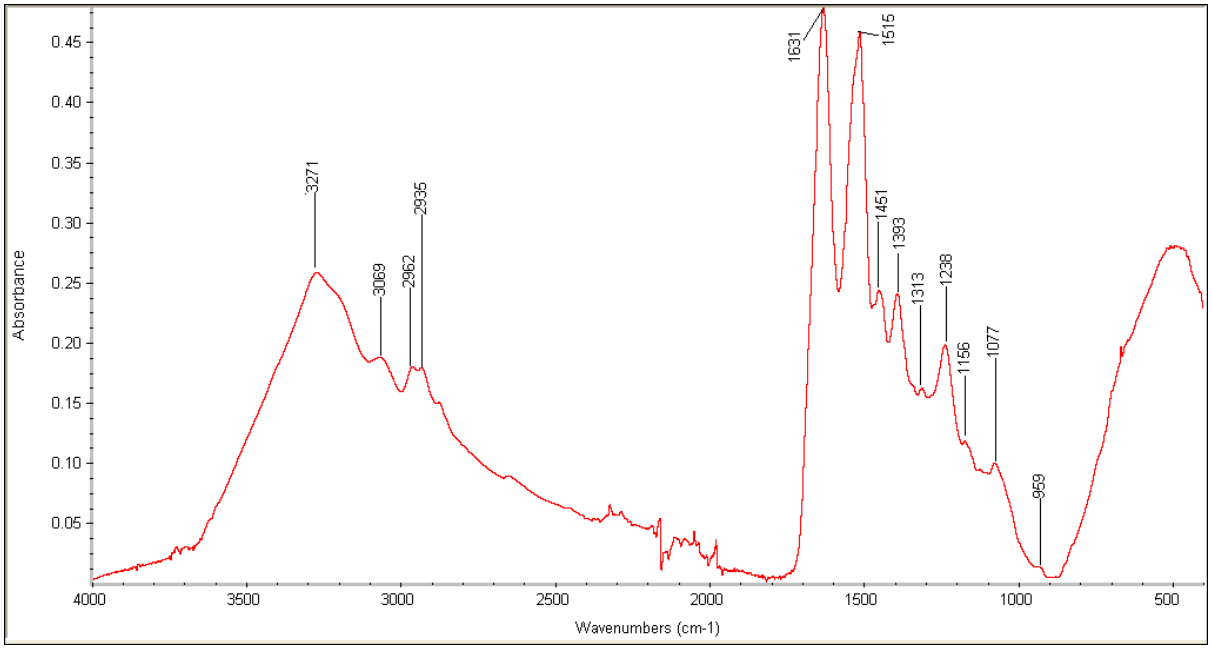

Fig 2(b) Average primary spectrum of goat hoofs.

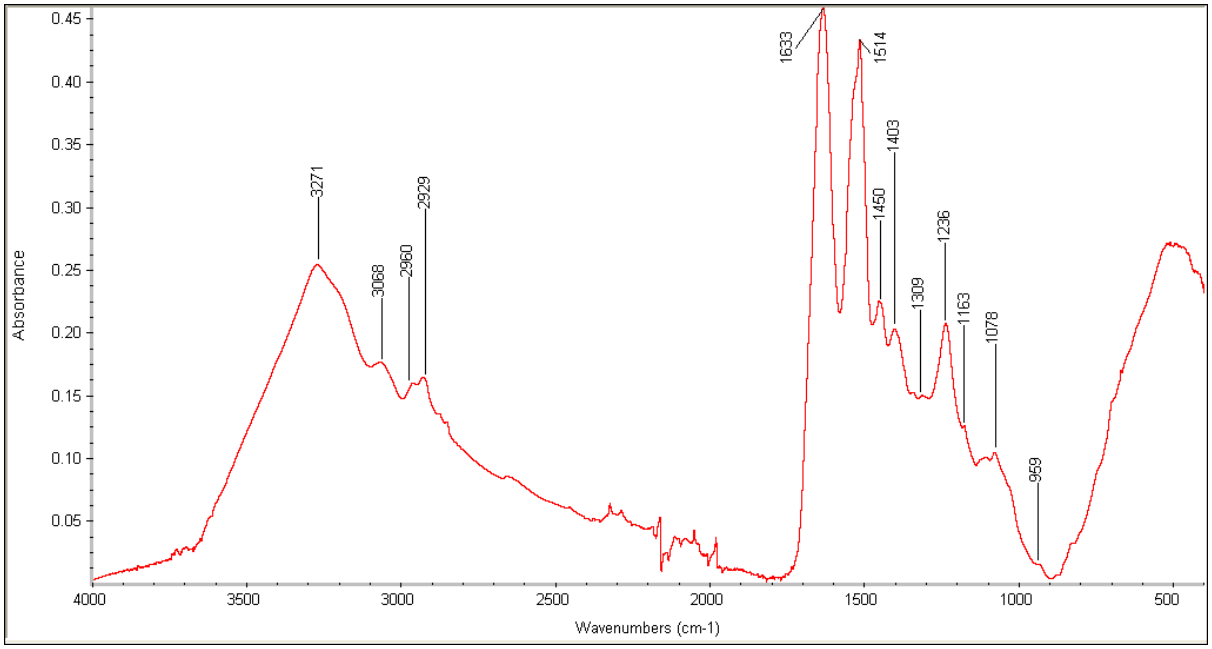

Fig 2(c) Average primary spectrum of leopard claws

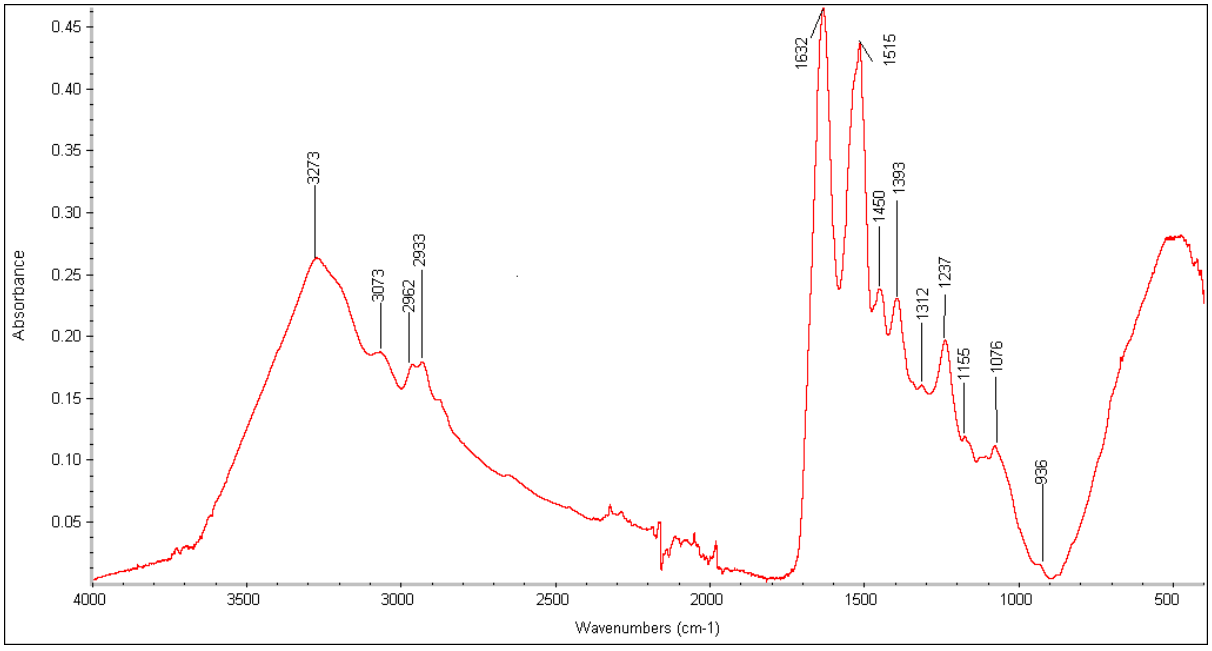

Fig 2(d) Average primary spectrum of spotted deer hoofs.

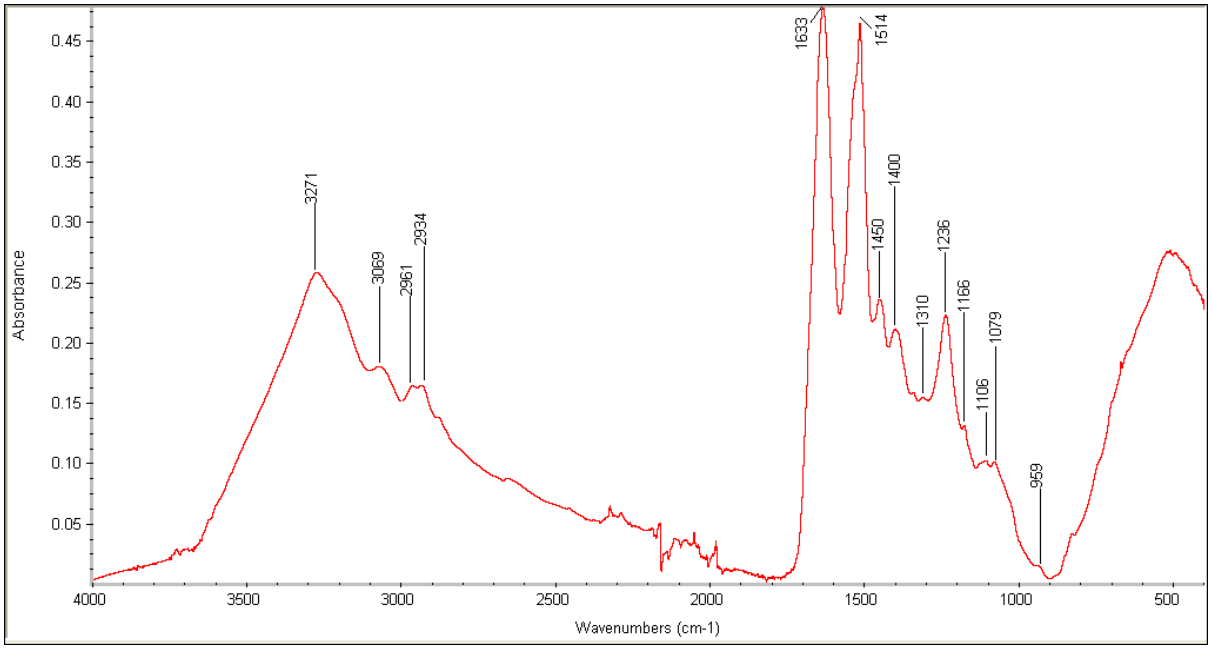

Fig 2(e) Average primary spectrum of tiger claws

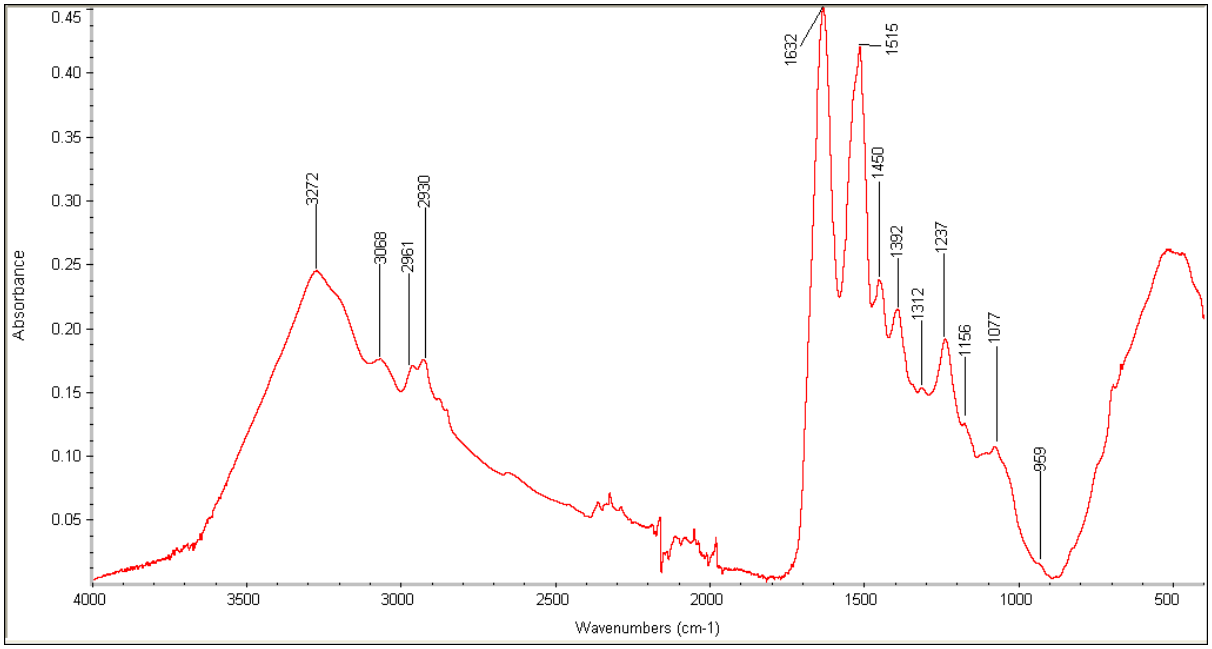

Fig 3(a) Average primary spectrum of cattle horns

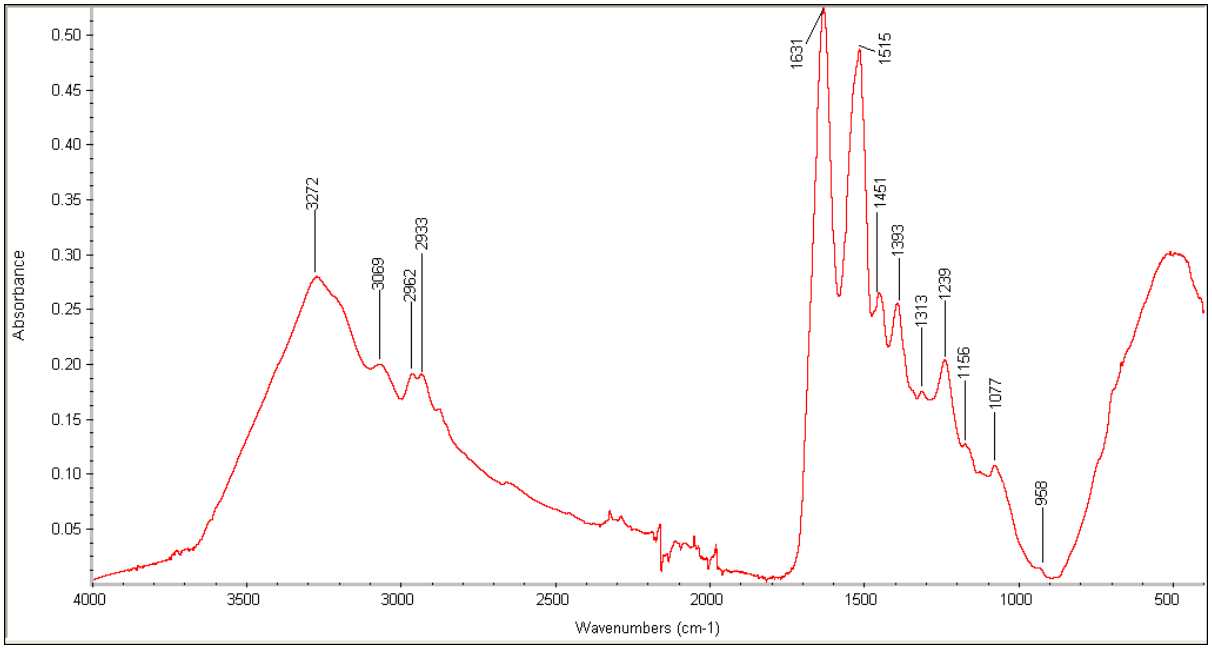

Fig 3(b) Average primary spectrum of goat horns

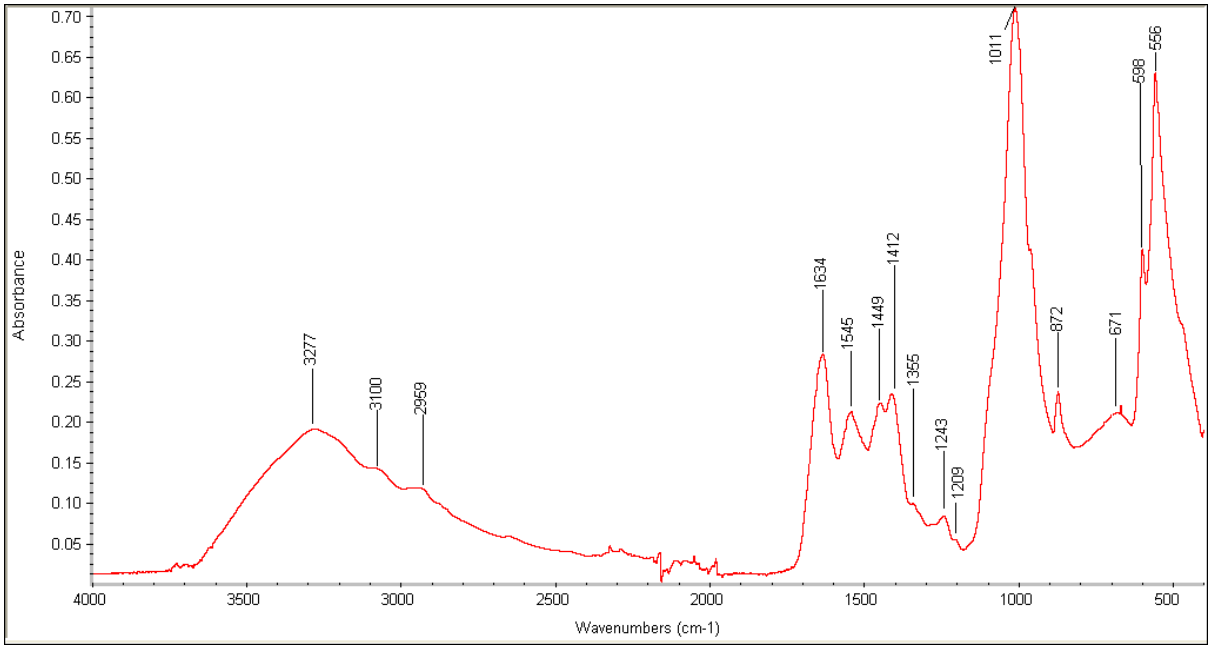

Fig 3(c) and 4(c) Average primary spectrum of spotted deer antlers.

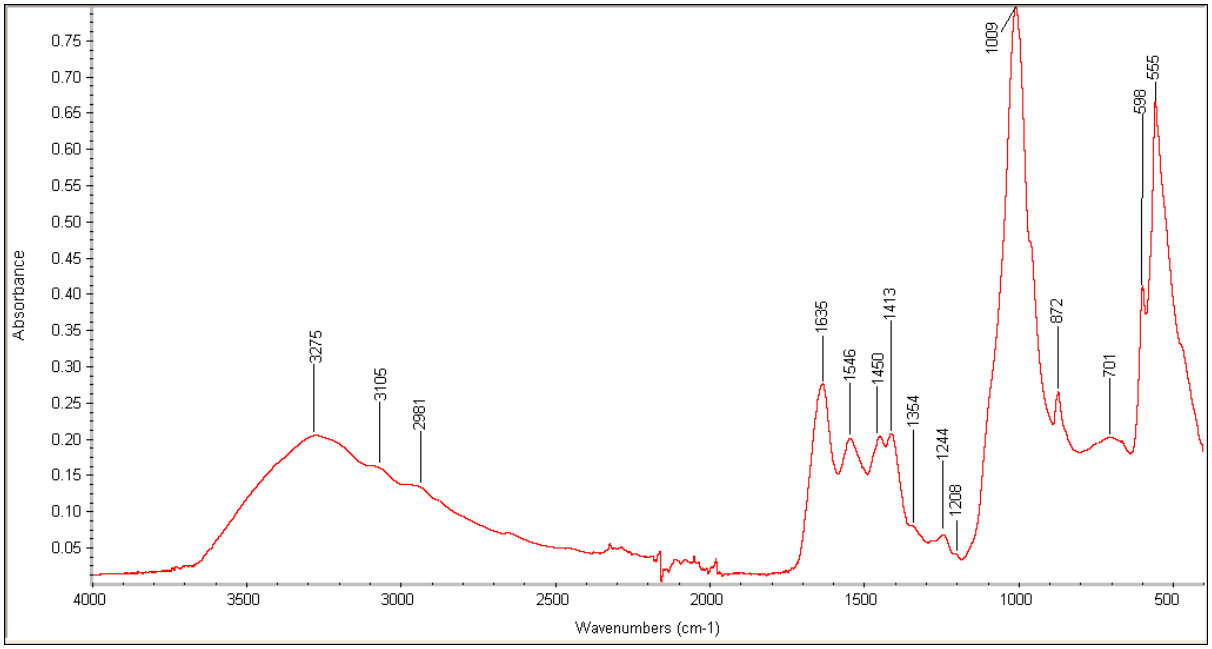

Fig 4(a) Average primary spectrum of wild boar ivory

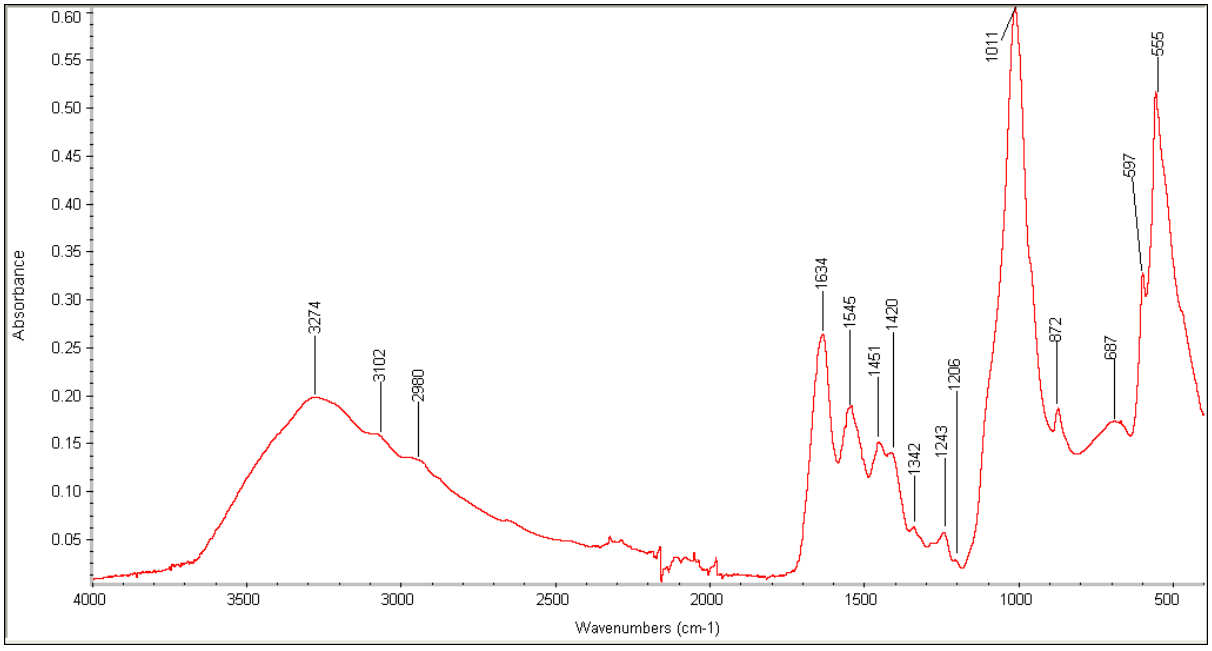

Fig 4(b) Average primary spectrum of elephant ivory

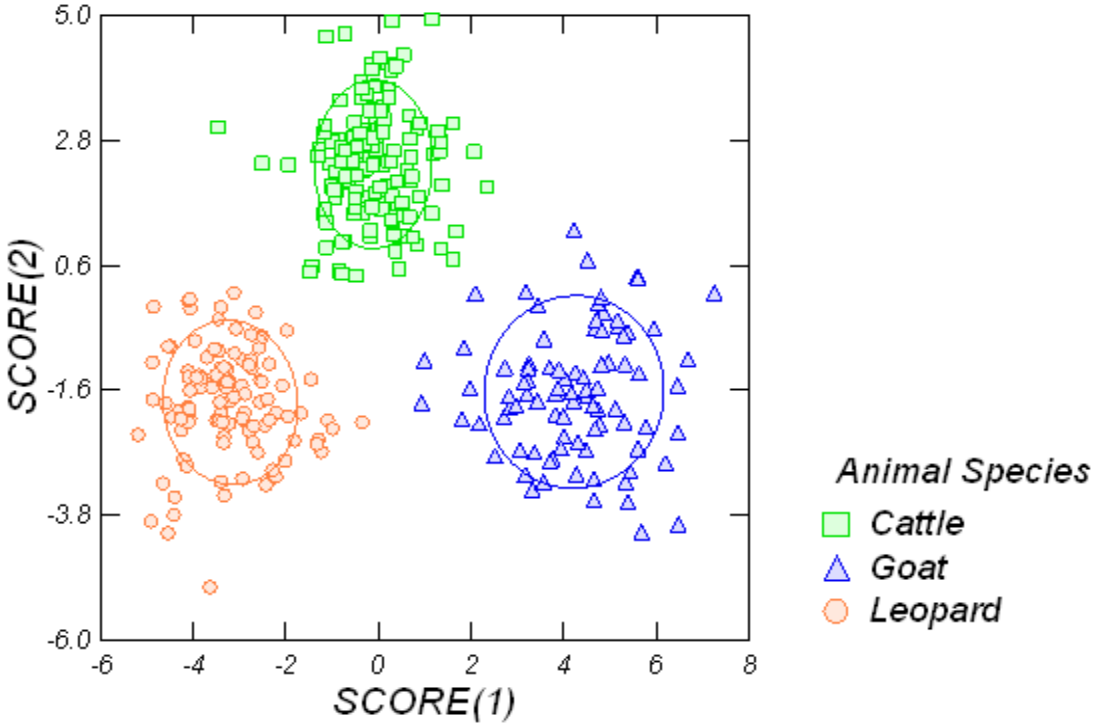

Fig 6 : Showing Peak Area, Peak Height and Peak Height Ratio Combined Canonical Score Plot of cattle, Goat and leopard hairs

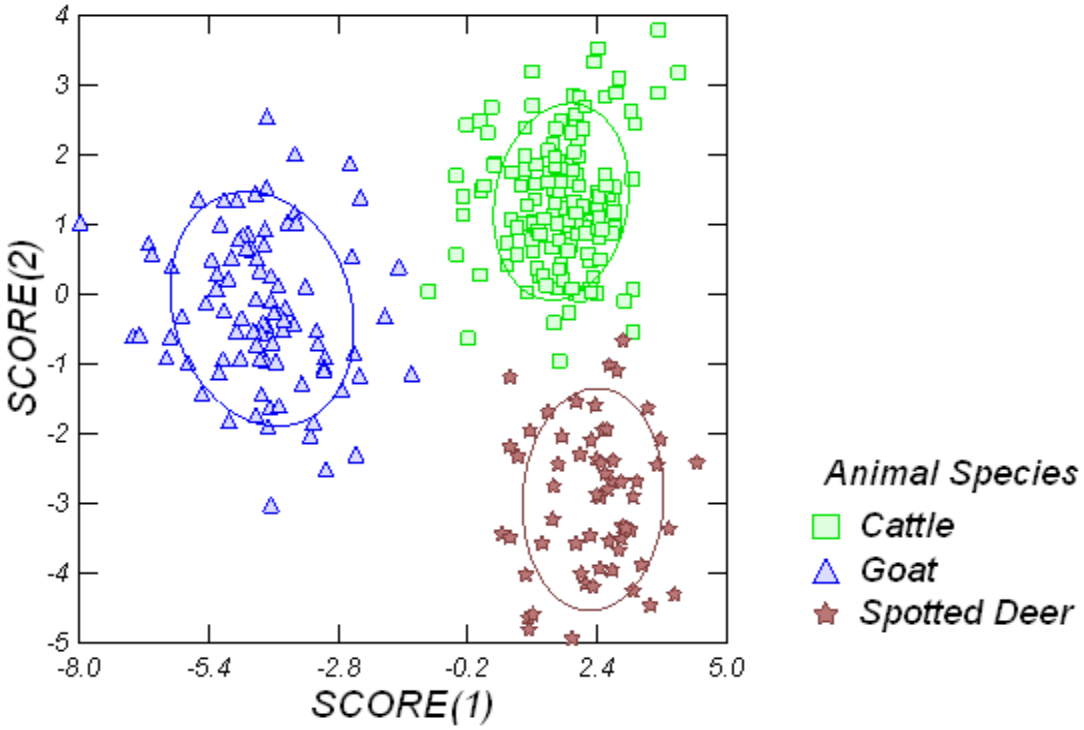

Fig 7 : Showing Peak Area, Peak Height and Peak Height Ratio Combined Canonical Score Plot of cattle, goat and spotted deer hairs

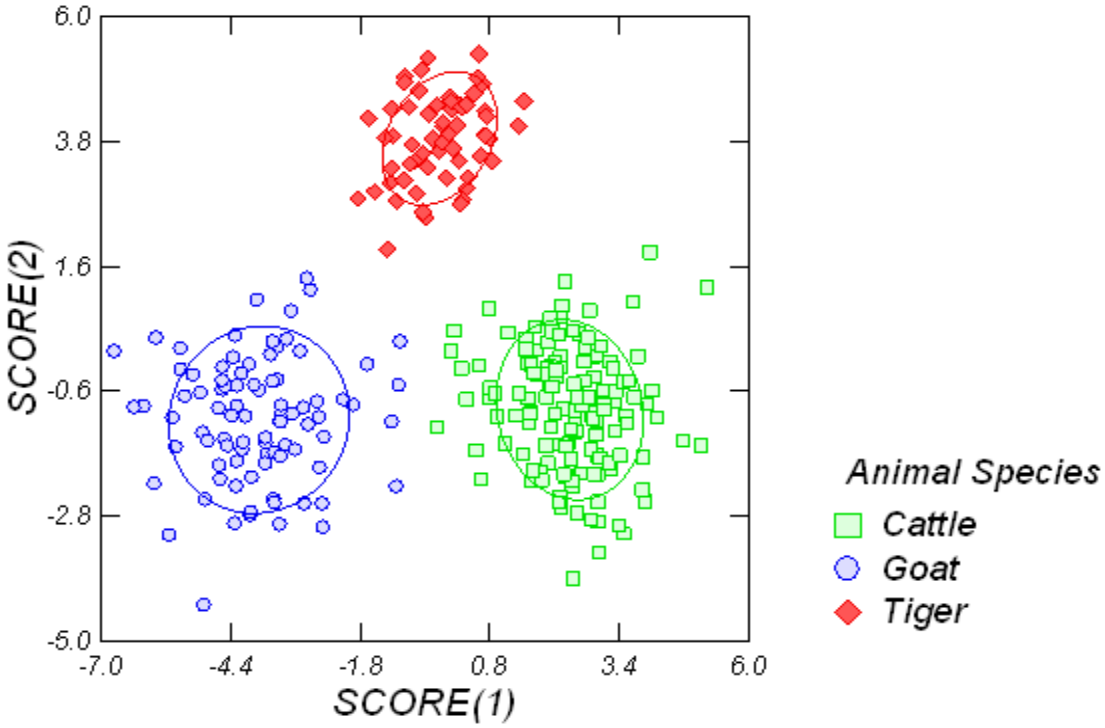

Fig 8 : Showing Peak Area, Peak Height and Peak Height Ratio Combined Canonical Score Plot of cattle, goat and tiger hairs

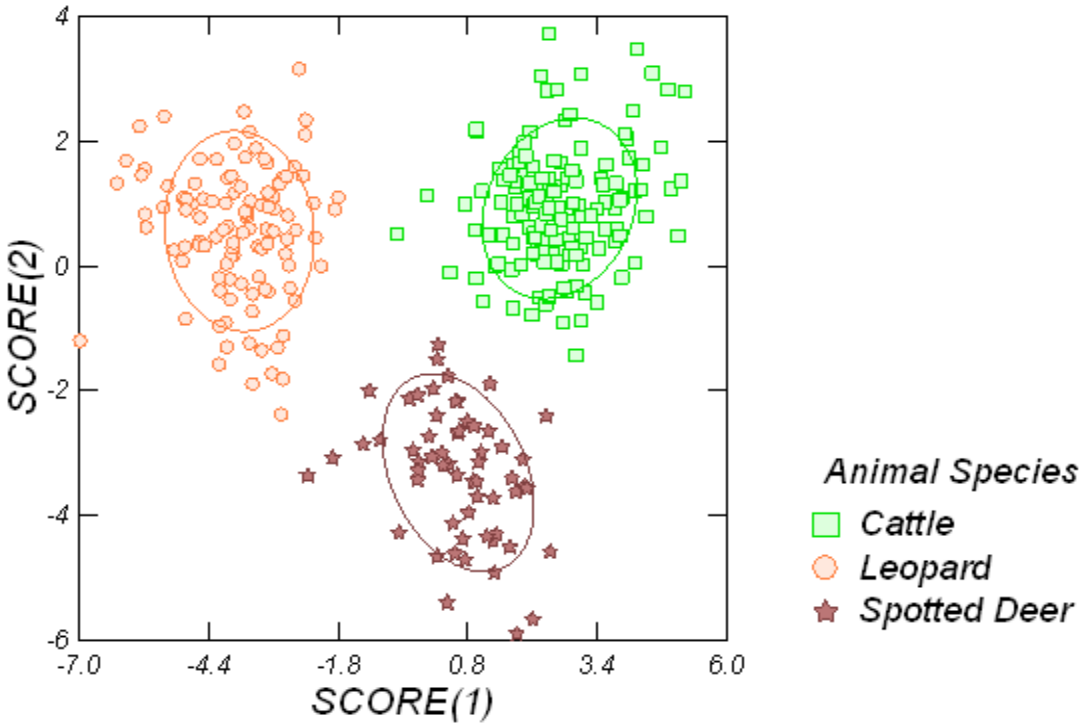

Fig 9 : Showing Peak Area, Peak Height and Peak Height Ratio Combined Canonical Score Plot of cattle, leopard and spotted deer hairs

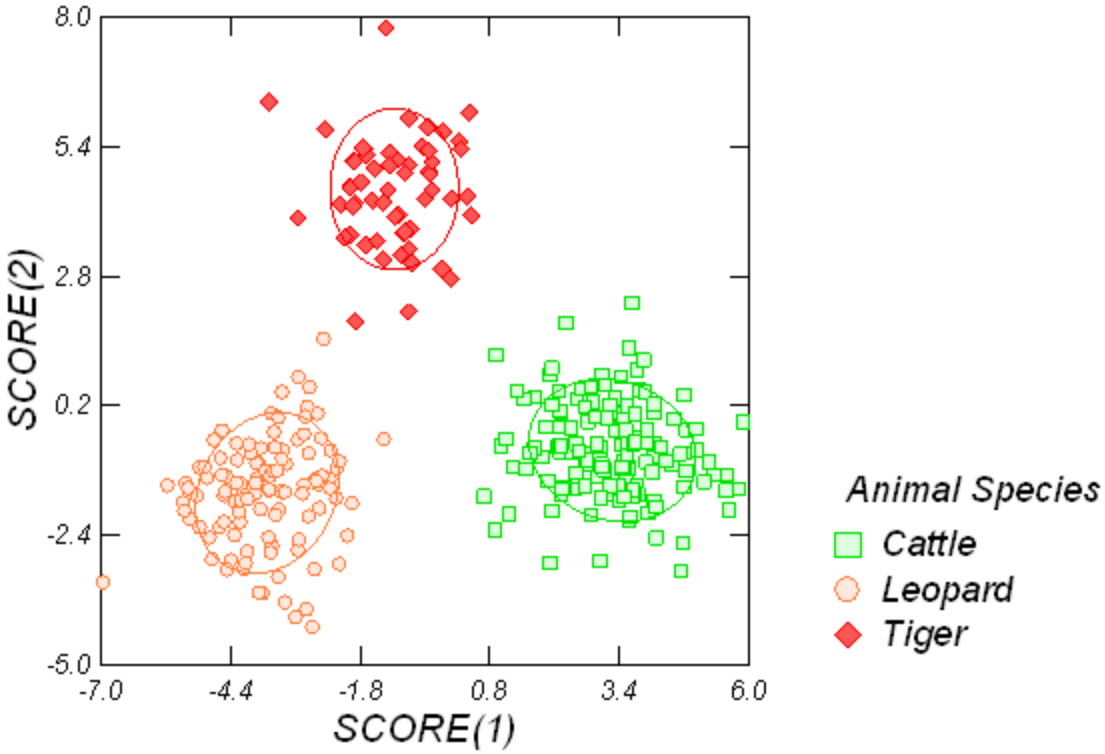

Fig 10 : Showing Peak Area, Peak Height and Peak Height Ratio Combined Canonical Score Plot of cattle, leopard and tiger hairs

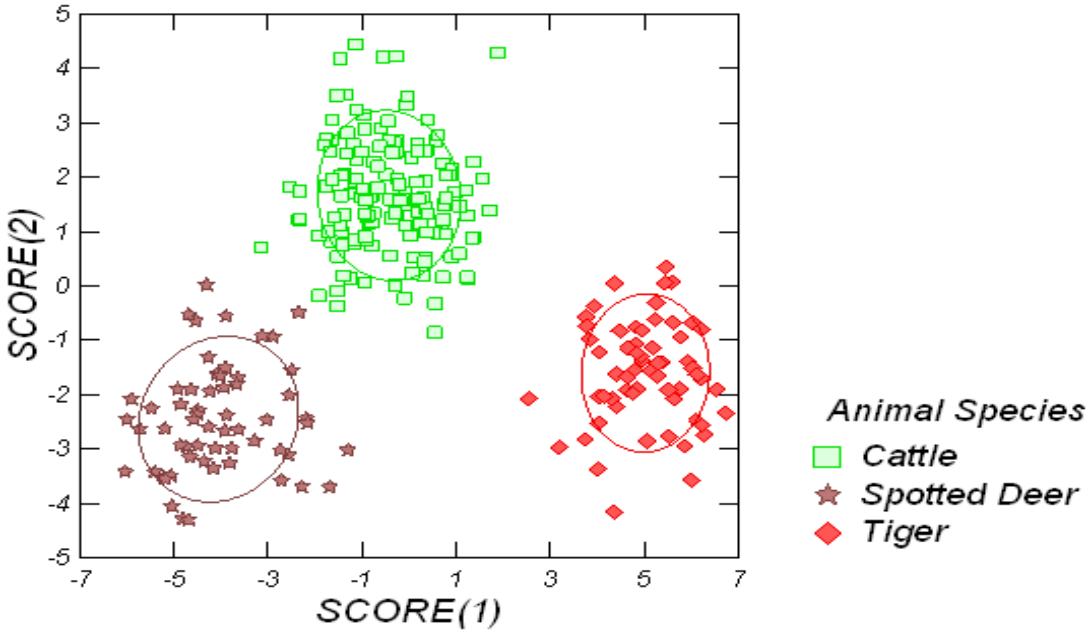

Fig 11 : Showing Peak Area, Peak Height and Peak Height Ratio Combined Canonical Score Plot of cattle, spotted deer and tiger hairs

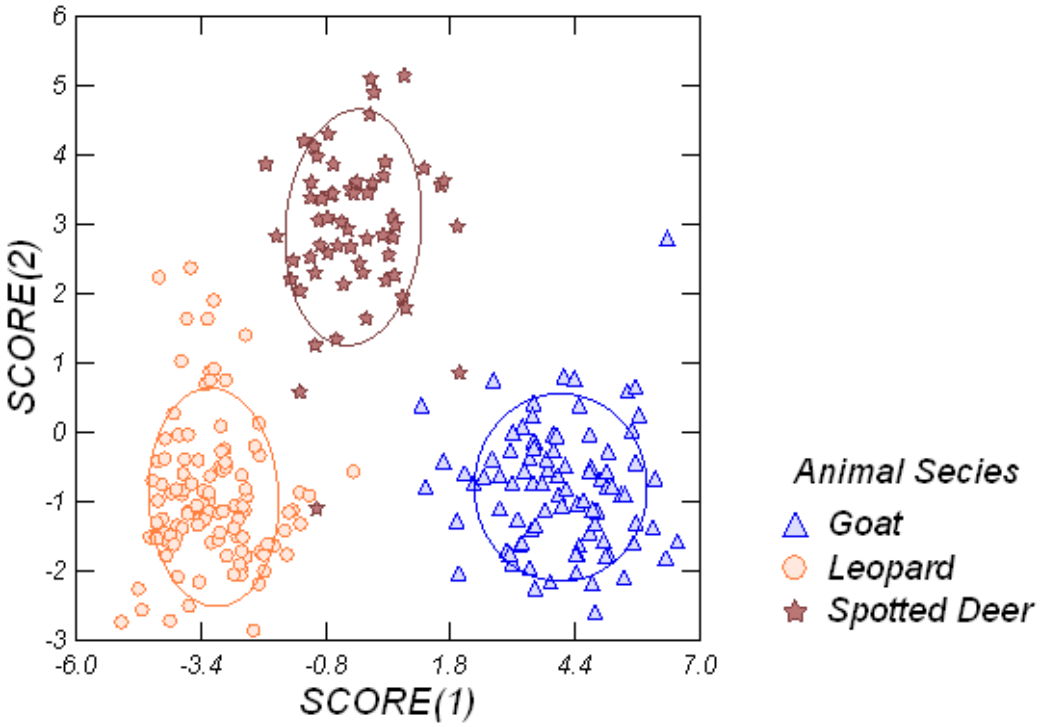

Fig 12 : Showing Peak Area, Peak Height and Peak Height Ratio Combined Canonical Score Plot of goat, leopard and spotted deer hairs

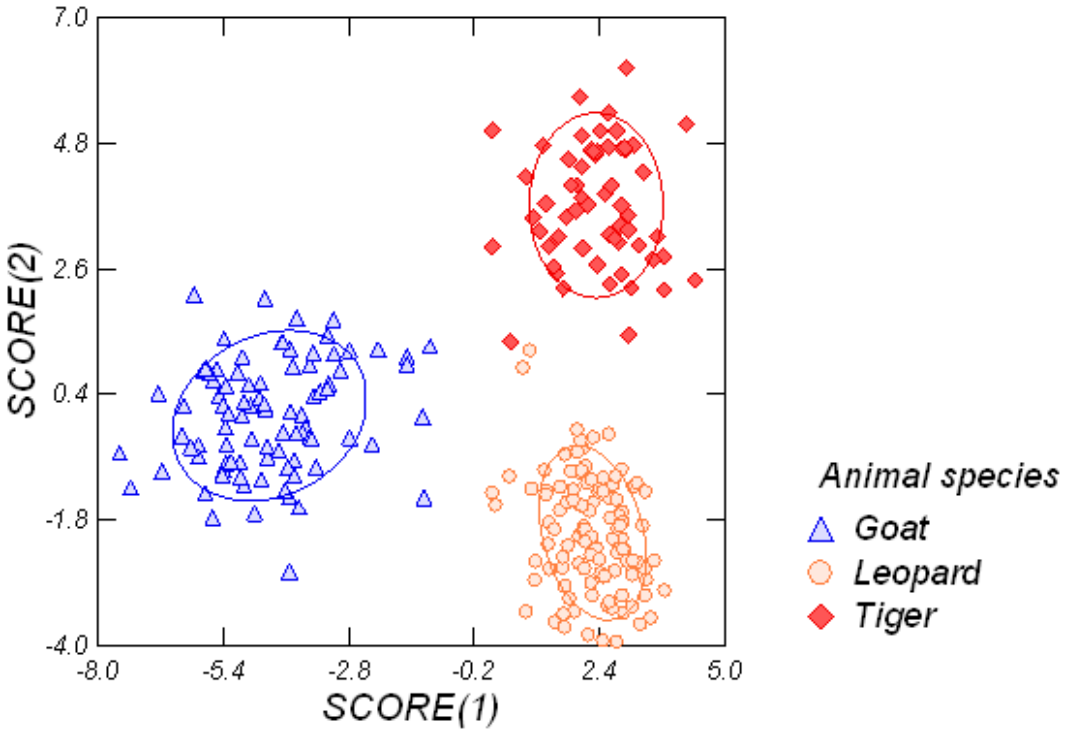

Fig 13 : Showing Peak Area, Peak Height and Peak Height Ratio Combined Canonical Score Plot of goat, leopard and tiger hairs

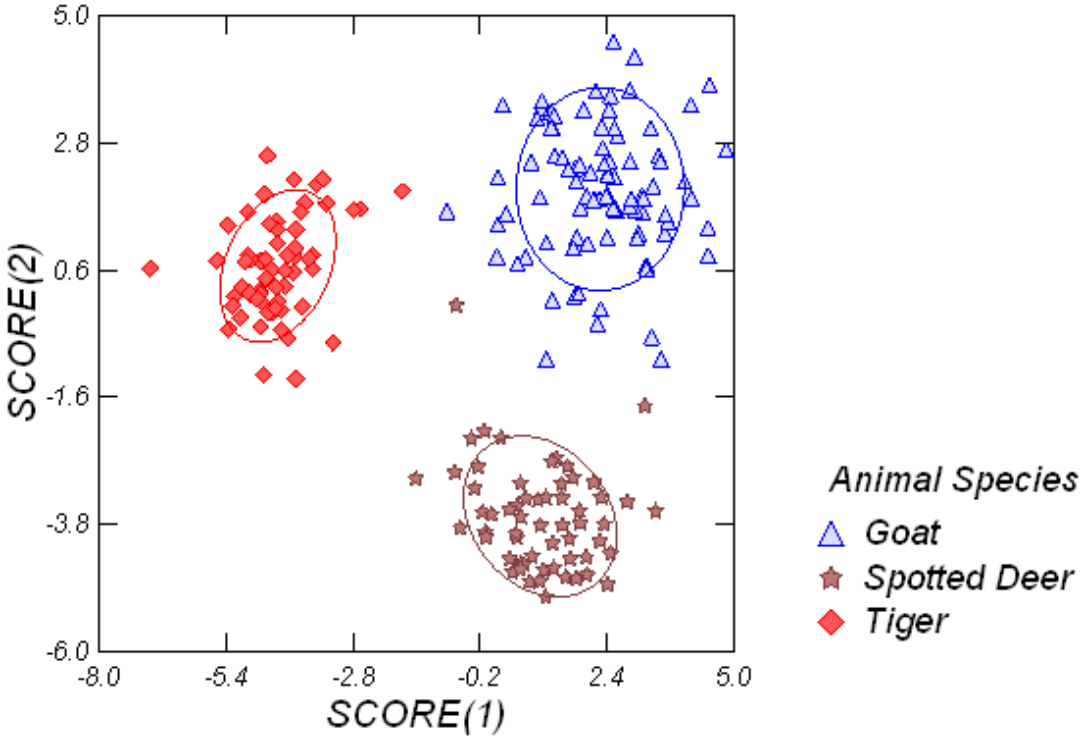

Fig 14 : Showing Peak Area, Peak Height and Peak Height Ratio Combined Canonical Score Plot of goat, spotted deer and tiger hairs

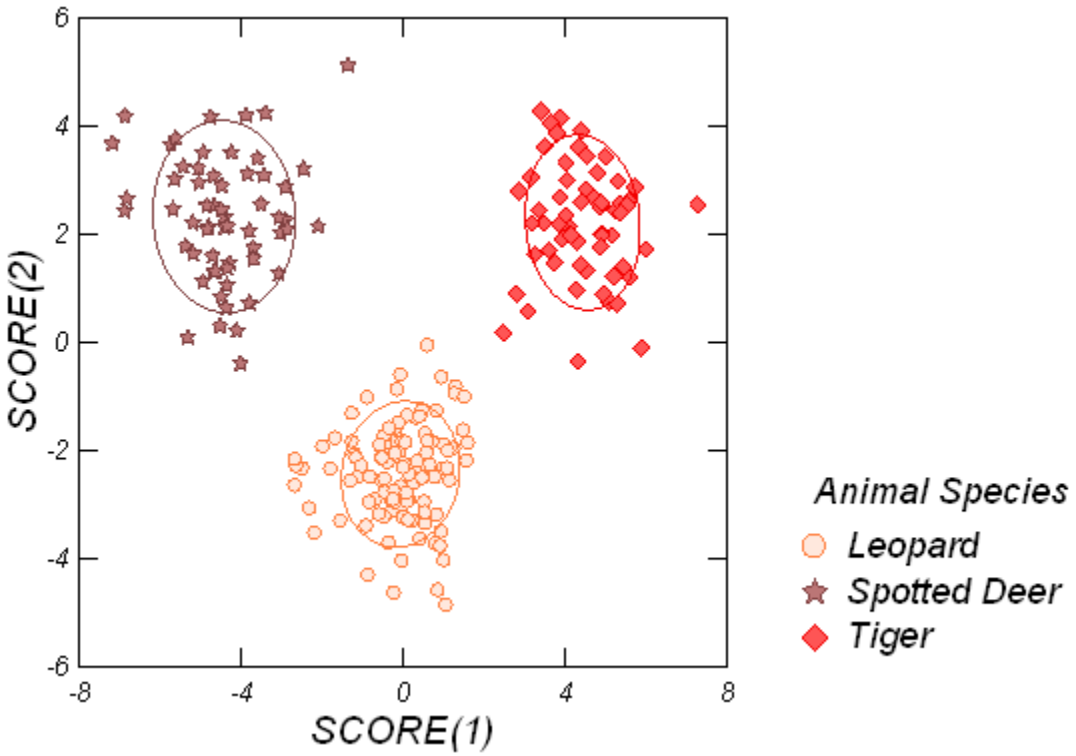

Fig 15 : Showing Peak Area, Peak Height and Peak Height Ratio Combined Canonical Score Plot of leopard, spotted deer and tiger hairs

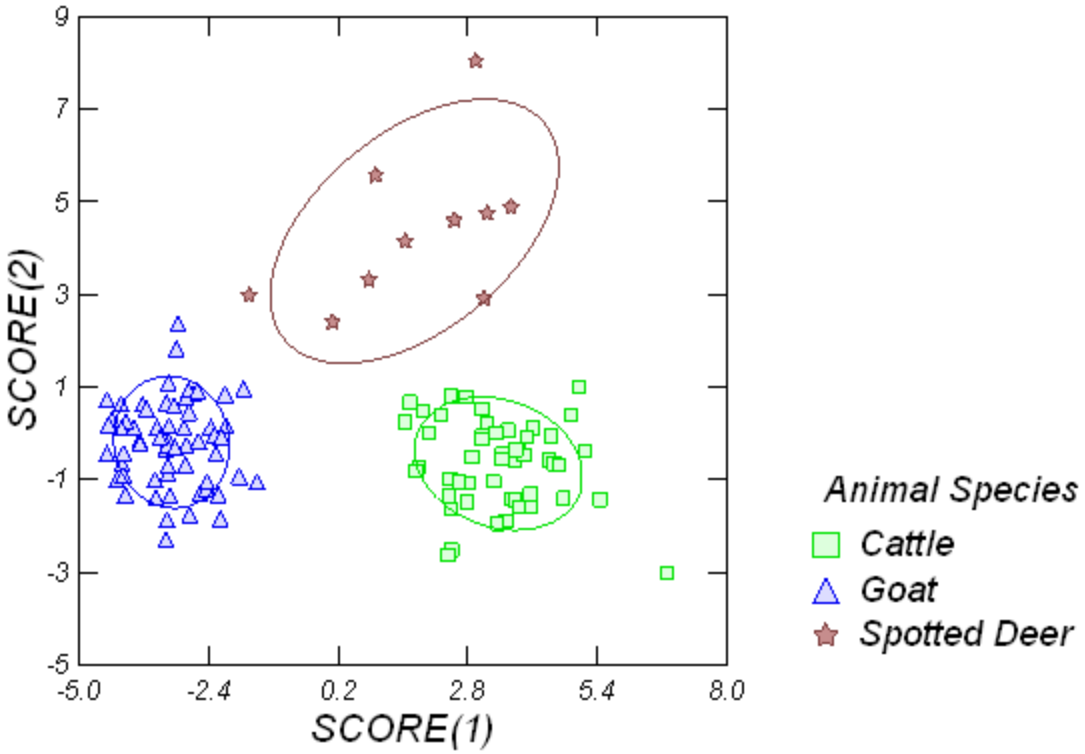

Fig 16 : Showing Peak Area, Peak Height and Peak Height Ratio Combined Canonical Score Plot of cattle, goat and spotted deer hoofs.

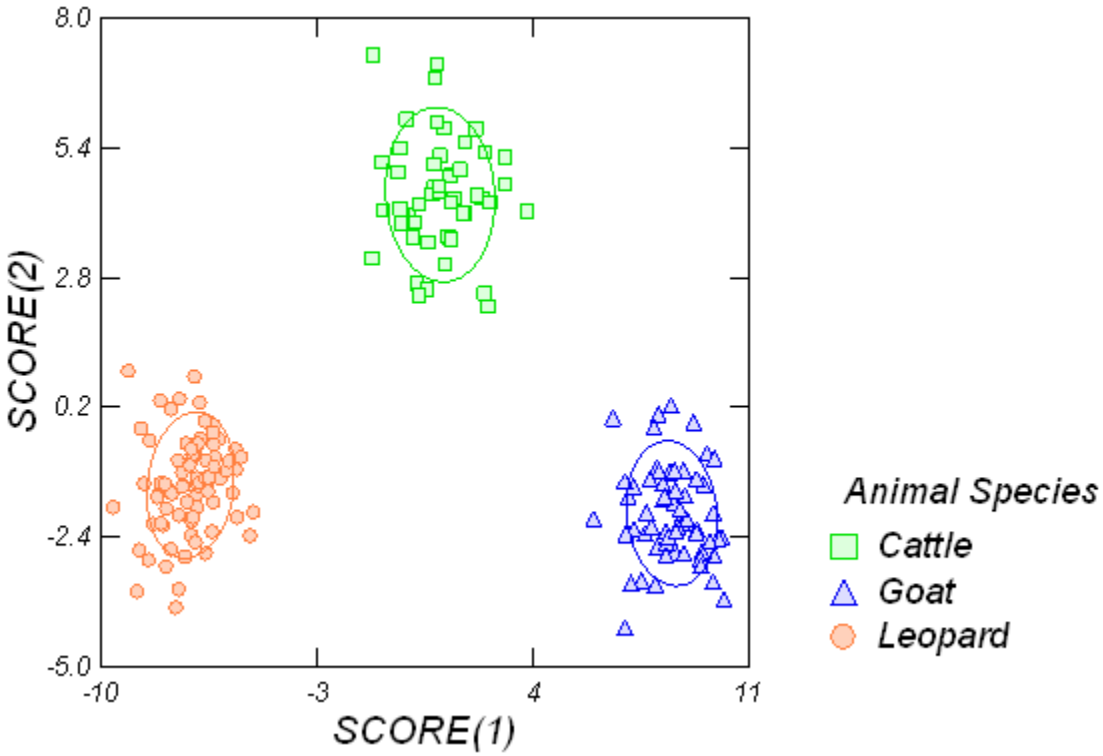

Fig 17 : Showing Peak Area, Peak Height and Peak Height Ratio Combined Canonical Score Plot of cattle, goat and leopard claws.

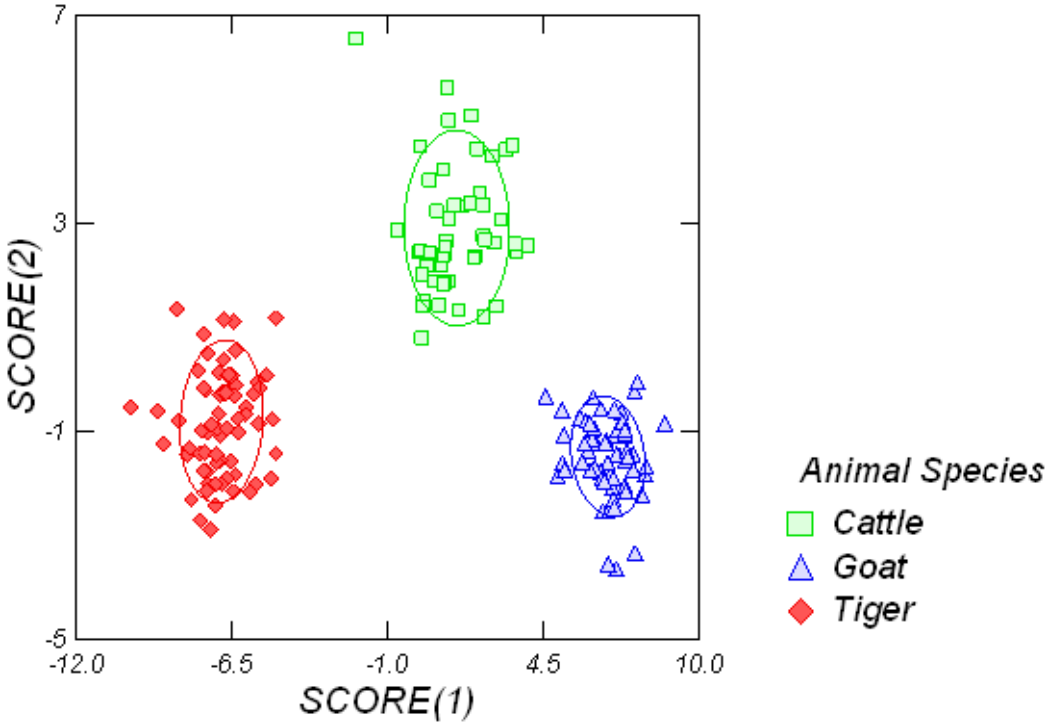

Fig 18 : Showing Peak Area, Peak Height and Peak Height Ratio Combined Canonical Score Plot of cattle, goat and tiger claws.

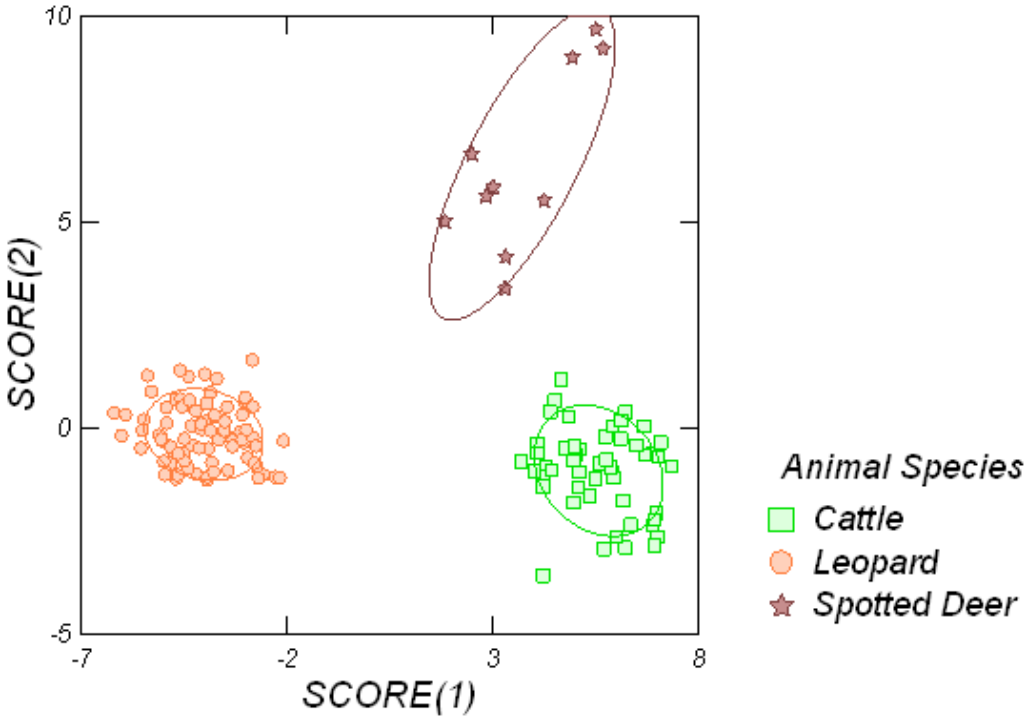

Fig 19 : Showing Peak Area, Peak Height and Peak Height Ratio Combined Canonical Score Plot of cattle hoofs, leopard claws and spotted deer hoofs.

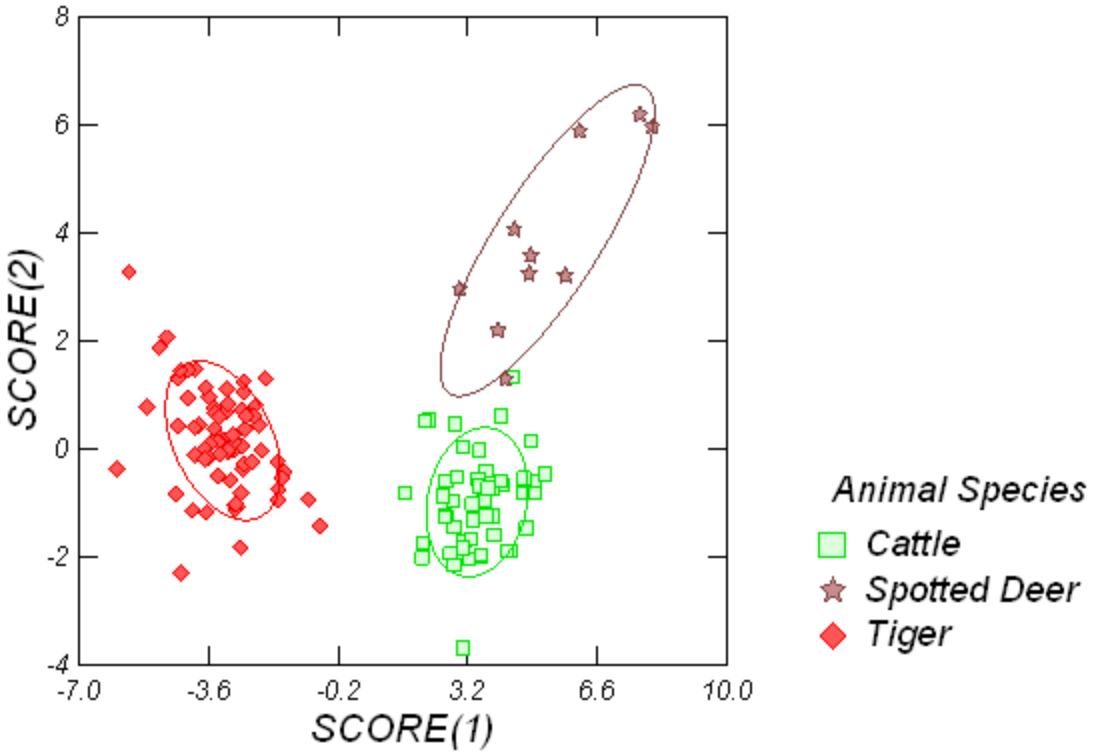

Fig 20 : Showing Peak Area, Peak Height and Peak Height Ratio Combined Canonical Score Plot of cattle, spotted deer hoofs and tiger claws.

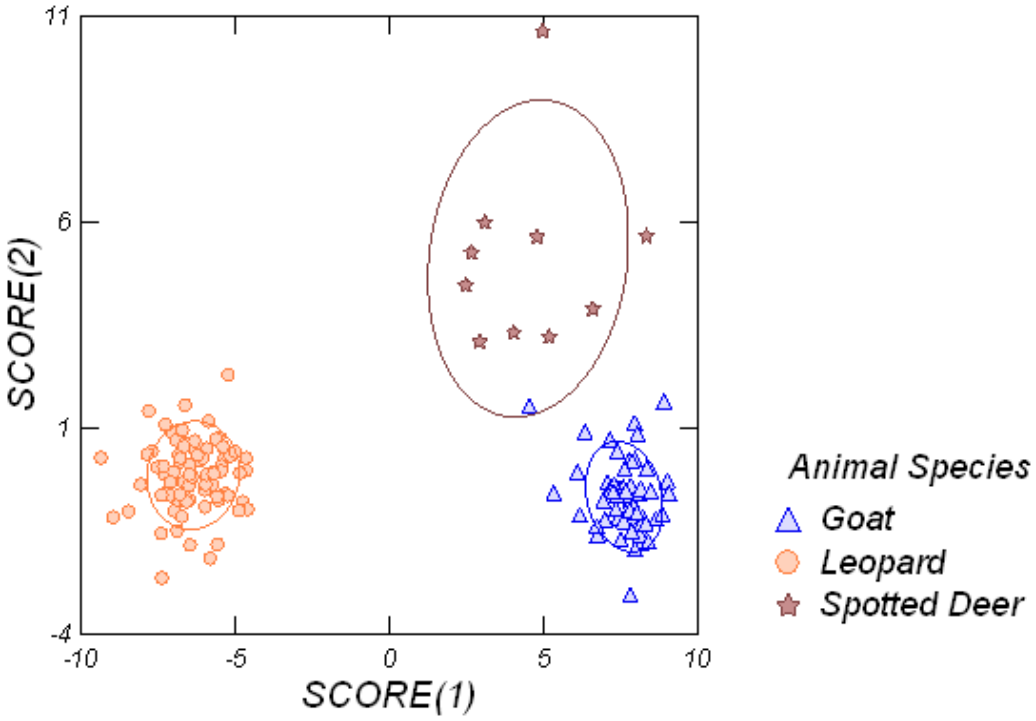

Fig 21 : Showing Peak Area, Peak Height and Peak Height Ratio Combined Canonical Score Plot of goat, spotted deer hoofs and leopard claws.

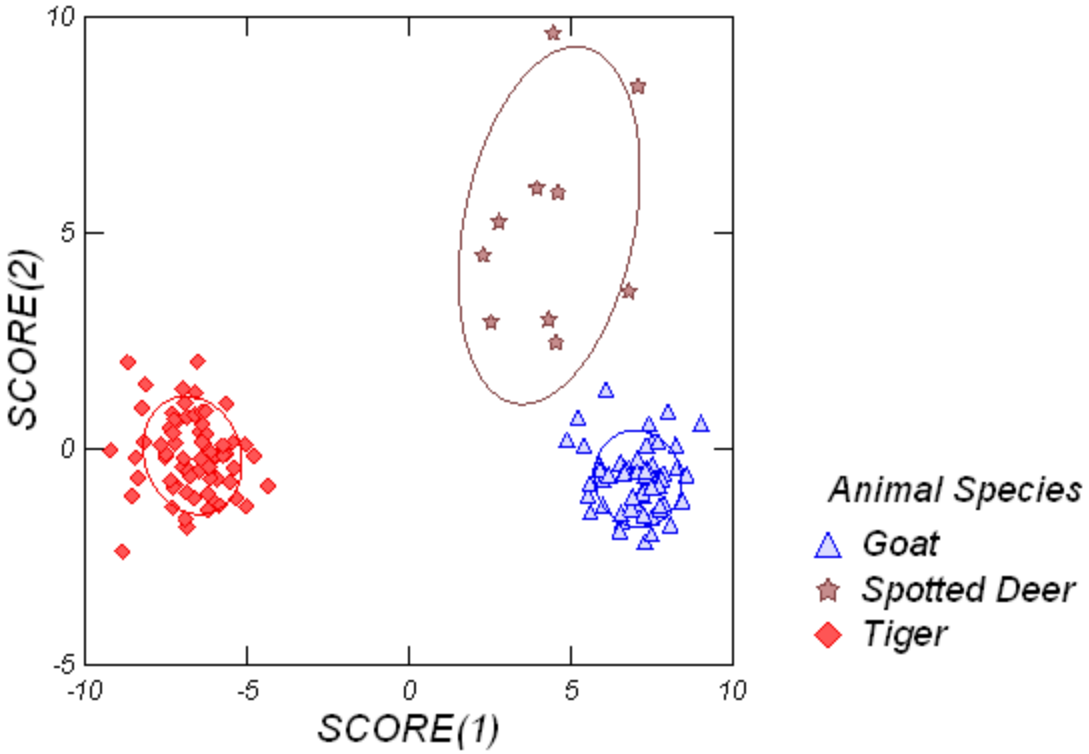

Fig 22 : Showing Peak Area, Peak Height and Peak Height Ratio Combined Canonical Score Plot of goat, spotted deer hoofs and tiger claws.

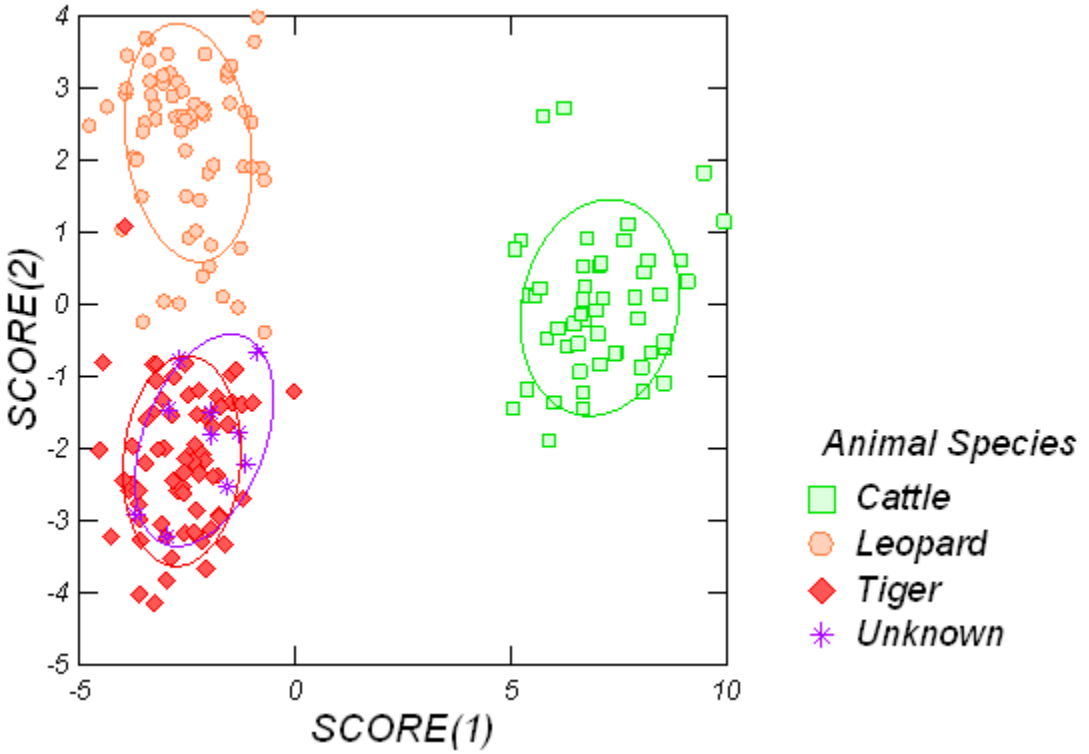

Fig 23 : Showing Peak Area, Peak Height and Peak Height Ratio Combined Canonical Score Plot of cattle, leopard and tiger claws.

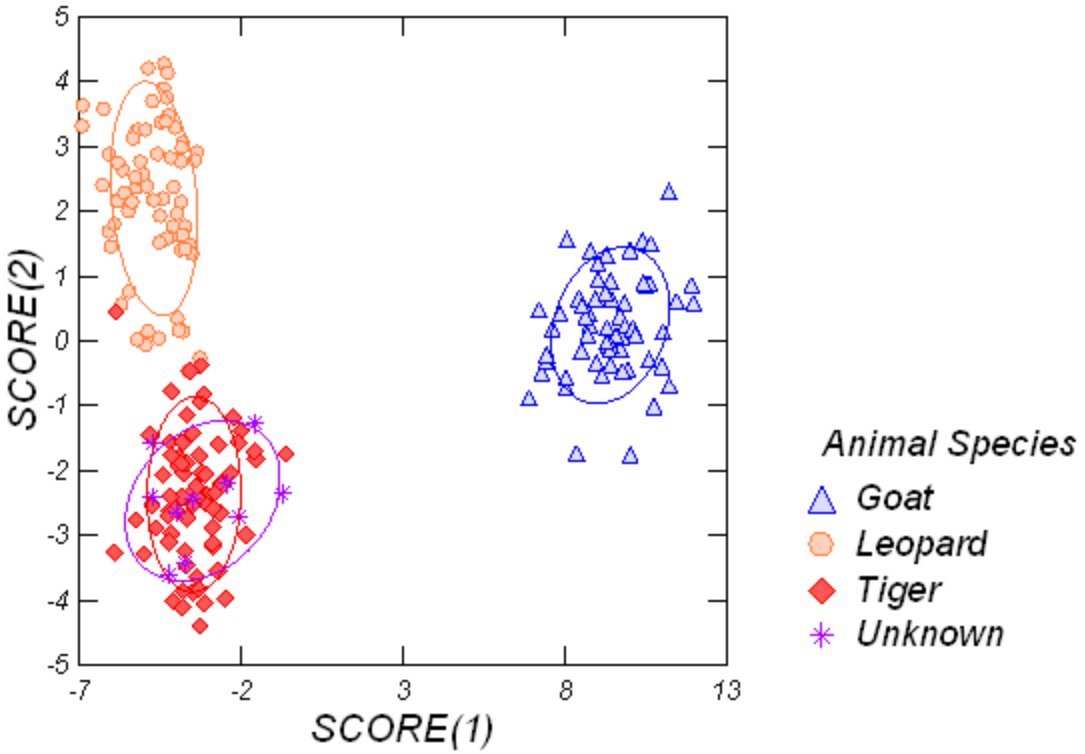

Fig 24 : Showing Peak Area, Peak Height and Peak Height Ratio Combined Canonical Score Plot of goat hoofs, leopard and tiger claws.

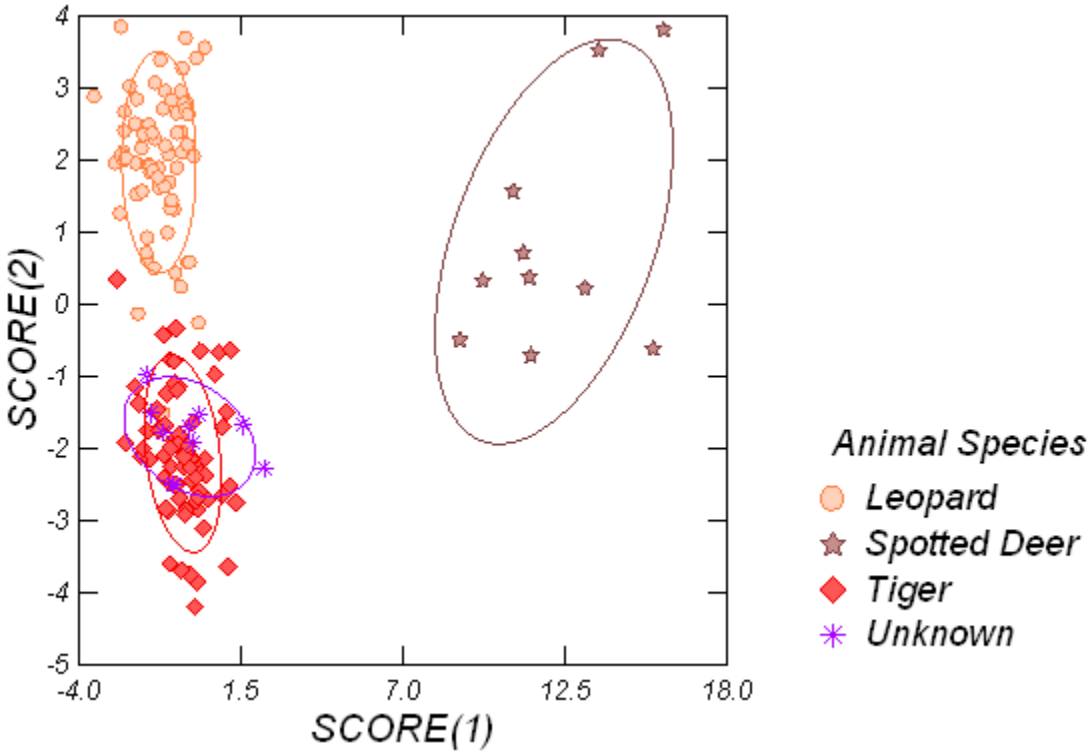

Fig 25 : Showing Peak Area, Peak Height and Peak Height Ratio Combined Canonical Score Plot of leopard claws, spotted deer hoofs and tiger claws.

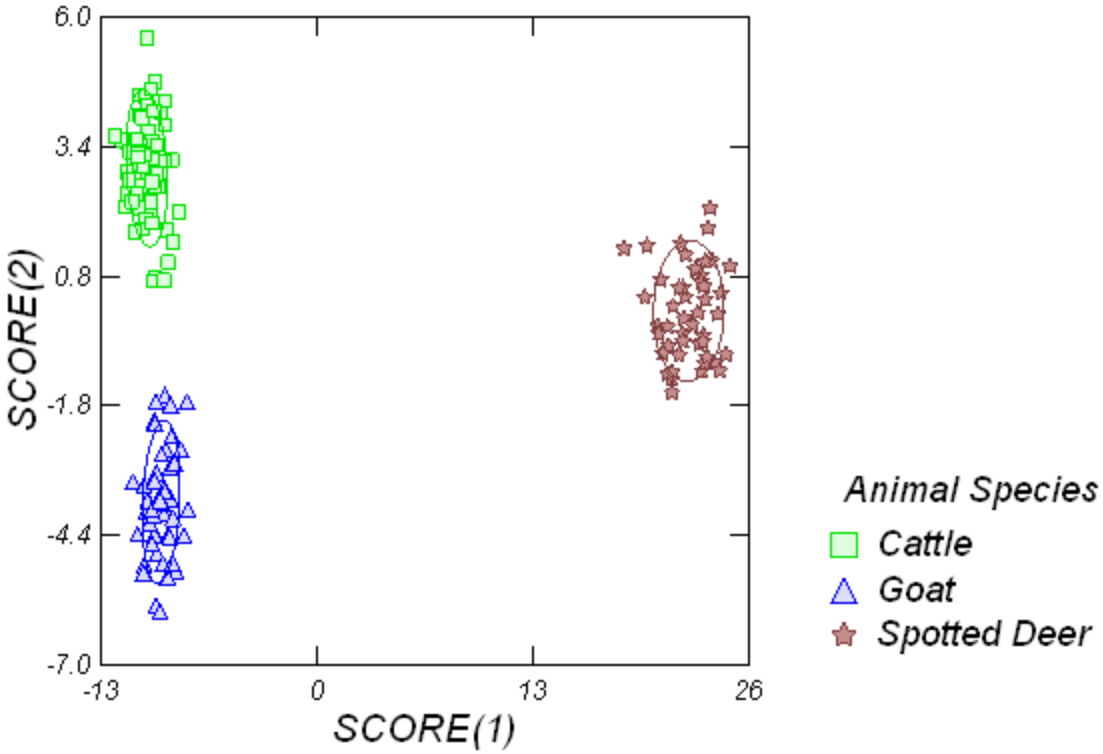

Fig 26 : Showing Peak Area, Peak Height and Peak Height Ratio Combined Canonical Score Plot of cattle, goat horns and spotted deer antlers.

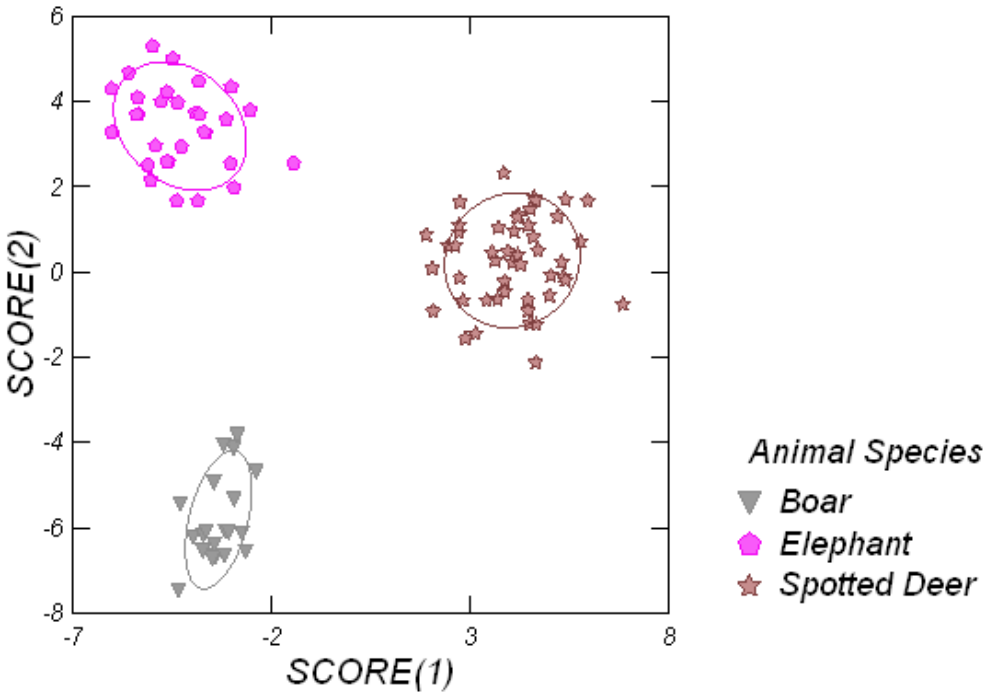

Fig 27 : Showing Peak Area, Peak Height and Peak Height Ratio Combined Canonical Score Plot of wild boar ivory, elephant ivory and spotted deer antlers.

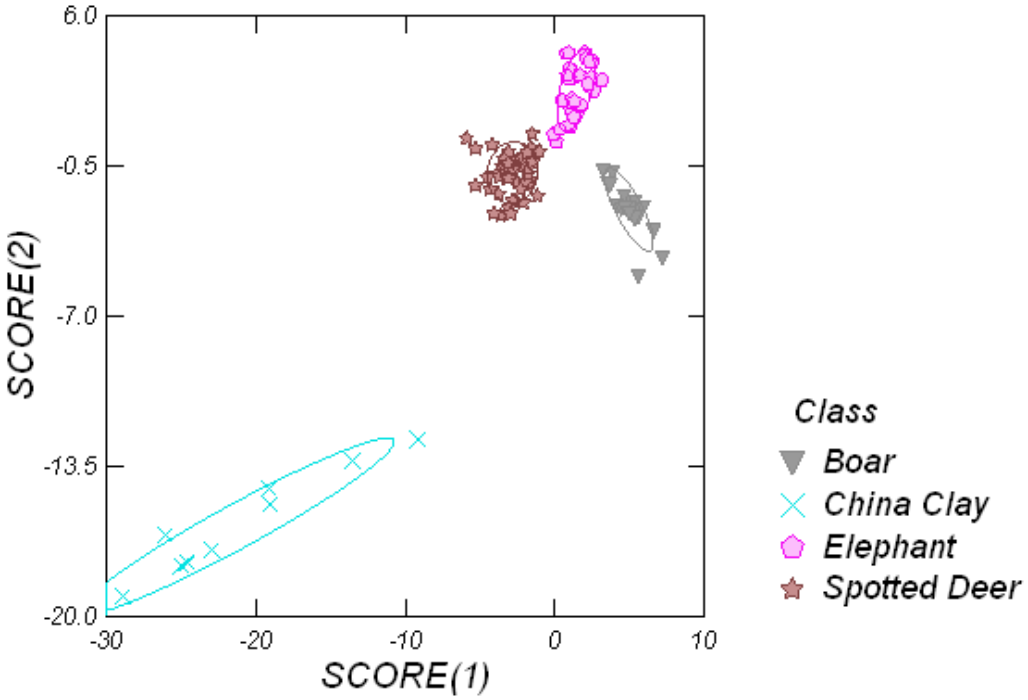

Fig 28 : Showing Peak Area, Peak Height and Peak Height Ratio Combined Canonical Score Plot of wild boar ivory, elephant ivory and spotted deer antlers with artifact.

Discussion

V DISCUSSION

The present study was conducted on the skins of wild and domestic animals namely tiger, leopard, spotted deer, cattle, goat, dog and cat. Most of the wild animals are facing the risk of extinction since they have been hunted by the poachers and so they have been considered as endangered species. The domestic animal skins are artificially painted to resemble wild animal skins and are sold at exaggerated prices in the grey market.

These wild animals and domestic animals belong to the Orders carnivore and artiodactyls respectively in the animal kingdom. Leopard and tiger belong to the family felidae whereas spotted deer belong to family Cervidae, the cattle and goats belong to family bovidae and capridae respectively. Among the domestic species cat and dog belong to family felidae and canidae. These domestic animals are used for the comparative study in order to differentiate the fake skin architecture from that of wild animals.

Trautmann and Fiebiger (1957) have described the five layers in the epidermis of domestic animals. However, in the present study skin layers were reduced in the leopard, spotted deer, goat, dog and cat, except in the tiger and cattle where all the five layers were recorded. Strickland and Calhoun (1963) reported decreased skin thickness from sub lumbar region to the base of the abdomen and also from the proximal end of the limbs to the distal end. Nickel and Schummer (1981) also described decreased cell layers in the epidermis of domestic animals. They also reported the absence of stratum granulosum and stratum lucidum in goat, dog, and cat.

5.1. Epidermis

In the present study the epidermis of leopard consisted of four layers namely stratum basale, stratum spinosum, stratum granulosum, and stratum corneum with the absence of stratum lucidum. In the tiger the epidermis consisted of five layers namely stratum basale, stratum spinosum, stratum granulosum, stratum lucidum and stratum corneum. Similarly the epidermis of spotted deer consisted of only three layers namely stratum basale, stratum granulosum, and stratum corneum.

In the epidermis of cattle all the five layers were seen, whereas in the goat only four layers namely stratum basale, stratum spinosum, stratum granulosum and stratum corneum were seen. In the dog there were three layers namely stratum basale, stratum spinosum and stratum corneum. In the cat, the epidermis consisted of distinct four layers without stratum lucidum. Strickland and Calhoun (1963) and Sar (1966) have also observed four distinct layers without stratum lucidum in the hairy skin of cat and goat respectively. Similar observation was recorded in the epidermis of leopard, cat and goat whereas Varicak (1941) had observed stratum lucidum in the cat. Trautmann and Fiebiger (1957) have described the presence of all five layers in the epidermis of domestic animals. However, Dellman and Brown (1981) have described the absence of stratum lucidum in the hairy regions of the epidermis of the domestic animals.

In the present study similar observation was seen in the epidermis of tiger and cattle. However darkly stained melanin pigments were observed at the junction of epidermis and dermis of the tiger. This was a characteristic feature of a tiger skin epidermis. The epidermis of spotted deer was very thin and consisted of only three layers

namely stratum basale, stratum granulosum and stratum corneum. No such observations were available in the literature reviewed, which is a significant observation in the present study. In the dog also the epidermis consisted of three layers namely stratum basale, stratum spinosum and stratum corneum. This is similar to the observations of Lovell and Getty (1957) and in contrast four layers with additional stratum granulosum were observed by Lloyd and Garthwaite (1982). The stratum spinosum was composed of elongated cells with multiple layers in dog whereas in spotted deer stratum spinosum and stratum lucidum were absent. This observation was significant and can be used to differentiate the skin of dog and spotted deer.

5.2. Dermis

The dermis was composed of collagen, elastic and reticular fibers, nerve components and blood vessels. Goldsberry and Calhoun (1959), Strickland and Calhoun (1963) and Marcarian and Calhoun (1966) have stated that there was indefinite division between the stratum papillaris and the stratum reticularis. However, in the present study distinct demarcation of papillaris and reticularis layers were observed in leopard.

In the papillary layer hair bundles were supported by the smooth muscle fibers. The stratum papillaris had fine, irregular collagenous fibers which were usually distributed along with dermal pegs. The stratum reticularis had dense, irregularly arranged collagenous fibers approximately two times larger than those of the stratum papillaris. Thick, irregular elastic fibers were observed at the stratum reticularis.

In tiger skin, the dermis was subdivided into two layers which blended without a distinct demarcation. The papillary layer originated immediately beneath the epidermis,

and the deeper portion of the dermis was the reticular layer, the papillary layer had more number of elastic fibers compared to the reticular layer. The papillary layer was composed of loosely arranged connective tissue elements. The collagenous bundles of the papillary layer were delicate and thin in contrast to those of the reticular layer.

Scanty reticular fibers were loosely arranged in the deeper part of the dermis. In cattle, goat, spotted deer and dog there was no clear cut demarcation of the dermis into stratum papillaris and stratum reticularis as described by Gossberry and Calhoun (1959) in Hereford and Aberdeen Angus cattle. The dermis consisted of interlacing elastic fibers and small collagen bundles extending in between the hair follicles .Distinct elastic fibers were observed in between layers of hair follicle in the spotted deer .Such arrangements were not observed in the cattle and goat. Fine strands of elastic fibers were observed at papillary region, these elastic fibers were not found at dermal pegs.

Nerve fibers were distinctly seen, penetrating through the root of hair follicle. Nerve fibers were distinctly seen in case of goat as compared to spotted deer and cattle. Reticular fibers were uniformly distributed surrounding the hair follicle in all the species and were described routinely in all domestic animals (Dellman and Brown, 1981; Talukdar et. al, 1972; Lovell and Getty, 1959). Cellular population of connective tissue were highly concentrated just below the epidermal layer where as the deeper part were more fibrous and less cellular in cattle, goat and spotted deer species under present investigations. However, Trautmann and Fiebiger (1957) described in ox, sheep and dog a felt work of delicate reticular fibers with an admixture of fibroblast elements in

superficial layers of the dermis. The remainder of the dermis consisted of bundles of collagen fibers with few elastic fibers.

In the papillary layer the fine collagenous bundles were densely interwoven. In cat skin, the deep part of the dermis consisted of blood vessels and muscle fibers. Skeletal muscle fibers were seen between adipose cells of the dermis and hypodermis and large quantity of adipose tissue was observed at the bottom of the dermis according to and Winkelman (1957) Strickland and Calhoun (1963).

The dermis of the cat skin showed definite division between stratum papillaris and stratum reticularis. The stratum papillaris was composed of collagen, elastic, reticular fibers and nerve components. Stratum reticularis was dense, irregularly arranged and was approximately three times larger than those of the stratum papillaris. However, in the present study no reticular fibers were observed in the dermis of cat.

5.2.1. Hair follicles

The distributions of hair follicles in the dermis are species specific; many differences exist in the arrangement of hair follicles among domestic animals (Dellman and Brown, 1981). In leopard the distribution of hair follicles had unique arrangement consisting of a single large primary hair follicle with circumferentially surrounded clusters of compound hair follicles. In each compound follicle there were six to eight secondary hair follicles located at one side along with one or two indistinct sebaceous glands. The clusters of compound follicles were densely surrounded by collagen fibers and reticular fibers.

Elastic fibers were associated with primary hair follicles. Each compound follicle was encapsulated by connective tissues through which nerve fibers penetrated into the interior of the hair follicle. Follicular folds were evident in primary follicle. Sar and Calhoun (1966) have also observed follicular folds in goat. Errector pilli muscles were attached around the clusters of compound hair follicles.

In the tiger, clusters of compound hair follicle consisted of one primary hair follicle with two to four secondary hair follicles at one end were seen. Fine elastic fibers encircled the compound hair follicles. Collagen fibers were associated with primary hair follicle and secondary hair follicles. These features are characteristic and aid in the identification of the skin as the hair follicle arrangements are species specific according to Dellman and Brown (1981).

There were plenty of fine, irregular reticular fibers located between the clusters of hair follicles; nerve fibers surrounded both primary and secondary hair follicles. The errector pilli muscles were located between the clusters of compound follicles in the deeper part of the dermis. These muscles were branched and extended to the adjacent hair follicles and sometimes appeared to connect two hair follicles or enclose a follicle in support.

In cattle, the distributions of hair follicles were irregular and isolated. Goldsberry and Calhoun (1966) studied the hair follicle in the Hereford and Aberdeen Angus cattle. They revealed a series of distinct follicular folds in the wall of the hair follicle. They were 15 to 25 folds which began at the opening of the sebaceous ducts and encircled the middle third of the hair. In goat, the primary hair follicles were arranged in

a linear fashion and were associated with 1-2 secondary hair follicles at the base. But the concentration and number of hair follicles were more as compared to cattle. Sar and Calhoun (1966) have reported that primary hair follicles were arranged in groups of three.

The distributions of hair follicles were characteristic in the spotted deer where in the primary hair follicles were associated with two to three secondary hair follicles in linear fashion. The sebaceous glands surrounded the primary follicle. This pattern of arrangement is characteristic in its identification. This can help in the identification of fake skin from the original skin thus aiding in forensic investigation. In the dog skin, the compound follicles were arranged in a capsular form, each compound follicle consisted of one large primary follicle with six to eight secondary follicles.

The compound follicles were encapsulated with fibrous connective tissue and associated with sebaceous and apocrine sweat glands. Lovell and Getty (1957) have described compound hair follicles in a group of two, three and four in dog. Dellman and Brown (1981) also described that primary hair follicle is associated with a group of smaller secondary hair follicles. In cat skin, the clusters of compound follicles were seen. Each primary hair follicle was surrounded by six to eight secondary follicles. These compound follicles were associated with the sebaceous gland but were lacking sweat glands. Strickland and Calhoun (1963) studied hair follicles in the cat; they reported that hair follicle occurred in clusters of 3 to 5 groups around a central guard hair,

5.2.2. Sebaceous glands:

Sebaceous glands associated with the hair follicles were appreciated in all the species studied. In case of leopard one or two indistinct sebaceous gland were located at

one side of secondary hair follicle. In tiger, they were observed within the compound hair follicles; in the spotted deer sebaceous gland surrounded the primary hair follicles. In cattle skin the sebaceous glands were appreciated at the base of the hair follicle. In the goat the sebaceous gland was located between the primary hair follicles along with errector pilli muscle; in dog and cat skin the sebaceous glands were associated with the primary hair follicles.

Trautmann and Fiebiger (1957) have described the sebaceous gland as simple alveolar holocrine gland and appeared as evaginations of the follicles. The size and number are dependent on the species and size of hair, who also described largest sebaceous gland in the dog. Strickland and Calhoun (1963) have described the sebaceous glands in cat as simple alveolar type, clustered around the hair follicles. No sebaceous glands were found in the non hairy region.

Dellman and Brown (1981) described the sebaceous glands as simple branched or compound alveolar type. In the present study the distribution of sebaceous gland and their association with primary and secondary hair follicles can also help in the identification of skins of animals. The secretion of sebaceous gland contained lipoid mixture high in cholesterol which keeps the skin and hairs pliable and protects them against drying and moisture (Trautmann and Fiebiger, 1957)

5.2.3. Sweat glands

Based on morphological and functional characteristics sweat (sudoferous) glands are named as apocrine and merocrine glands. The apocrine type is the most extensively developed in domestic animals as described by Dellman and Brown (1981). In leopard

simple tubular merocrine type of sweat glands were observed at the reticular part of the dermis which was serpentine in nature. According to Trautmann and Fiebiger (1957) similar observations were made in the ox, goat and dog. Whereas in tiger few sweat glands were observed at the base of the hair follicles. Both small and large sacular apocrine sweat glands were observed in the tiger, these sacular glands were associated with cuboidal epithelial cells. Strickland and Calhoun (1963) reported similar observations in the dog.

In cattle the present study revealed sweat glands frequently in the deeper part of the dermis, which was sacular, coiled with a large lumen, lined by simple cuboidal epithelium. The cytoplasm was highly eosinophillic and nuclei with round and indistinct cell boundaries .Whereas in case of spotted deer the simple tubular sweat glands were observed at the junction of the dermis and hypodermis.

In goat, the sweat glands were frequently seen at the base of the hair follicle, which were similar to that of cattle. Sar and Calhoun (1966) stated that sweat glands of goat were coiled tubular apocrine which varied in different body regions with exception of the compound tubular sweat glands in the planum nasale. In dog skin, very few simple tubular apocrine type sweat glands were seen which were in contrast to Trautmann and Fiebiger (1957) who described the sweat glands as serpentine in nature. Whereas in cat, few simple tubular sweat glands were observed between the reticular part and adipose tissue of the dermis. Similar observations were made by Trautmann and Fiebiger (1957). However, Strickland and Calhoun (1963) in contrast found sacular apocrine glands in the dermis of cat.

5.3. Spectral analysis of hairs

The present study was conducted on representative samples of keratotic and bony tissues from wild and domestic animals namely tiger, leopard, spotted deer, cattle, goat's hair, hoofs, claws, horns, antlers, and ivories of elephant, wild boar and artifacts.

These representative samples of different tissues collected from wild and domestic animals were subjected to FTIR analysis and FTIR spectra were obtained. The natural keratin fibers and bony tissues were investigated through the use of FTIR followed by linear discriminant analysis or canonical score variates. All samples studied in this work showed similar vibration spectra in the spectral region between 4000-400 cm^{-1}. Analysis of amide A region of all hair samples of all animals exhibited very similar peak positions (Table 3) and (Fig 1).

Differences were observed in the amide B regions at 3080cm^{-1} in cattle and goat. In spotted deer exhibited at 3076cm^{-1}, in tiger at 3070cm-1 and in leopard at 3069cm^{-1}. These results showed that in all animals the peaks were exhibited almost at same positions except in cattle and goat, which were due to over toning of Fermi resonance doublet of N-H stretching and O-H stretching between 3400-3300cm^{-1} (Stuart 2004). Similar observations were made by Panayiotou (2004) in cat, cattle, horse, human hair where spectra were found between 3300-3050cm^{-1}.

CH_3 mode vibrations were observed at 2961cm^{-1} in cattle and leopard, in goat hair at 2964cm^{-1}. In tiger hair it was at 2966cm^{-1}, in spotted deer at 2962cm^{-1}. All animals showed peaks at almost similar spectral position, except in tiger hair, where medium peak was observed. Panayiotou (2004) observed that cow, cat, horse, human, sheep hair

exhibited CH_3 modes of vibration at 2955cm^{-1} and 2933cm^{-1} respectively. Whereas in wool fiber these CH_3 modes of vibration of protein was not observed (Griebenow et. al., 1992). Fabian (2000) observed symmetric stretching vibration at 2956cm^{-1} and asymmetric stretching of CH_2 of acyl chain at 2922cm^{-1}.

The peak for Amide I band occurred due to C-O stretching and N-H bending vibration at 1638cm^{-1} in cattle hair, at 1629cm^{-1} in goat hair, at 1626cm-1in spotted deer hair, at 1628cm^{-1} in leopard hair, at 1626cm^{-1} in tiger hairs. Generally Amide I absorption occurs in the region between 1600-1700cm-1. Major contribution for this peak could be attributed to C=O stretching and minor contributions from C-N stretching. This band has been most widely studied for assignment of secondary structure of the protein and polypeptide.

Amide II band occurred due to C-N stretching and C-N-H bending vibration coupled with C=O stretching was observed at 1525cm^{-1} in cattle, at 1521cm^{-1} in goat, at 1520cm^{-1} in spotted deer and tiger at 1519cm^{-1} in leopard hair. All animals exhibited almost similar spectral peaks positions. Panayiotou (2004) observed amide I and amide II bands at 1657cm^{-1} and at 1537cm^{-1} respectively in cattle, sheep, cat, horse and human hair which could be attributed to refractive index of Kbr (potassium bromide) used for pelleting in the spectral collections.

Amide II absorption resulted from both N-H bending vibration and from C-N stretching vibration. The absorption for this band occurred in the region between 1500 to1600cm^{-1}. Similar observations were found at 1630cm^{-1} for amide I peak and at 1515cm^{-1} for amide II peak in the spectra of wool fiber according to Griebenow *et al,*

(1992). Elliot (1956) reported that folded forms of amide I band occurred at 1655cm^{-1}, amide II band occurred at 1540cm^{-1}. Whereas extended form of amide I peak observed at 1630cm^{-1} and amide II peak observed at 1540cm^{-1}. Pielesz et al., (2000) reported that amide I band found at 1652cm-1 and amide II band found at 1541cm-1, these peaks were similar to that of β chitin at 1630cm-1 and α chitin at 1562cm-1 (Bruner et. al.,2009).

Espinoza and Baker (2006) studied sea turtle and bovidae keratin using DRIFT method where amide II peak was recorded at 1516cm^{-1} in the sea turtle. The region between 1700-750cm^{-1} contains vibration from the CONH stretching primarily from protein structure with amide I and amide II bands occurring at 1647cm^{-1} and 1547cm^{-1} respectively (Baddiel *et al.*, 1968). Panayiotou (2004) reported strong band at 1652cm^{-1} for all keratin except feather.

Asymmetric CH_3 bending modes of the methyl groups of proteins, methylene deformation were observed at 1450cm-1 in cattle, goat, spotted deer ,leopard and tiger hairs, whereas aliphatic side groups of the amino acid residue peak was observed at 1394cm^{-1} in cattle, at 1399cm^{-1} in goat, at 1390cm^{-1} in spotted deer, while flat peak was recorded in leopard and tiger at 1403cm^{-1} and at 1399cm^{-1} respectively.

Amide III band attributed to C=O stretching was observed at 1237cm^{-1} in cattle, 1241cm-1 in goat, 1235cm^{-1} in spotted deer and tiger, 1234cm^{-1} in leopard. Cattle and spotted deer exhibited shoulder at 1158cm^{-1}, leopard exhibited shoulder at 1159cm^{-1}, whereas tiger and goat exhibited prominent peaks at 1160cm^{-1} and 1161cm^{-1} respectively.

Amide III absorption band occurred in the region 1220-1330 cm^{-1}. The amide III absorption band mainly arise from C-N stretching vibration as well as N-H in plane bending vibration with weak contributions from C-C stretching and C=O in plane bending vibration. Secondary structure determination of protein has also been done using this region. Generally alpha helix structure occurs in the region 1293 and 1328cm^{-1}, beta sheet in the region 1225, 1250cm^{-1} and unordered structures in the region 1257 and 1288cm^{-1} (Stuart, 2004).

Panayiotou (2004) reported that amide III band is seen at 1244cm^{-1} in cattle, cat, horse, goat and human hair whereas in parrot feather the intensity of this band was stronger. This observation was almost consistent with the comments made by Griebenow et al (1992); he opined that absorption bands of protein at 1230cm^{-1} was due to amide III peak which occurred because of heavily mixed vibrational modes.

The region of S-O stretching vibration related to the cystine monoxide, which was exhibited as twin peaks at 1077cm^{-1} and 1042cm^{-1} in cattle. whereas in goat, leopard, and spotted deer hairs these peaks were observed at 1076cm^{-1} and 1042cm^{-1} due to medium intensity of cystine monoxide interaction.

In tiger hairs additional peaks were found at 1125cm^{-1} and 1102cm^{-1} which was due to rocking of methylene group according peak assignment made by Akhtar and Edward (1997) and Edward et al (1998). Panayiotou (2004) reported in cow, goat, horse, human hair and cat fur the amide III band was found at 1040cm^{-1} where as in the parrot feather this band was attributed to a cystic acid.

5.4. Spectral analysis of hoofs, claws and horns

Hoofs, claws and horns are made up of the fibrous structural protein called keratin, the two major class of keratin are alpha-keratins and beta-keratins. Alpha keratins are characterized by helical structure, whereas beta keratins have a pleated structure.

The hoofs represented the harder tissue where as claws represented the intermediate tissues. All samples showed similar vibrational modes in the spectral region between 4000-400cm^{-1}. The amide A, B and amide I display similar characteristic band in all animals hoofs and claws. The amide II and III are very important bands because from their position and shape, information about protein structure (keratin) and conformation can be described.

Amide A band and amide B band were due to over toning of N-H stretching and O-H stretching .Amide A peak observed at 3273cm^{-1} in cattle hoof, spotted deer hoof, whereas in goat hoof, leopard claw and tiger claw it was found at 3271cm^{-1}

Amide B peak seen at 3069cm^{-1} in cattle hoof, goat hoof, tiger claw, whereas in spotted deer hoof it was observed at 3073cm^{-1}, in leopard claw it appeared at 3068cm^{-1} due to more interaction of vibrational bands. Panayiotou (2004) reported that the region between 3300-3050cm^{-1} corresponded to the O-H stretching. in contrast, Singquing *et al* (2011) described that sheep horn exhibited peaks at 3295, 3259, 3206 and 3060cm^{-1} .cattle horn exhibited weak peaks at 2907cm^{-1}, 2850cm^{-1}, in yak horn no such peaks were observed. In goat horn weak spectral bands appeared 2920cm^{-1}, 2850cm^{-1} 2450cm^{-1} compared to rhinoceros horn. In sheep the absorption peaks at 3295cm^{-1}, 3259cm^{-1},

3206cm^{-1}, 3060 cm^{-1} were stronger than rhinoceros horn which indicates cholesterol contents in sheep horn is more compared to goat, cattle, yak and rhinoceros horns.

In the present study the spectral peaks were almost at similar positions as described by Espinoza *et al* (2006) and Griebenow *et al* (1992) with their spectral peaks of keratin tissues.

Amide I peak observed at 1632cm-1 in cattle hoof, goat hoof, spotted deer hoof, tiger claw and leopard claw occurred due to C=O stretching vibration. In the goat horn prominent amide I peak observed at 1631cm^{-1} was due to more intensity of C=O stretching interaction. In rhinoceros horn, goat horn, yak horn cattle horn and sheep horn no such amide I peak was recorded (Shingqing *et al.*, 2011).

Prominent amide II peak observed at 1515cm^{-1} in goat hoof, spotted deer hoof and cattle horn, whereas in cattle hoof, leopard claw and tiger claw the same peak was observed at 1514 cm^{-1}. Singquing *et al* (2011) reported that the amide II peak occurred due to C=C stretching vibration at 1540cm^{-1} in rhinoceros horn and 1583cm^{-1} in yak horn. Usually amide II peaks observed between the regions 1580-1500cm^{-1} according to Akhtar *et al.*, (1997).

In the present study asymmetric CH_3 bending modes of the methyl group of protein and methylene deformation observed at 1451 cm^{-1} as weak peak in cattle hoof, goat hoof, goat horn and a prominent peak occurred at 1450 cm^{-1} in spotted deer hoof, leopard claw, tiger claw and cattle horn. The C-H bending vibration modes at 1446cm^{-1}

was stronger in rhinoceros horn compared to cattle horn and this peak was not recorded in sheep, goat, and yak horn as reported by Shengqing *et al* (2011).

The aliphatic side groups of the amino acid residue stretching vibration observed at the region of 1395-1389cm^{-1}. In cattle hoof, goat hoof, cattle horn, spotted deer hoof prominent peaks were observed, whereas in leopard and tiger claws weak aliphatic side groups of amino acid residue stretching seen at 1403 and 1400cm^{-1} which indicates that the amino acid contents were more in the carnivore's animals. Stronger peak of 1393cm^{-1} was observed in goat horn due to stronger intensity of stretching vibration. Espinoza and Baker (2004) were not described these peaks in the sea turtle and bovidae keratins ,similar observations were not reported in rhinoceros horn, cattle horn, sheep horn and goat horn by Singquing *et al* (2011).

A weak Amide III peak occurred at 1312cm^{-1} and medium peak at 1237cm^{-1} and shoulder observed at 1156cm^{-1} in cattle hoof, whereas in goat hoof and spotted deer hoofs amide III bands were observed at 1313cm^{-1} and 1238 cm^{-1}. In leopard and tiger claws the amide III peaks were observed at 1236cm^{-1} and shoulder observed at 1163 cm^{-1}, whereas shoulder was observed at 1166cm^{-1} in tiger claw. In cattle horn and goat horn similar observations were made.

The S-O symmetric stretching vibration of cystine monoxide was observed at 1078cm^{-1} in cattle hoof, leopard claw; at 1077cm^{-1} in goat horn, cattle horn; whereas tiger claw exhibited additional peak at 1106cm^{-1} due to asymmetric S-O stretching. No S-O stretching was reported by Shengqing *et al* (2011) in yak, goat and rhinoceros horn except in cattle horn where S-O stretching vibration was reported similar to our finding.

5.5. Spectral analysis of Elephant, Boar ivory and spotted deer antlers

Proper identification of these biological materials is very important, since various ceramic (artifacts) and other biological materials are often used as substitute materials. Rigorous methods for identifying ivories, antlers are also interest to police and forest officials, who monitor the illegal trade in endangered and threatened species. HATR-FTIR coupled with discriminant analysis is the most effective method for the non-destructive identification of ivory, antler and ceramic artifacts (Sila Tripati *et al.*, 2007 and Banerjee *et al.,* 2008). Hence, the present study has been undertaken by using HATR-FTIR coupled with discriminant analysis to differentiate the ivory, antler and ceramic artifacts.

Spectra of elephant ivory, wild boar ivory and spotted deer antler samples revealed similar spectral features in all the three sample types. Spectral peaks of ivory of boar and antler of spotted deer were very much similar compared to peaks of ivory of elephant. Clear differences existed amongst these species in the region from 600 cm^{-1} to 800 cm^{-1}, whereas elephant ivory (*Elephas maximus indicus*), boar ivory (*Sus crofa cristatus*) and deer antler (*Axis axis*) showed maximal absorbance at 687, 701 and 671 cm^{-1} respectively. Another spectral difference was found in the region 1300 to 1500 cm^{-1} as described above. The shoulder at 1111 cm^{-1} was observed only in Elephant spectrum.

The FTIR spectra of ivory artifact (ceramic) clearly differed with all spectral features from ivory and antler of animals studied. No further test was required to classify the sample. Spectral peaks and minima of second derivative spectra were used to assign functional groups. Table 2 gives the details of peak assignment based on second

derivative spectra (Miller and Wilkins 1952; Espinoza E.O. *et al*., 2008; Movasaghi Z. 2007 and Kourkoumelis and Tzaphlidou 2010).

A comparison between transmission and ATR spectra was studied in elephant ivory samples. The primary transmission and ATR spectra were quite different. Banerjee *et al.* (2008) reported that the main Phosphate peak was observed at 1030 cm^{-1} cm in transmission who observed that s this peak was quite broader with a shoulder at 1079cm^{-1} and weaker shoulder at 1110 cm^{-1}. Whereas our study revealed a sharp peak at 1011 cm^{-1} in ATR spectra and a rather weak shoulders at 1078 cm^{-1} and 1111 cm^{-1}. But second derivative spectra of these primary spectra revealed identical peaks which were not evident in the primary spectra. But most of the peaks in the ATR spectra were weak.

The shoulder at 1111 cm^{-1} was slightly different from the earlier report (Banerjee *et al*., 2008). The main Peak at 1011 cm^{-1} was corresponding to PO_4^{-3} stretch which shifted to lower wave number in ATR spectra compared to transmission spectra. But the real peak occurring at 1012 cm^{-1} was evident from the second derivative spectra. The second derivative spectra were being used to find the exact location of shoulders in the original spectra and for finding exact peak locations, since peaks in the second derivative appeared at the same location as peaks in the original spectrum but as a negative peak (Stuart, 2007).

5.6. Discriminant analysis

Discriminant analysis is concerned with deriving helpful rules for allocating observations to one or other set of priories defined classes in some optimal way, using the information provided by a series of measurements made of each sample member. The

technique is used in situations in which group membership is known with certainity a priori, and a second set, the test sample, consisting of the observation for which group membership is unknown, with which we require to allocate to one of the known groups with a few misclassification as possible. If we know that our classifying variables are normally distributed within groups we can use a classification procedure called linear discriminant analysis (LDA). Another approach is canonical variate analysis. Canonical variate analysis (CVA) separates objects into classes by minimizing the within class variance and maximizing between class variance. The aim of CVA is to find directions (i.e., linear combination of original variables) in the data space, that maximize the ratio of the between class to within class variance. These directions are called discriminant functions or canonical variates (Ballabio and Todeschini. 2009)

5.6.1. Discriminant analysis of Hairs

In the present analysis the spectral data of known classes were deduced first into common covariance matrix shared by the groups. The covariance matrix was used to calculate the Mahalanobis distances. These distances were calculated between cases we want to classify and the center of each group in a multidimensional space. The Mahalanobis distances were used to calculate canonical scores. These canonical scores were used to graphically deduce group classes as canonical score plots (Systat 12, 2007, Kimsley, 1998).

We used 145 replicate spectra of cattle hairs, 88 replicate spectra of goat hairs 111 replicate spectra of leopard hairs, 57 replicate spectra of spotted deer hairs and 60 replicate spectra of tiger hairs. In this analysis the spectral data of known classes were

deduced first into common co-variance matrix shared by the groups, the canonical scores were used to geographically deduce group classes.

The performance index of all species lies between 95 to 100%. The performance index between goat and leopard was 99%, spotted deer and goat was 95%, tiger and spotted deer was 98% which indicates all animals compared exhibited the performance index of more than 95%. The results exceeded 90% of the performance index (Espinoza *et al.,* 2007) and Wilks lambda close to 0 indicates the accuracy of the samples (Ballabio and Todeschini, 2009). Our studies can be compared to the results obtained by Espinoza and Baker (2004) who while analyzing sea turtle and bovidae keratin reported a performance index of 95.5% and in an another study by Espinoza *et al.,* (2007) differentiated elephant hair with giraffe hair with a performance index of 97%.

5.6.2. Discriminant analysis of hoofs, claws, Horns

There are no major differences observed in the spectrum of cattle hoof, goat hoof, spotted deer hoof, tiger claw and leopard claw. The classical classification matrix was observed by combination of three different species. Utilizing the canonical score plots the performance index of all these three grouped animals such as cattle, goat, and tiger were 100%, leopard, cattle, and spotted deer were 99%.

5.6.3. Discriminant analysis of Elephant, Boar ivory and spotted deer antlers

For the linear discriminant analysis, we used 20 replicate spectra of 4 boar ivory samples, 30 replicate spectra of 6 elephant ivory samples and 48 replicate spectra of 5 spotted deer antler samples. The performance index was 100% for all the 3 test species.

The results indicating in excess of 90% of performance index (Espinoza *et al*, 2007) and the value of Wilks lambda closer to zero (Ballabio and Todeschini 2009) then it can be inferred that the accuracy of the classification as accurate. Further, the value of Wilks lambda varies between 0 and 1 and the value close to 0 indicates group means are different and validates the classification.

The analysis was also validated by correct assignment of external quality control standards. The test ivory sample was also correctly assigned to Elephant. The test sample was further authenticated using non spectroscopic histological finding.

We performed the linear discriminant analysis using different spectral measurements rather than direct spectral data points normally being used for the analysis. Still we were able to get correct classification of species. All the spectral measurements were subjected to normalization by dividing with a constant variable from each spectrum and thus minimizing the variation within the spectra of each group and which also helped in correct classification.

Summary

VI SUMMARY

Forest and police officials are facing difficulties in identifying the confiscated skin specimens, which are prepared using skins of domestic animals and selling them as skins of wild animals. Hence, to identify the original skin from the fake, histological studies using several staining techniques and FTIR with linear discriminant analysis (for identifying and differentiating the skin appendages such as hairs, claws, hoofs, horns ,antlers and ivories) have been employed in the present study.

The epidermis of cattle and tiger showed all the five layers. Cat, Goat and leopard showed four layers, whereas dog and spotted deer consisted of only three layers. In the leopard, there was clear demarcation between papillary layer and reticular layer of the dermis. In the papillary layer hair bundles were supported by the smooth muscle fibers. Densely irregular connective tissue along with branched alveolar sebaceous glands was observed. Whereas, in tiger the dermis consisted of interlacing elastic fibers and small collagen bundles extending in between the hair follicles.

Distinct elastic fibers were observed in between layers of hair follicle in the spotted deer. Such arrangements were not observed in the cattle and goat. In the tiger skin fine stranded elastic fibers were observed at papillary region, these elastic fibers were not stranded at dermal pegs. The distribution and arrangement of hair follicles in the dermis were species specific. In the spotted deer, hair follicles were arranged in a linear fashion. In the cattle, hair follicles were irregular and isolated. In the goat primary hair follicle was associated with 1-2 secondary hair follicles. In the Bengal tiger, clusters of

compound hair follicles were observed; within each compound follicle one large primary hair follicle located at one end was surrounded by 2-4 secondary follicles peripherally.

In the leopard, single large primary follicle was surrounded circumferentially by clusters of compound follicles; within each compound follicle 6-8 secondary hair follicles were found. In dog, compound follicles arranged in a capsular form, each compound follicle consisted of one large primary follicle with six to eight secondary follicles. in cat clusters of compound follicles uniformly distributed and large quantity of adipose tissue was observed at the base of dermis. In leopard sebaceous glands were branched alveolar type, in tiger one or two simple alveolar sebaceous glands were seen at the base of the primary hair follicle. The sweat glands were simple tubular merocrine in leopard and sacular apocrine in tiger. In case of cattle the sebaceous glands were present on either side of hair follicle whereas in goat the sebaceous glands were present in between hair follicles, having large segment supported by two minor segments of the glands. In case of spotted deer the sebaceous glands were present at the base of the hair follicles which were divided into two major segments.

In cattle sweat glands frequently in the deeper part of the dermis, whereas in case of spotted deer the simple tubular sweat glands were observed at the junction of the dermis and hypodermis, in the goat sweat glands were frequently seen at the base of the hair follicle.

FTIR spectroscopy has become a well-accepted and newly used method to characterize the keratinous and bony tissues of tiger, leopard, spotted deer and domestic animals. The technique of FTIR spectroscopy has also become a technique of choice for

forensic scientists interested in finding the structural properties of original and fake skins, hairs, hoofs, claws, antlers and ivories. Spectrum of amide A and B region of all hair samples of all animals exhibited very similar peak positions.

Amide I band due to C-O stretching and N-H bending vibration observed at 1638cm^{-1} in cattle hair, in goat hair these peak observed at 1629cm^{-1}, in spotted deer hairs at 1626cm-1, in leopard hairs at 1628cm^{-1} in tiger hairs at 1626cm^{-1}.

Amide II band due to C-N stretching and C-N-H bending vibration coupled with C=O stretching observed at 1525cm^{-1} in cattle, 1521cm^{-1} in goat, 1520cm^{-1} in spotted deer and tiger, 1519cm-1 in leopard hair. Amide III band due to C=O stretching was observed at 1237cm^{-1} in cattle, 1241cm-1 in goat, 1235cm^{-1} in spotted deer and tiger, 1234cm^{-1} in leopard. Cattle and spotted deer exhibited shoulder at 1158cm^{-1}, leopard exhibits shoulder at 1159cm^{-1}, whereas tiger and goat exhibited prominent peaks at 1160cm^{-1} and 1161cm^{-1} respectively.

Amide I peak observed at 1632cm-1 in cattle hoof, goat hoof, spotted deer hoof, tiger claw and leopard claw which is due to C=O stretching vibration. In the goat horn prominent amide I peak observed at 1631cm^{-1} due to more intensity of C=O stretching interaction. Prominent amide II peak observed at 1515cm^{-1} in goat hoof, spotted deer hoof and cattle horn, whereas in cattle hoof, leopard claw and tiger claw observed at 1514 cm^{-1}

Amide III peak was a weak at 1312cm^{-1} and medium peak at 1237cm^{-1} and shoulder observed at 1156cm^{-1} in the cattle hoof, whereas in goat hoof and spotted deer

hoofs amide III bands were observed at 1313 and 1238 cm^{-1}. In leopard and tiger claws the amide III peaks were observed at 1236cm^{-1} and shoulder observed at 1163 cm^{-1}, whereas shoulder observed at 1166cm^{-1} in tiger claw. In cattle horn and goat horn similar observation were found.

Spectral peaks of ivory of boar and antler of spotted deer are very much similar compare to ivory of elephant. Clear differences were observed in the region from 600 to 800 cm^{-1}, whereas Elephant (*Elephas maximus indicus),* wild boar *(Sus crofa cristatus)* and spotted deer (*Axis axis)* were showing maximal absorbance at 687, 701 and 671 cm^{-1} respectively. Another spectral difference was found in the region 1300 to 1500 cm^{-1}. The shoulder at 1111 cm^{-1} is only seen in Elephas spectrum. In this study the performance index lies between 97 to 100%. A resulting performance index shows that HATR FTIR, combined with discriminant analysis, is a powerful, nondestructive, qualitative technique for distinguishing ivories, hairs, claws, hoofs, horns, and antlers often encountered in museum collections and the modern wildlife trade.

Bibliography

VII BIBLIOGRAPHY

AKHTAR, W. and EDWARDS, H.G., 1997. Fourier-Transform Raman Spectroscopy of Mammalian and Avian Keratotic Biopolymers. *Spectrochimica Acta Mol. Biomol. Spectrosc*., **53A**: 81–90

ALEXANDER, N.J., PARAKKAL P.F., 1969 Formation of α- and β-type keratin in lizard epidermis during the molting cycle. Cell Tissue Res **101**:72–87

ALIBARDI, L., 2003a. Immunocytochemistry and keratinization in the epidermis of crocodilians. Zoological Studies, **42**(2): 346–56

ALIBARDI, L., 2003b. Adaptation to the land: the skin of reptiles in comparison to that of amphibians and endoderm amniotes, Journal of Experimental Zoology Part B: Molecular and Developmental Evolution, **298** (1): 12– 41

ALIBARDI, L., 2003c. Proliferation in the epidermis of chelonians and growth of the horny scutes. *J Morphol* **265**:52–69

AMBROSE, E. J. and ELLIOTT, A., 1951a, Infra-red spectra and structure of fibrous proteins, *Proceedings of the Royal Society of London, Series A, Mathematical and Physical Sciences*, **206** (1085): 206–19

AMBROSE, E.J. and ELLIOT, A., 1951b. Infra-red spectra and structure of fibrous proteins. Proc R Soc Lond A Math Phys Sci., **206**: 206–219

AMIEL, C., MARIEY, L., DENIS, C., PICHON, P., and TRAVERT, J., 2001. FTIR spectroscopy and taxonomic purpose: contribution to the classification of lactic acid bacteria, Le Lait, **81**(1–2): 249–255

BACHA, W. J. and BACHA, J. L. M., 1990. Integument, color atlas of Veterinary Histology, *Edn 2nd*, Lippincott Williams and Wilkins Philadelphia., *pp* 85-86

BADDIEL, C.B., 1968. Structure and Reaction of Human Hair; an Analysis of by infrared spectroscopy, *J. Mol. Biol.*, **38:** 181-199

BADDI, S.Y., 2009. Morphological studies on the skin of carnivorous wild animals. M.V.Sc. Thesis, Karnataka Veterinary, Animal and Fisheries Sciences University.Bidar

BAETEN, V. and APARICIO, R., 2000. Edible oils and fat authentication by Fourier transform Raman spectrometry, *Biotechnology, Agronomy, Society and Environment*, **4**(4): 196–203

BALLABIO, D., and TODESCHINI, R., 2009. Multivariate Classification for Qualitative Analysis in Infrared Spectroscopy for Food Quality Analysis and Control. Edn. Sun D.Academic Press Burlington.

BANERJEE, A. AND BORTOLASO, G. 2004. Digenetic changes of collagen in mammoth ivory as revealed by Isotopic Ratio Mass spectrometry (IRMS) and FTIR spectroscopy, *Geobiology* ,p. 53.

BANARJEE A., BORTOLASO G. and DINDORF W. 2008. Distinction between African and Asian Ivory in Ivory and Species Conservation Proceedings of INCENTIVS – Meetings (2004-2007) Bundesamt fur Natuschutz Bonn. 37-50

BANDEKAR, J., 1992. *Biochim. Biophys. Acta.*, **1120**: 123–143

BARTH, A., 2000. *Prog. Biophys. Mol. Biol.*, **74**, 141–173

BHAYANI, D.M., VYAS, K.N., VYAS, Y. L. and PANDYA, S. P., 1995. Histomorphological Study on the Skin of Lion *(Fells led). Indian J. Vet. Anat.,* **7**(1/2): 44-51

BITOSSI, G., GIORGIO, R., MAURO, M., SALVADORI, B., DEI, L., 2005. Spectroscopic techniques in cultural heritage conservation: a survey. *Appl. Spectroscope Rev.,* **40**:187–228

BLOOM and FAWCETT, 1986. A Text Book of Histology, 11th Edn. W.B. Saunders Company, Philadelphia, *pp*.543-578

BREKHMAN, J. T., Y. L DUBRYAKOV and A. L. TANEYEVA. 1969. The biological activity of the antlers of deer and other deer species. Ivestio Sibirskogo Ordelemia Akalemi Nank SISR. Biological Series No. **10** (2):112-115

BRUNNER, E., EHRLICH, H., SCHUPP, P., HEDRICH, R., HUNOLDT, S., KAMMER, M., MACHILL, S., PAASCH, S., BAZHENOV, V.V., KUREK, D.V., ARNOLD, T.BROCKMANN, S., RUHNOW, M., and BORN, R., **2009**. Chitin based scaffolds are an integral part of the skeleton of the marine demo sponge Ianthella *basta*. *J. Struct. Biol.* **168**: 539–547

CHURCH, J.S., 1999. Velvet Antler: Its historical medical use, performance enhancing effects and pharmacology. Elk Tech International Research Centre http: / www. Elk tech. Com / research. htm.

CITES, 1994. Resolutions of the Conference of the Parties, Conf. 10.10, Annex 2.

COPENHAVER, W.M., BUNGE, R.P. and BUNGE, M.B., 1971. Bailey's Textbook of Histology.**16**th Edn. Williams and Welkin's Company, Baltimore, Calcutta.

CULLING, C.F.A., 1981. Hand Book of Histological and Histochemical Techniques 3rd Edn. Butterworth's, London, *pp*. 422-438

DELLMAN, H.D., and BROWN, E.M., 1981. Text Book of Veterinary Histology. 2nd Edn. Lea and Fiebiger, Philadelphia, *pp.* 382-388

DERRICK, M. R., STULIK, D. C., and LANDRY, J. M., 2000. *Infrared spectroscopy in conservation science: scientific tools for conservation*, Getty Trust Publications, Getty Conservation Institute, Los Angeles, CA.

DHARMARAJ, S., JAMALUDIN, A. S., RAZAK, H. M., VALLIAPPAN, R., AHMAD, N. A., HARN, G. L., and ISMAIL, Z., 2006. The classification of *Phyllanthus niruri* Linn. According to location by infrared spectroscopy, *Vibrational Spectroscopy*, **41**(1): 68–72

EDWARD, G. and BATRICK., 2002**.** Applications of Vibrational Spectroscopy in Criminal Forensic Analysis *Handbook of Vibrational Spectroscopy* John M. Chalmers and Peter R. Griffiths (Editors) John Wiley & Sons Ltd, Chishester,

EGAN, W. J., MORGAN, S. L., BATRICK, E. G., MERRILL R. A., and TAYLOR III, H. J., 2003. Forensic discrimination of photocopy and printer toners. II. Discriminant analysis applied to infrared reflection–absorption spectroscopy, *Analytical and Bioanalytical Chemistry*, **376**(8): 1276–85

ELLIOTT, A., and AMBROSE, E. J., 1950. *Nature*, **165**, 291.

ELLIOTT, A., 1953. *Proc. Roy. Soc.* A, **221**, 104.

ELLIOTT, A., 1956. *Proc. IIIrd Int. Congr. Biochem.* p. 106. New York: Academic Press.

ENLOW, E. M., KENNEDY, J. L., NIEUWLAND, A. A., HENDRIX, J. E., and MORGAN, S. L., 2005. Discrimination of nylon polymers using attenuated total reflection mid-infrared spectra and multivariate statistical techniques, *Applied Spectroscopy*, **59**(8): 986–992

EPLING, G.P., 1953. The Anatomy of the Skin .In "Canine Medicine". American Veterinary Publications, Inc., Evanscon.

ESPINOZA, E., PRZYBYLA, J., and COX, R., 2006. Analysis of fiber blends using horizontal attenuate total reflection Fourier transform infrared and discriminant analysis, *Applied Spectroscopy*, **60**(4): 386–91

ESPINOZA, E.O., BAKER, B.W., and BERRY, C.A., 2007. The analysis of sea turtle and bovid keratin artefacts using DRIFT spectroscopy and discriminant analysis. Archaeometry **49:** 685–698

ESPINOZA, E.O., BAKER, B.W., MOORES, T.D., and VOIN, D., 2008. Forensic identification of Elephant and Girafffe Hair Artifacts Using HATR FTIR Spectroscopy and Discriminant Analysis. *Endanger. Species Res.,* **9**: 239-246

EVANS, H. E., and CHRISTENSEN, G. C., 1967. Miller's Anatomy of the dog. *Edn 2nd*., W.B.Saunders company philadolphia.London, Toronta,Mexico city, *pp.*78-97

FABIAN, H., 2000, 'Fourier Transform Infrared Spectroscopy in Peptide and Protein Analysis', in *Encyclopedia of Analytical Chemistry*, Vol. 7, Meyers, R. A. (Edn.), Wiley, Chichester, UK, *pp*.5779–5803

FRAZIER, J., 2005. Marine turtles—the ultimate tool kit: a review of worked bones from marine turtles, in From hooves to horns, from mollusc to mammoth: manufacture and use of bone artefacts from prehistoric times to the present (eds. H. Luik, A. M. Choyke, C. E. Batey and L. Lõugas), 359–82, Proceedings of the 4th Meeting of the ICAZ Worked Bone Research Group at Tallinn, 26th–31st of August 2003, International Council for Archaeozoology, Tallinn Book Printers.

FULDER, S. 1980a. The Hammer and the pesstle. New Scientist. **87** (1209): 120-123

GALLAGHER, W.H., TAO, F., and WOODWARD, C., 1992. *Biochemistry,* **31**: 4673-4680

GOLDSBERRY, S., and CALHOUN, M.L., 1959. The Comparative Histology of the Skin of Hereford and Aberdeen Angus Cattle. *Am .J. Vet. Res.,* **20**: 61-68

GRIEBENOW K., SANTOS A. M., CARRASQUILLO K. G., 1992. Secondary structure of proteins in the amorphous dehydrated state probed by FTIR spectroscopy, The Internet of Vibrational Spectroscopy Vol. **3**, Edn. 1.

HANSEN, A.E., SINCLAIR, J.G., AND WIESE, H.G., 1954. Sequence of Histologic Changes in Skin of Dog in Relation to Dietary Fat. *J. Nutr.,* **52:** 541-556

HOPKINS. J, BRENNER. L, and TUMOSA C.S, 1991. Variation of the amide I and amide II peak absorbance ratio in human hair as measured by Fourier transform infrared spectroscopy. *Forensic Sci. Int.,* **50**: 61–65

JALKANEN, K.J., WU¨RTZ JU¨RGENSEN, V., CLAUSSEN, A., RAHIM, A., JENSEN, G.M., WADE, R.C., NARDI, F., JUNG, C., DEGTYARENKO, I.M., NIEMINEN, R.M., HERRMANN, F., KNAPP-MOHAMMADY, M., NIEHAUS, T.A., FRIMAND, K., and JOY M, LEWIS D.M., 1991. The uses of Fourier transform infrared spectroscopy in the study of the surface chemistry of hair fibers. *Int. J. Cosmetic Sci.,* **13**: 249–261

KAPTCHUK, T., and. CROUCHER. M., 1987. The Healing Arts: Exploring the Medical Ways of the World. New York, Summit Books.

KIMSLEY E.K. 1998. Discriminant Analysis and Class Modelling of Spectroscopic Data. John Wiley & Sons Chishester

KIRKBRIDE K.P, TUNGOL M.W, 1999. Infrared micro spectroscopy of fibers, In: Robertson J, Grieve M (Edn) Forensic examination of fibers, 2nd Edn. Taylor & Francis Inc., Philadelphia, A, pp 179–222

KOURKOUMELIS, N., and TZAPHLIDOU, M., 2010. Spectroscopic Assessment of Normal Cortical Bone: Differences in Relation to Bone Site and Sex. *The Scientific World J*. **10**: 402-412

LEHNINGER, L., 1982. *Principles of biochemistry*, Worth, New York.

LLOYD, D. H., and GARTHWAITE, G., 1982. Epidermal Structure and Surface Topography of Canine Skin. *Res. Vet. Sci.* **33**(1): 99-104

LOVELL. J. E., and GETTY, R., 1957. The Hair Follicles, Epidermis, Dermis, and Skin Glands in the Dog. *Am .J. Vet. Res.,* **18**, (Oct); 873-885

LOW, M.J.D., and BAER, N.S., 1977. Application of infrared Fourier transforms spectroscopy to problems in conservation. Stud Conserve **22**; 116–128

LUNA, L.G., 1968. Manual of Histological Staining Methods of the Armed forces Institute of Pathology. 3rd Edn. McGraw-Hill Book co. New York, pp.85-95

LYMAN D.J., MURRAY-WIJELATH, J., and FEUGHLMAN, M., 2001. Effect of temperature on the conformation of extended α-keratin. Appl Spectroscope **55**; 552–554

MARCARIAN, H.Q., and CALHOUN, M.L., 1966. Microscopic Anatomy of the Integument of Adult Swine. *Am. J. Vet. Res.,* **27**(118):765-772

MARSHALL, R.C., ORWIN, D.F.G., GILLESPIE, J.M., 1991. Structure and biochemistry of mammalian hard keratin. Electron Microsc Rev **4**:47–83

MARGOLENA, H, A., 1959. Skin and Hair Follicle Development in Dairy Goats. *Virginia J. Sci.,* **10:** 33-47

MARIGHETO, N.A., KIMSLEY, E.K., DEFERNEZ, M., and WILSON, R.H., 1998. A comparison of mid-infrared and Raman spectroscopies for the authentication of edible oils, *J. Am. Oil Chem. Soc.,* **75**; 987- 992

MILLER, F.A., and WILKINS, C.H., 1952. Infrared Spectra and Characteristic Frequencies of Inorganic Ions Their Use in Qualitative Analysis.Anal.Chemistry **24**:1253 –1294.

MOVASAGHI, Z., REHMAN, S., REHMAN, I., 2008. Fourier Transform Infrared (FTIR) Spectroscopy of Bilogical Tissues. *Appl. Spectroscopy Rev.,* **43**: 134-179

NICKEL, R., SCHUMMER, A., and SEIFERLE, E., 1981. The Anatomy of the Domestic Animals. **3**: 487-505

PANAYIOUTOU, H., 2004. Vibrational Spectroscopy of Keratin Fibbers, A Forensic Approach. Ph D thesis submitted to the School of Physical and Chemical Sciences, Queensland University of Technology.

PARIJ, S.C., and BHATTACHARYA, S., 2001. Guest editorial, the tragedy of tigers: Lesson to Learn from Nandankanan Episode *Indian J. Med. Microbiol.*, **19**; 116

PARIS, C., LECOMTE, S., and COUPRY, C., 2005. ATR–FTIR spectroscopy as a way to identify natural protein-based materials, tortoiseshell and horn, from their protein-based imitation, galalith, *Spectrochimica Acta Part A Molecular and Biomolecular Spectroscopy*, **62**(1–3);532–538

PASCHALIS, E.P., VERDELIS, KDOTY, S.B., BOSKEY, A.L., MENDELSOHN, R., and YAMAUCHI, M., 2001. Spectroscopic characterization of collagen cross-links in bone. Journal of bone and mineral Research Volume **16**, pp1821-1828

PIELESZ, A., WESEŁUCHA-BIRCZYNSKA., 2000. The identification of structural changes in the keratin of wool fiber dyed with an azo dye using the Raman and Fourier transform infrared spectroscopy methods Journal of Molecular Structure, **555:** 325–334

PRICE, J.S., B.O., OYAJOBI, A.M., NALIN, 1996. Chondrogenesis in the regenerating antler tip in red deer: expression of collagen types I, hA, IIB, and X demonstrated by in situ nucleic acid hybridization and Immunocytochemistry. *Dev Dyn*., **205**(3); 332-347

ROUGHLEY, P.J. AND LEE, E.R. 1994 .Cartilage proteoglycans: structure and potential functions. Microscop. Res. Technique, **28**, 385-397.

RENATA ŽEMAITYTĖ, VAIDA JONAITIENĖ, RIMVYDAS MILAŠIUS, SIGITAS STANYS, and REGINA ULOZAITĖ. 2006. Analysis and Identification of Fiber Constitution of Archaeological Textiles**.** *ISSN 1392–1320 materials science (medžiagotyra). Vol.* ***12****, No.* ***3.***

RINTOUL, L., PANAYIOTOU, H., KOKOT, S., GEORGE. G., and OTHERS, 1998. Fourier transforms infrared spectrometry: a versatile technique for real world samples. Analyst (Lond) **123**; 571–577

SAR, M., and CALHOUN, M. L., 1996. Microscopic Anatomy of the Integument of the Common American Goat. *Am. J. Vet. Res.*, **27**; 444

SHENGQING, ZU ENDONG and LIU LIJUN., 2011. Identification of Rhinoceros Horn and its Substitutes *Advanced Materials Research Vol., **177** pp 636-63 © Trans Tech Publications, Switzerland.*

SILA TRIPATI, and IAN GODFREY., 2007. Studies on elephant tusks and hippopotamus teeth collected from the early 17th century Portuguese shipwreck off Goa, west coast of India: Evidence of maritime trade between Goa, Portugal and African countries. *Current science vol.*, **92** No .3, *pp* 333-339

SINGH, U.B., and SULOCHANA, S., 1996. Hand Book of Histological and Histochemical Techniques. 2nd Edn. Premier Publishing House, Hyderabad, pp.39-41

SISSON.S. and GROSSMAN, J. D., 1958. Anatomy of Domestic Animals. 3nd Edn. W.B.Saunders Co., Philadelphia,

SOLOMON, S. E., HENDRICKSON, J. R., and HENDRICKSON, L. P., 1986. The structure of the carapace and plastron of juvenile turtles, *Chelonian mydas* (the green turtle) and *Caretta caretta* (the loggerhead turtle), *Journal of Anatomy*, **145**: 123–31

STINER, M. C., WEINER, S., BAR-YOSEF, O., and KUHN, S. L., 1995. Differential burning, fragmentation, and preservation of archaeological bone. *Journal of Archaeological Science*, **22:** 223–237

STRICKLAND. S., and CALHOUN. M.L., 1963. The Integumentary System of the Cat. *Am. J. Vet. Res*., **24**; 1018-1029

STUART, B., 2004. Infrared Spectroscopy – Fundamentals and Applications. John Wiley & Sons, Ltd.

SUNWOO, H. H., 1998. Isolation and characterization of proteoglycans in growing antlers of wapiti (Cervus Elephas). Chapter 8 In Chemical characterization of growing antlers of Wapiti (Cervus Elephas). Ph. D. thesis, University of Alberta.

SYSTAT SOFTWARE, INC., 2007. Chicago IL USA.

TALUKDAR, A.M., CALHOUN, M.L., and STINSON, AL .W, 1972. Microscopic Anatomy of the Skin of Horse. *Am. J. Vet. Res*., **33**; 2365-2390

THERMO FISHER SCIENTIFIC INC., 2009. Madison, WI, USA.

TIMMINS, E.M., HOWELL, S.A., ALSBERG, B.K., NOBLE, W.C., and GOODACRE, R., 1998. Rapid differentiation of closely related *Candida* species and strains by pyrolysis-mass spectrometry and Fourier transform-infrared spectroscopy. *J Clin Microbiol.,* **36**; 367–374

TRAUTMANN and FIBIGER. J., 1957. Fundamentals of the Histology of Domestic Animals. 8th and 9th Edn. Comstock Publishing Associates, A Division of Cornell University Press, Ithaca, New York, *pp.* 334-355

VARICAK, T., 1941. Observations concerning the Epidermis in Domestic Animals. Vet Archive, **11**: 189-200

WANG, F. DUAN, J. A., NANJING UNIV, J., 2007. *Traditional Chin. Medicine*, **23**; 36

WANG, W., and PALIWAL, J., 2007. Near-infrared spectroscopy and imaging in food quality and safety. *Sens and Instrumen. Food Qual.*, **1**; 193-207

WIDJAJA, E., and SEAH, R. K. H., 2006. Use of Raman spectroscopy and multivariate classification techniques for the differentiation of fingernails and toenails, *Applied Spectroscopy*, **60** (3); 343–345

WILD LIFE PROTECTION SOCIETY OF INDIA (WPSI) 2000. Census, India

WILD LIFE INSTITUTE OF INDIA (WII) 2003 census, India

WINKELMANN, R.K., 1957. The sensory End organ of the Hairless Skin of the cat. *J.Invest. Dermt.*, **29**; 274-280

XING, J., NGADI, M., GUNENC, A., PRASHER, S., and GARIEPY, C., 2007. Use of visible spectroscopy for quality classification of intact pork meat. *J. Food Eng.*, **82**; 135-141

YASUI, N., and NIMNI, M.E., 1998. Cartilage collagens. In: Collagen, Volume I. M.E. Nimmi, ed. Boca Raton: CRC Press. 225-241

Abstract

VIII ABSTRACT

The histological study was conducted on the skin of wild and domestic animals, the epidermis of cattle and tiger showed all the five layers; Cat, Goat and leopard showed four layers, whereas spotted deer and dog consisted of only three layers. In the leopard, single large primary follicle was surrounded by clusters of compound follicles; within each compound follicle 6-8 secondary hair follicles were found. In dog, compound follicles arranged in a capsular form, each compound follicle consisted of one large primary follicle with six to eight secondary follicles. Whereas in cat, hair follicles arrangement was similar to that of tiger but there was large quantity of adipose tissue was observed at the base of dermis. In the spotted deer, hair follicles were arranged in a linear fashion. In the cattle, hair follicles were irregular and isolated. In the goat primary hair follicle was associated with 1-2 secondary hair follicles. In the Bengal tiger, clusters of compound hair follicles were observed; within each compound follicle one large primary hair follicle located at one end was surrounded by 2-4 secondary follicles peripherally. By using histological technique structural pattern of epidermis, hair follicle arrangement and glandular location can be appreciated, which are species specific. Thus help in solving the veterolegal cases and punishing the poachers. The representative samples of different tissues collected from wild and domestic animals were subjected to FTIR analysis and FTIR spectra were obtained. The natural keratin fibers and bony tissues were investigated through the use of FTIR followed by linear discriminant analysis or canonical score variates. All samples studied in this work showed similar vibration spectra in the spectral region between 4000-400cm^{-1}. A resulting performance index of above 90% shows that HATR FTIR, combined with discriminant analysis, is a powerful, nondestructive, quantitative technique for distinguishing ivories, hairs,claws,hoofs, horns and antlers often encountered in museum collections and the modern wildlife trade.

Appendices

APPENDICES

Table – A - FTIR Peak assignment for Keratinaceous Appendages resolved by secondary derivative spectra.

(Hopkins et. al., 1991, Joy and Lewis 1991, Akhtar and Edwards et. al., 1998).

Mean Peaks	Assignment
3274, 3273, 3272, 3271	Stretching O-H symmetric, N-H stretching, Amide A band
3066, 3065, 3064, 3063, 3062	C_2 aromatic stretching, Amide B band
2667, 2965, 2964, 2963	CH_3 modes
2931, 2930, 2929, 2927	C-H stretching bands
2925	C-H stretching bands
2874, 2873	ν st CH3 , Stretching C-H, N-H
2853, 2852, 2851	Symmetric CH_2 stretch
1693	Antiparallel β-sheet of amide I
1683, 1682, 1681, 1679	Unordered random coils and turns of amide I
1664, 1663	Amide I (disordered structure-solvated), 3 turn Helix
1647,1646, 1645	Amide I Random Coil
1642, 1640, 1637	Amide I β-sheet
1630	Amide I β-sheet
1625, 1623, 1622	Amide I β-sheet
1611, 1610, 1609, 1608	Amide I Unordered
1568, 1567	Amide II Ring base
1553	CO stretching Predominately a-sheet of amide II (Amide II band mainly stems from the C-N stretching and C-N-H bending vibrations weakly coupled to the C=O stretching Ring base
1552, 1551, 1550, 1549	Amide II Ring base (an N-H bending vibration coupled to C-N stretching)
1539, 1538, 1537, 1536	Amide II β-sheet, Stretching C=N, C=C (an N-H bending vibration coupled to C-N stretching
1519, 1518, 1517, 1516, 1515	Amide II (tyrosine side chain)
1513, 1512	ν(C=C)pigment , Amide II (an N-H bending vibration coupled to C-N stretching)
1498, 1497	CH in-plane bending
1451, 1450	Asymmetric CH_3 bending modes of the methyl groups of proteins, Methylene Deformation
1400	COO- symmetric stretching of acidic amino acids aspartate and glutamate Aliphatic side groups of the amino acid residues
1397	CH3 symmetric deformation
1395, 1393, 1392, 1391, 1390, 1389	Aliphatic side groups of the amino acid residues
1380, 1379, 1378, 1377, 1376	δCH_3, Stretching C-O, deformation C-H, deformation N-H
1371, 1369, 1368	Deformation N-H, C-H, δ(CH2), ν(CC)
1341, 1340	CH_2 wagging
1316, 1315, 1314, 1313,	Amide III band components of proteins

1312	
1308, 1307, 1306, 1305	Amide III
1303, 1302	Amide III
1290, 1289	Amide III
1286, 1285, 1284	Amide III, Deformation N-H
1273, 1271, 1270	CHα' rocking
1269, 1268, 1266, 1265	Amide III, CHα' rocking
1236, 1235, 1234, 1233	Amide III
1209, 1207, 1205, 1204, 1203, 1202	C-O-C , Ring vibrations, PO_2^- asymmetric (phosphate I), proteins-amide III
1200	Protein
1166	C-O stretching mode of C-OH groups of serine, threosine, & tyrosine of proteins), ν(CC), δ(COH), ν(CO) stretching
1163	CH_9, , CH_7, CH 7 deformations, C-O stretching
1161, 1160, 1159, 1158, 1156, 1155	νC-O of proteins,
1127, 1126	ν(C-O)
1108, 1107, 1106, 1105, 1104	ν asym(SO) Cystein dioxide, ν(CO), ν(CC)
1102, 1100	SO stretch (cysteine residue)
1078, 1077, 1076	ν sym(SO) Cysteine monoxide
1048, 1047, 1046, 1045	ν sym(SO) Cysteine monoxide
1043, 1042	ν st(SO) Cysteine monoxide
950, 948	Pigments
944, 942, 940, 939, 938	Pigments

Table - B: FTIR Peak Assignment for Antler or Ivory (Boney appendages)

(Miller and Wilkins 1952, Espinoza E.O. et al 2008 and Movasaghi Z. 2007, Kourkoumelis and Tzaphlidou 2010)

Wave umber (Mean)	Assignment
3279	– OH stretch symmetric
2875	νs Stretch C-H
2847	Symmetric stretch Methoxy, C-H stretch , Cholesterol, Phospholipids
1693,1694	Anti parallel β- sheet of Amide I
1680, 1681, 1683	C=O Guanine deformation N-H in plane
1680	Unordered random coil turns Amide I
1668	Amide I - Anti parallel β- sheet, inorganic Sulfate
1663, 62	C = O Cytosine, Uracyl
1654	Amide I, C2 = O Cytosine / C = O, C = N, N - H of Adenine, Thiamine, Guanine and Cytosine
1648, 1647	Amide I
1633, 34, 36	β- sheet – Amide I
1630, 1629	Amide I / C = C Uracyl C = O, Inorganic Sulfate
1567, 1566	Ring base
1563, 1560, 1557	Ring base
1548, 49, 50	Amide II
1528, 1531	C = N modified Guanine C = N Adenine, Cytosine Stretching C=N, C=C
1526, 1525, 1524	C = N Guanine, Stretching C=N, C=C
1522, 1521, 1519	Amide II ?
1513, 1512	CH in-plane bend.
1499, 1498	C = C, deformation C-H
1472, 1470	CH2 bending of the methylene chain in lipids
1453, 1452, 1451	Asymmetric CH3 bending of methyl groups of proteins, Inorganic carbonate
1379,1378, 1377	δ CH3, C – O stretching, deformation - C – H, deformation N – H .
1338	CH2 wagging / Collagen
1317	Amide III proteins / Collagen
1284, 1283	Amide III proteins – Collagen
1240	ν_{as} PO_2^- , Collagen, Amide III
1202, 1201	PO_2^- (Phosphate I) asymmetric
1162, 1161, 1160	CO stretching, Stretching vibrations of hydrogen-bonding C-OH groups, n(CC), d(COH), n(CO) stretching, Stretching modes of the C-OH groups of serine, threonine, and tyrosine residues of cellular proteins
1111	Symmetric Stretching P-O-C ?, Inorganic Phosphate
1097	Phosphate II stretching PO_2 symmetric
1085,1084	νs PO_2^-, DNA (PO_2^- vibrations), νs PO_2^- of nucleic acids, PO_2 symmetric (phosphate II)
1079	νs PO_2
1059, 1058	Stretching C-O deoxyribose, Oligosaccharide C-OH stretching band
1012, 1011	$CH_{\alpha\alpha'}$ out of plane and $C_\alpha = C_\alpha$ out of plane bending, Stretching C-O

	deoxyribose
1010	Stretching deoxyribose
958	Inorganic Phosphate, CH out of plane bending vibrations (700 – 1000)
872	CO_3^{-2} (carbonate), CH out of plane bending vibrations (600 – 900)
668, 666, 664	Inorganic sulfate, CH out of plane bending vibrations (600 – 900)
599, 600	CH out of plane bending vibrations (600 – 900)
576,557,522, 21	$C_\alpha = C_{\alpha'}$ torsion and C-OH_3 torsion of Methoxy group

Table-C: FTIR Peaks Assignments for Artifacts

Mean peaks	SD	Peak Assignment
469.41	2.705565	
539.5856	0.464384	
651.8533	0.079057	C-S Stretching
698.9856	0.094089	C-H Out of Plane Bending
741.7689	0.187779	C_H Out of Plane Bending
847.87	0.080178	
872.7089	0.108218	
1041.928	0.240936	S=O Stretching
1066.411	0.148277	S=O Stretching
1118.741	0.239867	C=O Stretching and Bending
1263.138	0.656521	C-O Stretching; C=O Stretching and Bending
1413.316	1.977885	C-H Bending
1491.918	0.300574	C-H Bending - Aromatic
1541.093	0.028702	C-H Bending - Aromatic
1580.627	0.18775	C-H Bending - Aromatic
1600.282	0.211174	C=C Stretching
1720.581	0.347291	C=O Stretching
2287.053	0.661784	
2324.148	0.071375	
2517.214	1.898145	S-H Stretching
2642.486	4.093984	
2927.879	1.219851	CH Stretching -CH2 Group
3027.326	0.352353	
3061.061	0.546064	CH Stretching
3423.977	4.71418	

Table – 1: Second derivatives spectra of hairs

Cattle Hair		Goat Hair		Spotted Deer Hair		Leopard Hair		Tiger Hair	
Mean	SD	Mean	SD	Mean	SD	Mean	SD	Mean	SD
3272	3.82	3272	4.02	3272	3.74	3272	3.57	3271	4.19
3065	4.93	3063	6.89	3066	3.33	3063	6.69	3065	5.14
2963	1.71	2965	4.74	2964	3.48	2963	2.24	2967	3.6
2925	5.43	2927	5.54	2927	5.63	2929	3.8	2925	5.99
2874	0.38	2874	0.762	2874	0.454	2873	0.472	2873	0.316
2851	0.927	2851	0.476	2851	0.508	2851	0.9	2851	0.406
1693	1.35	1693	1.47	1693	1.14	1693	1.34	1693	1.25
1681	2.57	1682	2.35	1682	2.78	1681	2.51	1683	1.41
1663	2.87	1664	2.81	1663	1.87	1663	2.45	1663	0.213
1647	1.59	1645	5.28	1646	2.01	1646	2.49	1646	1.92
1623	2.92	1625	3.5	1622	1.3	1622	0.344	1622	0.328
1608	1.16	1608	2.61	1609	0.588	1609	0.36	1609	0.337
1568	3.16	1567	2.9	1567	1.91	1567	3.08	1567	1.9
1550	3.02	1549	3.58	1551	2.41	1550	3.01	1551	2.41
1538	3.11	1539	2.96	1538	2.63	1538	2.52	1538	2.44
1518	1.41	1518	0.401	1518	0.999	1519	2.58	1518	1.71
1513	0.38	1513	0.716	1512	0.342	1512	0.332	1512	0.29
1498	0.184	1498	0.539	1498	0.152	1498	0.278	1498	0.199
1451	1.93	1450	3.83	1451	1.74	1451	2.17	1451	1.09
1392	5.1	1395	5.82	1391	3.49	1390	3.84	1397	5.36
1380	5.07	1378	5.66	1377	6.15	1376	6.47	1379	4.67
1341	1.89	1341	1.31	1341	1.63	1341	2.15	1340	1.05
1315	2.77	1313	2.72	1316	2.85	1314	1.97	1313	1.8
1303	2.04	1305	2.31	1303	1.74	1302	1.11	1302	0.654
1285	3.74	1285	4.42	1285	1.47	1284	2.4	1284	2.11
1273	3.59	1270	5.12	1271	4.62	1270	5.02	1271	5.18
1236	2.4	1236	1.37	1236	1.31	1234	2.14	1233	1.4
1200	2.89	1200	4.43	1202	0.894	1203	0.993	1203	0.618
1158	1.76	1161	3.32	1158	1.91	1159	3.32	1160	1.04
1126	2.01	1126	3.68	1126	2.7	1126	0.769	1127	2.08
1104	5.21	1105	3.17	1102	1.06	1100	2.33	1102	1.46
1077	0.76	1076	1.03	1077	0.488	1076	1.01	1076	0.812
1042	1.7	1042	1.27	1042	1.01	1042	0.965	1043	0.543
948	6.51	948	4.59	950	0.609	948	3.3	950	0.533

Table –2: Second derivatives spectra of claws and hoofs

Tiger Claw		Leopard Claw		Cattle Hoof		Goat Hoof		Spotted Deer Hoof	
Mean	SD	Mean	SD	Mean	SD	Mean	SD	Mean	SD
3271	2.49	3272	1.73	3273	4.99	3272	3.87	3274	7.3
3064	5.15	3062	6.64	3062	5.76	3065	3.61	3065	3.78
2963	1.02	2962	1.59	2964	0.894	2964	1.25	2964	0.549
2930	4.25	2925	6.2	2931	1.63	2931	3.62	2930	1.72
2873	0.493	2874	0.502	2874	0.427	2874	0.549	2873	0.296
2851	0.783	2851	0.716	2852	1.69	2853	4.58	2851	0.41
1693	1.4	1693	0.17	1693	0.607	1693	0.142	1693	0.198
1681	2.38	1679	1.83	1681	2.45	1681	2.36	1682	2.34
1663	0.2	1663	0.122	1663	0.214	1663	0.142	1663	0.109
1646	2.31	1647	1.42	1640	6.18	1637	6.17	1640	6.51
1630	0.465	1630	0.497	1630	0.582	1630	0.35	1630	0.63
1611	1.79	1610	1.93	1610	1.68	1609	1.07	1609	1.55
1567	1.82	1568	1.24	1568	1.28	1568	0.777	1567	1.95
1552	1.64	1552	1.4	1552	1.98	1553	1.09	1552	2.14
1537	2.05	1537	1.57	1537	2.21	1537	1.77	1536	1.32
1515	1.81	1516	1.88	1516	1.76	1516	1.86	1516	1.96
1513	0.422	1513	0.345	1513	0.787	1513	0.394	1513	0.369
1498	0.78	1498	1.16	1499	1.32	1498	0.641	1498	0.459
1451	1.91	1451	3.2	1450	3.29	1451	3.06	1451	0.641
1393	5.23	1400	4.84	1389	1.14	1389	1.54	1389	1.22
1379	5.16	1379	5.33	1369	3.45	1369	1.87	1368	0.27
1340	2.08	1340	1.27	1341	1.89	1340	1.07	1341	1.28
1313	1.56	1313	1.2	1312	2.05	1313	0.778	1313	0.7
1306	1.29	1305	1.11	1308	1.95	1308	1.91	1306	1.63
1290	2.9	1289	1.88	1284	1.82	1286	0.635	1286	0.853
1269	1.11	1268	1.95	1270	5.65	1266	4.54	1265	3.6
1234	1.28	1233	1.28	1235	1.72	1236	0.982	1236	0.68
1205	1.58	1204	0.992	1207	3.82	1209	3.57	1205	0.645
1166	3.04	1163	5.46	1156	0.51	1156	0.41	1155	0.432
1127	1.46	1126	2.85	1126	0.923	1127	0.841	1126	1.14
1106	0.555	1106	1.47	1107	3.33	1106	1.16	1106	0.801
1077	0.884	1077	1.14	1078	0.625	1078	0.528	1078	0.584
1046	0.929	1046	2.01	1045	1.44	1048	1.2	1046	1.41
940	6.31	939	4.31	939	5.51	942	7.53	938	1.22

Table – 3: Second derivatives spectra of horns

Cattle Horn		Goat Horn	
Mean	SD	Mean	SD
3273	5.52	3273	4.45
3065	5.47	3064	2.55
2963	1.5	2964	1.18
2925	6.2	2929	5.33
2873	0.471	2874	0.398
2851	1.36	2851	0.831
1693	0.499	1693	0.202
1681	2.46	1681	2.31
1663	0.185	1663	0.211
1642	5.92	1637	5.84
1630	0.58	1630	0.431
1609	2.44	1609	1.68
1568	0.863	1568	0.963
1552	1.73	1552	1.56
1536	1.63	1536	2.06
1516	1.84	1517	1.29
1513	0.667	1513	0.635
1497	2.35	1497	1.74
1451	1.78	1451	0.708
1389	1.17	1389	1.5
1371	5.34	1369	2.19
1341	1.83	1341	1.84
1313	0.867	1313	1.11
1307	1.78	1307	1.72
1285	1.48	1285	0.86
1269	4.54	1265	4.35
1236	1.13	1237	0.896
1205	1.18	1207	3.12
1156	0.478	1156	0.376
1126	1.96	1126	0.834
1106	2.11	1108	2.68
1077	1.65	1078	1.39
1043	1.56	1047	1.42
948	9.81	944	10

Table – 4: Second derivatives spectra of ivories and antlers.

Boar Ivory		Elephant Tusk		Spotted Deer Antler	
Mean Peaks	**SD**	**Mean Peaks**	**SD**	**Mean Peaks**	**SD**
3279	10	3275	8.66	3276	9.28
2875	0.733	2875	0.967	2875	0.938
2847	3.74	2851	4.54	2851	1.96
1693	1.33	1694	0.896	1693	1.57
1680	2.63	1683	1.38	1681	2.98
1668	0.438	1668	0.566	1668	0.429
1663	0.114	1662	0.432	1663	0.249
1654	1.48	1654	1.55	1654	1.23
1647	1.45	1648	1.69	1647	2.02
1633	0	1636	2.44	1634	1.19
1630	0.168	1629	1.32	1630	0.233
1567	1.12	1566	1.07	1567	1.39
1557	2.57	1560	5.39	1563	5.13
1548	2.69	1550	4.67	1549	3.77
1531	1.65	1528	2.9	1531	2.68
1526	1.84	1524	1.02	1525	1.7
1519	1.16	1522	1.82	1521	2.5
1513	0.446	1512	1.72	1512	0.969
1499	0.147	1498	0.166	1498	0.86
1470	1.09	1470	1.51	1472	3.39
1470	0.999	1470	1.52	1471	1.65
1451	0.374	1453	0.657	1452	0.665
1379	0.187	1377	1.77	1378	1.42
1338	0.558	1338	0.371	1338	1.08
1317	0.565	1317	0.231	1317	0.544
1284	0.436	1284	0.698	1283	0.641
1240	0.827	1240	0.613	1240	0.621
1201	0.339	1202	0.266	1201	0.344
1160	1.62	1161	1.13	1162	1.2
1097	1.01	1111	2.07	1097	3.94
1084	1.19	1079	3.45	1085	2.49
1059	0.773	1058	1.38	1058	0.966
1010	2.99	1012	1.4	1012	1.94
958	0.201	958	0.26	958	0.318
872	0.971	872	1.24	872	0.575
664	2.18	666	3.2	668	1.08
600	0.19	599	0.331	600	0.154
576	0.398	576	1.24	575	1.06
557	0.253	557	0.483	557	0.381
522	3.62	521	3.07	516	5.87

Table-5: Performance index (P.I.) and Wilks's lambda of hairs of different grouped animals

Classification Matrix (Cases in row categories classified into columns)

Species	Cattle	Goat	Leopard	P.I(%correct)
Cattle	145	0	0	100
Goat	0	88	0	100
Leopard	0	0	111	100
Total	145	88	111	100
Species	Cattle	Goat	Spotted Deer	%correct
Cattle	145	0	0	100
Goat	0	88	0	100
Spotted Deer	2	0	57	97
Total	147	88	57	99

Test Statistics

Statistic (for (Cattle, Goat and Leopard)	Value
Wilks's Lambda	0.022
Statistic(Cattle, goat and spotted deer)	Value
Wilks's Lambda	0.03

Canonical Scores of Group Means

Species	1	2
Cattle	-0.112	2.379
Goat	4.224	-1.631
Leopard	-3.202	-1.815
species	1	2
Cattle	1.678	1.327
Goat	-4.321	-0.211
Spotted Deer	2.32	-2.945

Table-6: Performance index and Wilks's lambda of hairs of different grouped animals

Classification Matrix (Cases in row categories classified into columns)

Species	Cattle	Goat	Tiger	%correct
Cattle	145	0	0	100
Goat	0	88	0	100
Tiger	0	0	60	100
Total	145	88	60	100
Species	Cattle	Leopard	Spotted Deer	%correct
Cattle	144	1	0	99
Leopard	0	111	0	100
Spotted Deer	0	0	59	100
Total	144	112	59	100

Test Statistics

Statistic (for Cattle, Goat and Tiger)	Value
Wilks's Lambda	0.025
Statistic (for Cattle, Leopard and Spotted Deer)	Value
Wilks's Lambda	0.03

Canonical Scores of Group Means

Species	1	2
Cattle	2.409	-0.925
Goat	-3.828	-1.102
Tiger	-0.208	3.852
species	1	2
Cattle	2.643	0.922
Leopard	-3.778	0.557
Spotted Deer	0.613	-3.314

Table-7: Performance index and Wilks's lambda of hairs of different grouped animals

Classification Matrix (Cases in row categories classified into columns)

Species	Cattle	Leopard	Tiger	%correct
Cattle	145	0	0	100
Leopard	0	111	0	100
Tiger	0	0	60	100
Total	145	111	60	100
Species	Cattle	Spotted Deer	Tiger	%correct
Cattle	145	0	0	100
Spotted Deer	1	58	0	98
Tiger	0	0	60	100
Total	146	58	60	100

Test Statistics

Statistic (for Cattle, Leopard and Tiger)	Value
Wilks's Lambda	0.015
Statistic(Cattle, spotted deer and Tiger)	Value
Wilks's Lambda	0.021

Canonical Scores of Group Means

Species	1	2
Cattle	3.267	-0.692
Leopard	-3.666	-1.551
Tiger	-1.113	4.541
Species	1	2
Cattle	-0.428	1.663
Spotted Deer	-4.055	-2.453
Tiger	5.022	-1.606

Table-8: Performance index and Wilks's lambda of hairs of different grouped animals

Classification Matrix (Cases in row categories classified into columns)

Species	Goat	Leopard	Spotted Deer	%correct
Goat	87	0	1	99
Leopard	0	111	0	100
Spotted Deer	1	2	56	95
Total	88	113	57	98
Species	Goat	Leopard	Tiger	%correct
Goat	87	1	0	99
Leopard	0	110	1	99
Tiger	0	0	60	100
Total	87	111	61	99

Statistics

Statistic (for Goat, Leopard and Spotted Deer)	Value
Wilks's Lambda	0.025
Statistic (for Goat, Leopard and Tiger)	Value
Wilks's Lambda	0.015

Canonical Scores of Group Means

Species	1	2
Goat	4.1	-0.797
Leopard	-3.133	-0.938
Spotted Deer	-0.22	2.954
Species	1	2
Goat	-4.435	0.027
Leopard	2.258	-2.026
Tiger	2.328	3.709

Table-9: Performance index and Wilks's lambda of hairs of different grouped animals

Classification Matrix (Cases in row categories classified into columns)

Species	Goat	Spotted Deer	Tiger	%correct
Goat	87	1	0	99
Spotted Deer	1	58	0	98
Tiger	0	0	60	100
Total	88	59	60	99
Species	Leopard	Spotted Deer	Tiger	%correct
Leopard	111	0	0	100
Spotted Deer	0	59	0	100
Tiger	0	0	60	100
Total	111	59	60	100

Test Statistics

Statistic (for Goat, Spotted Deer and Tiger)	Value
Wilks's Lambda	0.016
Statistic (for Leopard, Spotted Deer and Tiger)	Value
Wilks's Lambda	0.013

Canonical Scores of Group Means

Species	1	2
Goat	2.263	1.998
Spotted Deer	1.033	-3.663
Tiger	-4.336	0.672
Species	1	2
Leopard	-0.055	-2.437
Spotted Deer	-4.413	2.329
Tiger	4.442	2.219

Hoof, Horn and Claw Keratin Canonical Score Plots

Table-10: Performance index and Wilks's lambda of hoofs and claws of different grouped animals

Classification Matrix (Cases in row categories classified into columns)

	Cattle	Goat	Spotted Deer	%correct
Cattle	50	0	0	100
Goat	0	60	0	100
Spotted Deer	0	1	9	90
Total	50	61	9	99
	Cattle	Goat	Leopard	%correct
Cattle	50	0	0	100
Goat	0	60	0	100
Leopard	0	0	79	100
Total	50	60	79	100

Test Statistics

Statistic (for Cattle, Goat and Spotted Deer Hoof)	Value
Wilks's Lambda	0.031
Statistic (for Cattle, Goat Hoof and Leopard Claw)	Value
Wilks's Lambda	0.003

Canonical Scores of Group Means

Species	1	2
Cattle	3.422	-0.648
Goat	-3.14	-0.187
Spotted Deer	1.732	4.366
Species	1	2
Cattle	0.994	4.46
Goat	8.505	-1.927
Leopard	-7.089	-1.36

Table-11: Performance index and Wilks's lambda of hoofs and claws of different grouped animals

Classification Matrix (Cases in row categories classified into columns)

Species	Cattle	Goat	Tiger	%correct
Cattle	50	0	0	100
Goat	0	60	0	100
Tiger	0	0	70	100
Total	50	60	70	100
Species	Cattle	Leopard	Spotted Deer	%correct
Cattle	50	0	0	100
Leopard	0	79	0	100
Spotted Deer	0	0	10	100
Total	50	79	10	100

Test Statistics

Statistic (for Cattle, Goat Hoof and Tiger Claw)	Value
Wilks's Lambda	0.006
Statistic (for Cattle, Spotted Deer Hoof and Leopard Claw)	Value
Wilks's Lambda	0.01

Canonical Scores of Group Means

species	1	2
Cattle	1.454	2.911
Goat	6.789	-1.477
Tiger	-6.858	-0.813
species	1	2
Cattle	5.587	-1.033
Leopard	-4.007	-0.158
Spotted Deer	3.723	6.409

Table-12: Performance index and Wilks's lambda of hoofs and claws of different grouped animals

Classification Matrix (Cases in row categories classified into columns)

Species	Cattle	Spotted Deer	Tiger	%correct
Cattle	50	0	0	100
Spotted Deer	1	9	0	90
Tiger	0	0	70	100
Total	51	9	70	99
Species	Goat	Leopard	Spotted Deer	%correct
Goat	60	0	0	100
Leopard	0	79	0	100
Spotted Deer	0	0	10	100
Total	60	79	10	100

Test Statistics

Statistic (for Cattle, Spotted Deer Hoof and Tiger Claw	Value
Wilks's Lambda	0.029
Statistic (for Goat, Spotted Deer Hoof and Leopard Claw)	Value
Wilks's Lambda	0.007

Canonical Scores of Group Means

Species	1	2
Cattle	3.446	-0.985
Spotted Deer	5.292	3.858
Tiger	-3.217	0.153
Species	1	2
Goat	7.625	-0.662
Leopard	-6.362	-0.144
Spotted Deer	4.506	5.115

Table-13: Performance index and Wilks's lambda of hoofs and claws of different grouped animals

Classification Matrix (Cases in row categories classified into columns)

Species	Goat	Spotted Deer	Tiger	%correct
Goat	60	0	0	100
Spotted Deer	0	10	0	100
Tiger	0	0	70	100
Total	60	10	70	100
Species	Cattle	Leopard	Tiger	%correct
Cattle	50	0	0	100
Leopard	0	64	5	93
Tiger	0	1	69	99
Total	50	65	74	97

Test Statistics

Statistic (for Goat, Spotted Deer Hoof and Tiger Claw)	Value
Wilks's Lambda	0.007
Statistic (for Cattle Hoof and Leopard, Tiger Claw)	Value
Wilks's Lambda	0.011

Canonical Scores of Group Means

Species	1	2
Goat	7.063	-0.691
Spotted Deer	4.332	5.171
Tiger	-6.673	-0.147
Species	1	2
Cattle	7.061	-0.048
Leopard	-2.465	2.24
Tiger	-2.614	-2.174

Table-14: Performance index and Wilks's lambda of hoofs and claws of different grouped animals

Classification Matrix (Cases in row categories classified into columns)

Species	Goat	Leopard	Tiger	%correct
Goat	60	0	0	100
Leopard	0	67	2	97
Tiger	0	1	69	99
Total	60	68	71	98
Species	Leopard	Spotted Deer	Tiger	%correct
Leopard	67	0	2	97
Spotted Deer	0	10	0	100
Tiger	1	0	69	99
Total	68	10	71	98

Test Statistics

Statistic (for Goat Hoof and Leopard, Tiger Claw)	Value
Wilks's Lambda	0.005
Statistic (for Spotted Deer Hoof and Leopard, Tiger Claw)	Value
Wilks's Lambda	0.017

Canonical Scores of Group Means

	1	2
Goat	9.402	0.241
Leopard	-4.678	2.193
Tiger	-3.448	-2.369
	1	2
Leopard	-1.278	1.974
Spotted Deer	12.129	0.871
Tiger	-0.473	-2.071

Table-15: Performance index and Wilks's lambda of horns and antler of different grouped animals

Classification Matrix (Cases in row categories classified into columns)

Species	Cattle	Goat	Spotted Deer	%correct
Cattle	60	0	0	100
Goat	0	49	0	100
Spotted Deer	0	0	48	100
Total	60	49	48	100

Test Statistics

Statistic	Value
Wilks's Lambda	0.001

Canonical Scores of Group Means

Species	1	2
Cattle	8.179	-2.413
Goat	8.387	2.932
Spotted Deer	-18.785	0.023

Table-16: Performance index and Wilks's lambda of ivories and antler of different grouped animals

Classification Matrix (Cases in row categories classified into columns)

Species	Boar	Elephant	Spotted Deer	%correct
Boar	20	0	0	100
Elephant	0	30	0	100
Spotted Deer	0	0	48	100
Total	20	30	48	100

Test Statistics

Statistics	Value
Wilks's Lambda	0.003

Canonical Scores of Group Means

species	1	2
Boar	-3.327	-5.808
Elephant	-4.289	3.426
Spotted Deer	4.067	0.278

Table-17: Performance index and Wilks's lambda of ivories, antler and artefact of different grouped animals

Classification Matrix (Cases in row categories classified into columns)

species	Boar	Elephant	Spotted Deer	%correct
Boar	19	0	0	100
Elephant	0	30	0	100
Spotted Deer	0	0	48	100
Total	19	30	48	100

Test Statistics

Statistics	Value
Wilks's Lambda	0.019

Canonical Scores of Group Means

Species	1	2
Boar	4.95	-2.39
Elephant	1.399	2.783
Spotted Deer	-2.834	-0.793